

Oil Shale Pyrolysis by Triple Quadrupole Mass Spectrometry: Comparisons of Gas Evolution at 10°C/min Heating Rate.

John G. Reynolds, Richard W. Crawford, and Alan K. Burnham,
University of California,
Lawrence Livermore National Laboratory,
Livermore, CA 94550.

Abstract

Kimmeridge, Phosphoria, LaLuna, Teistberget, New Albany, Janus, Lias ϵ , Maoming, Fushun, Woodford, and three Green River oil shales were subjected to programmed temperature pyrolysis at a heating rate of 10°C/min using Triple Quadrupole Mass Spectrometry (TQMS) as the detection method. Volatile compound evolution, including hydrocarbons, non-condensable gases, and heteroatomic compounds were monitored by on-line, real-time detection. As expected, the temperatures of maximum evolution depended on the oil shale and the species evolving. Generally, the T_{\max} values for total light volatile organic compound generation were between 430 to 500°C, with the New Albany giving the lowest values and Brotherson A from Green River giving the highest values. The heteroatomic species had T_{\max} values which were slightly lower than those for hydrocarbon evolution. Non-condensable gas formation was highly dependent upon the mineral matrix of the shale.

Introduction

Locating oil in a formation, and predicting where generation will occur are relevant contemporary problems for geochemistry. We are studying the kinetics of oil generation through laboratory simulated pyrolysis of source rocks to better address these problems.¹ To extend our data base, we have selected several oil shales from various geographical locations, from both marine and lacustrine source types and subjected them to programmed temperature pyrolysis at various heating rates, from room temperature to 900°C using Triple Quadrupole Mass Spectrometry (TQMS) as the detection method. This technique has been utilized previously for several studies on pyrolysis of oil shale,²⁻⁵ tar sands,⁶⁻⁸ and coal.⁹

TQMS is particularly suited for this type of study because it provides on-line, real-time analysis. By these experiments, we follow the evolution as a function of temperature of various light hydrocarbons, N-, S-, and O-containing compounds, and non-condensable gases. The pyrolysis profiles obtained allow determination of evolution range and T_{\max} . Multiple heating rates allow determination of kinetic parameters for which the ultimate aim is extrapolation to geological conditions. This report is a preliminary account of the evolution behavior of several oil shales at the heating rate of 10°C/min. A full report will be issued later. In addition, the kinetics derived from multiple heating rates will be reported separately.

Experimental

Instrumentation. The TQMS utilizes both MS and MS/MS detection coupled with computer controlled acquisition which allows for the detection of over 40 components in mat-

ters of seconds. Full details of this technique have been published elsewhere.^{10,11} Compounds analyzed for are C₁- through C₇-hydrocarbons, C₂- through C₅- volatile sulfur compounds, the non-condensable gases, H₂, CO, CO₂, H₂S, SO₂, and COS, as well as H₂O, CS₂, and several nitrogen- and oxygen-containing compounds. In these experiments, the pyrolysis reactor was a 1/4 inch quartz tube holding approximately 0.5 grams of oil, and was heated at a rate of 10°C/min with a constant Ar sweep of 30 cc/min. The evolving components flowed into a trap kept at 140°C. This allowed for light volatile hydrocarbon and heteroatom (N,S,O) compounds up to C₈ to pass through to the mass spectrometer, while the heavy components were retained. In addition to qualitative detection, several of the volatile components were also quantitated. Total evolution data will be reported later. The width of the T_{max} values indicate in all cases multiple activation energies. This will also be discussed in detail in the kinetics report.

Most of the samples were also characterized pyrolysis in a Pyromat (Lab Instruments) micropyrolysis instrument. 15 mg of sample is held in a quartz tube with a type K thermocouple inside. The sample is heated at a programmed heating rate, chosen to be 9.2°C/min in this case for comparison to the TQMS results. The total pyrolysate is monitored with an adjacent FID detector operated at 500°C.

Samples. Table 1 describes the shales examined in this study. Both marine and lacustrine samples from several locations throughout the world were examined. Pyrolysis experimental conditions and errors were determined by multiple runs on Woodford and NA-13 shales. Less abundant samples were examined generally 1 to 2 times.

Sources of several of the shales have been described previously.¹ In addition, NA-13 is from the New Albany formation; AP-24, Government 33-4, and Brotherson A are from the Green River formation; Wenzen comes from the Lias ϵ formation. AP-24 comes from the Mahogany zone in Colorado. Government 33-4 and Brotherson A come from well cores in Utah. Government 33-4 contains 10% vitrinite and 5% exinite. (Numbers provided by DGSi company of The Woodlands, TX.) Brotherson A is just above the oil window. The Wenzen sample is from J. Rullkotter (KFA); LaLuna from S. Talukdar (INTEVEP); Janus and Teistberget from B. Dahl (Norsk Hydro).

Two samples each of Maoming and Fushun shales were also examined. These samples were from the same formation but obtained from different sources. The samples appended with I were obtained from R. C. Rex, Jr. (Hycrude Corporation) and those appended with II were obtained from Zhang Shi Ko of Sinopec International. Janus is a terrestrial shale with some marine mixed in. Full descriptions of the samples will be presented elsewhere.

Results and Discussion

Hydrocarbon Evolution. Figure 1 shows the pyrolysis profiles for the evolution of C₃H₈ for several of the shales listed in Table 1 (some were not presented for figure clarity). These profiles are typical of evolution seen for all the hydrocarbons, having an approximate Gaussian shaped prominent maximum with a temperature of maximum evolution (T_{max}) around 450 to 500°C, depending upon the hydrocarbon species evolving and the particular shale. This maximum has been assigned as due to kerogen breakdown and bitumen cracking.^{2,12-14} Little or no intensity is seen at temperatures below and above this

maximum, except in methane evolution and isolated cases for higher hydrocarbons (see below).

Table 2 shows the T_{\max} for the total light organics evolved, and compares this value to the T_{\max} for the $C_4H_9^+$ ion and the T_{\max} measured by Pyromat. The total light organics evolution value comes from taking the total ion current of all the species evolving (which pass through the 140°C trap) at a specific temperature and subtracting the ion current contributions from non-hydrocarbon gases (SO_2 , CO_2 , H_2S , HS , O_2 , S , H_2O , NH_3 , H_2) and the carrier and analysis gases (Ar, Kr). The $C_4H_9^+$ ion is from monitoring m/z 57 and is a result of contributions from most hydrocarbons of C_4H_{10} and higher. It is meant to be an indicator of these larger alkyl hydrocarbons as opposed to only butane. The Pyromat analysis was included to give a comparison measurement of total hydrocarbons which is not based on MS methods. Generally, for a given sample, the absolute values of the Pyromat technique are slightly lower than the total light organics from the TQMS, but the trends are the same.

Comparing T_{\max} for total volatile organics, two groupings are observed. The marine shales have temperature maxima between 447 and 471°C and the lacustrine shales between 471 and 484°C. This is normal behavior for these types of shales. The Maoming shales, however, are the exceptions. The T_{\max} , as well as other properties (see below), are much more like marine shale than lacustrine shale. The same grouping is observed for the $C_4H_9^+$ ions, but with slightly different temperatures ranges.

Comparing corresponding T_{\max} values for total light organics and $C_4H_9^+$ ions, in general, the values are similar. NA-13 has the lowest T_{\max} for both sets, while Brotherson A has the highest for both sets. The biggest differences between the two sets are for Wenzen, where the T_{\max} for total light organics evolution is 8 °C higher than for the $C_4H_9^+$ fragment. In some cases (Phosphoria, Wenzen, Woodford, Government 33-4, Maoming II) the T_{\max} for total light organics generation is higher than the T_{\max} for $C_4H_9^+$ ion, but in many cases it is the same or lower (NA-13, Janus, Maoming I, Kimmeridge, AP-24, Teistberget, Fushun I, Fushun II, Brotherson A, LaLuna).

The Pyromat derived T_{\max} values are generally lower than the corresponding T_{\max} values and exhibit a much smaller spread in values than for both total light organics and $C_4H_9^+$ generation. However, the trends are roughly same. In this case, Phosphoria has the lowest T_{\max} , instead of NA-13. Brotherson A has the highest T_{\max} . Also, the lacustrine shales have a T_{\max} which is around 460°C, while the marine shales have a T_{\max} around 445°C. As in the case for total light organics generation, Maoming shale behaves more like a marine than lacustrine shale.

Table 3 shows the T_{\max} values for C_2H_4 , C_2H_6 , C_3H_8 , and C_4H_{10} evolution. The value in parentheses in the T_{\max} column indicates another maximum is observed having a T_{\max} at the listed temperature in addition to the maximum assigned to hydrocarbon evolution. This low temperature maximum can be assigned to entrapped material in the mineral matrix which becomes labile when the bitumen in the shale begins to soften. This behavior is very prominent in tar sands where the bitumen content is much higher than in oil shale and has been assigned as such.⁶⁻⁸

For all cases, the C_2H_4 evolution T_{max} values are higher than the T_{max} for total light organics evolution for the corresponding shale. For the lacustrine shales, Fushun I, Fushun II, Government 33-4, and Brotherson A show very little difference between the C_2H_4 T_{max} and the total light organics evolution T_{max} (2 to 6 °C) as shown in Table 2. For the marine shales, the difference between the T_{max} for C_2H_4 evolution and the T_{max} for total light organics evolution is very large (15 to 35 °C). The two Maoming samples, however, behave like marine samples also which has been seen above for the total light organics, $C_4H_9^+$ evolution, and Pyromat T_{max} .

Interestingly, the lacustrine samples tend to have T_{max} values for total light organics evolution which are *higher* than that for the marine shales, but in the case of C_2H_4 evolution, the T_{max} values are *lower*. Fushun I and Fushun II have the lowest C_2H_4 evolution T_{max} values for all the shales listed. Brotherson A which has the highest T_{max} for total light organics and $C_4H_9^+$ ion evolution, and Pyromat T_{max} , is not even close for that value in Table 3.

Contrary to total light organics and C_2H_4 evolution, the T_{max} values for C_2H_6 evolution show no apparent grouping according to type. However, the differences in the T_{max} values for C_2H_6 evolution compared to the T_{max} values for total light organics evolution are generally much larger for the marine shales than the lacustrine shales. Even the Maoming samples are consistent with this.

The difference in the T_{max} values for C_2H_4 evolution and C_2H_6 evolution are much larger for the marine shales than the lacustrine shales. (The ethane to ethene ratio are much closer to 1 for the marine shales). Once again, the Maoming samples are the exception as noted above. Brotherson A is also an exception. This shale is different than the other samples in that it is just above the oil generation window. As seen in Table 2, it has the highest T_{max} for total light organics and $C_4H_9^+$ ion evolution. This is consistent with the lighter material being converted in the formation.

Our results are similar to earlier results for eastern Devonian shale,^{2,13} Chinese shale,² and Green River shale.^{2,12} Our T_{max} values are generally higher because our faster heating rate, but these appear to be minor differences from the earlier work¹²⁻¹⁴ due to improvements in techniques.

The T_{max} values for C_3H_8 evolution listed in Table 3 are lower than the T_{max} values for C_2H_4 and C_2H_6 evolution, and are similar to the T_{max} for total light organics evolution, for a given shale. This has been seen before NA-13 oil shale at 4°C/min¹³ and for several tar sands.⁶⁻⁸ Only Fushun II and Brotherson A counter this trend.

Of all the hydrocarbons listed in Table 3, C_4H_{10} had the lowest T_{max} for a given shale. These values are significantly lower than the T_{max} for total light organics evolution. The differences in T_{max} values of C_2H_4 and C_4H_{10} for a given shale ranged from 54 °C to 10 °C. The lacustrine shales generally had smaller differential than the marine shales, which is expected. However, as seen before, the Maoming shales had behavior which was similar to marine shales. Brotherson A was another exception, which exhibited very little difference in the T_{max} values for all the hydrocarbons listed in Table 3. As stated above, Brotherson A is located above the oil generation window, which is probably responsible for its aberrant behavior. The T_{max} for C_4H_{10} generation for NA-13 is slightly lower (3°C)

than the value found at 4°C/min, but probably within experimental error.¹³ The AP-24 value is higher as expected for the higher heating rate.¹²

Methane. Figure 2 shows the pyrolysis profiles for the evolution of methane as a function of pyrolysis temperature for selected shales. In contrast to the other hydrocarbon evolution profiles, the typical methane profile exhibits not only the prominent maximum at hydrocarbon evolution temperatures, but also a shoulder on the high temperature side of this maximum. The prominent maximum has a T_{max} higher than for the corresponding other hydrocarbons, ranging from 2 to 146 °C above the T_{max} for total light organics generation, depending upon the shale. This has also been assigned to kerogen breakdown and bitumen cracking reactions.¹²⁻¹⁴

The evident shoulder on many of the profiles in Figure 2 has been assigned to evolution of methane by secondary charring reactions. As the kerogen is further pyrolyzing, and the non-volatile bitumen is laying down as pre-coke and coke on the mineral matrix, more methane is evolved. This behavior has been seen previously for oil shale¹² and tar sands.⁶⁻⁸ However, for several shales (LaLuna, Phosphoria, Government 33-4) have shoulders in the methane profiles on the low temperature side of the prominent maximum. This behavior has been seen before for NA-13 shale.² This suggests the major peak is due to charring reactions instead of organic evolution. Because at the higher heating rates, the shoulders are poorly resolved, this aspect will be examined in more detail at the 1°C/min heating rate.

Table 4 lists the T_{max} for methane evolution for all the shales studied. Kimmeridge exhibits the highest T_{max} while AP-24 exhibits the lowest. The AP-24 value is 15°C higher than the T_{max} reported earlier at a 4°C/min heating rate, which is consistent with the higher heating rate.¹² The T_{max} for NA-13 also agrees with values for eastern shales heated at 4°C/min reported by Coburn¹³ and Oh et al.² We also observe a shoulder on the low temperature side of the prominent maximum at about 470°C. This is in agreement with Oh et al. who see the shoulder at 450°C and assign it as probably due to CH₄ generation from kerogen pyrolysis. Oh et al. also reports the Maoming I and Fushun I shales having T_{max} at 500°C. These values are reasonably close to those in Table 4 which would not be expected at the different heating rates. Because of the broad nature of the CH₄ peak, T_{max} values are difficult to assign when the signal-to-noise is not optimal. In addition, they observed shoulders at temperature around 600°C, which is also consistent with Table 4.

Regardless of the T_{max} for a particular shale, the shoulder appears at approximately 100°C higher. Although there is no shoulder temperature listed for Janus, examination of the profile in Figure 2 shows a very broad peak which defies resolution in the temperature range expected for the shoulder. This could be due to the noise in the profile, or the two methane forming reaction pathways being about equal in intensity. Experiments at different heating rates will help clarify this, and are in progress.

Evident in Figure 2 for Government, LaLuna, Teistberget, and AP-24 oil shales are small maxima in the 700 to 900°C evolution range. Because the data is from the unique MS/MS combination of 16/14, these are not artifacts of other species which produce m/z 16 ions.¹¹ Examination of the CO₂ profiles show that these maxima coincide with intense CO₂ evolu-

tion for the same shale. This suggests CO₂ gasification of organic char (from decomposing kerogen and bitumen) in the mineral matrix. Equation (1) describes this reaction:



Carbon Oxide Evolution. The CO₂ evolution profiles for the shales can be grouped into three types: 1) high carbonate shales (LaLuna, Wenzen, Brotherson A, Government 33-4, Teistberget, and AP-24), 2) low CO₂ mineral shales (Phosphoria, Woodford, Kimmeridge, and Janus), and 3) high siderite shales (Maoming I, Maoming II, Fushun I, and Fushun II). The high carbonate type shales show a very small maximum around 400 to 450°C, and prominent evolution in the 650 to 900°C range. The former has been previously tentatively assigned in oil shales and tar sands to be due to the decomposition of oxygen-containing organic compounds, such as carboxylic acids and salts, and ketones.^{6-8,12,13,15,16} The high temperature evolution is has been assigned to carbonate mineral decomposition dominating the CO₂ evolution. Table 1 lists Brotherson A, Wenzen, LaLuna, and AP-24 having calcite and/or dolomite as the major mineral. Government and Teistberget are the only other shales that have any appreciable carbonate minerals. Independent acid carbonate determinations show this is the case for AP-24, Wenzen, and LaLuna (Government and Teistberget are being determined). These results are in agreement with previously published results on AP-24 and NA-13 shales.^{2,12,13}

The low mineral shales show CO₂ evolution behavior which is very complex. In most cases, CO₂ evolution correlates well with water and H₂S evolution in the temperature range around 475 to 600°C. Some of this evolution can be described by: 1) the α to β transition for quartz around 560°C (evolves not only water, but some CO₂),¹⁷ and 2) the reaction of H₂S is also known to react with iron and mixed metal carbonates¹⁸ at fairly moderate temperatures.

The high siderite shales (Chinese shales), minerals release CO₂ at relatively low temperatures (Shale, T_{max}: Maoming I, 465°C; Maoming II, 462°C; Fushun I, 497°C; Fushun II, 487°C) most likely due to the decomposition of siderite. For the Maoming shales, CO₂ release is coincidental with H₂S and hydrocarbon evolution, indicating reaction of H₂S (probably generated from organo-sulfur compound decomposition) with minerals may be catalyzing the release in this temperature range.

No evolution of CO is seen below 300°C, after which evolution begins. In most of the profiles, a small maximum is evident around 440°C and falls in the range of hydrocarbon evolution due to kerogen breakdown and bitumen cracking reactions. The chemical species responsible for this evolution is not certain, but may be the decarbonylation of carboxylic acids and salts.¹⁹

The majority of the CO evolved occurs above 600°C, and is not directly related to hydrocarbon generation. This high temperature CO could have a variety of origins²⁰: 1) the water-gas shift reaction, 2) the Boudouard reaction (similar to equation 1), and 3) char gasification by water from mineral breakdown.

Hydrogen. Figure 3 shows the H₂ evolution profiles as a function of temperature for several of the oil shales studied. Except for Wenzen, the profiles show no hydrogen evolution before approximately 350°C. Several maxima are seen above this temperature, depending

upon the oil shale. For AP-24, Teistberget, Maoming I, Maoming II (not shown), Fushun I (not shown), Fushun II (not shown), the best defined maximum is around 475°C. This is also evident to a lesser extent for all the other shales. Table 5 lists the T_{max} for this maximum, along with the % of total evolution (by integration) accounted for by this maximum, and the total evolution of hydrogen (cc/gr of TOC) for the entire profile. No correlation between shale type and T_{max} was observed. This maximum occurs at the same temperature range as the maximum for total light organic evolution and is attributed to kerogen breakdown, aromatization, cracking, and dehydrogenation reactions of non-volatile bitumen. The differences between this T_{max} , and the T_{max} for total light organic evolution (see Table 2) depended upon the shale, varying from 0 (Wenzen) to 48°C (NA-13). This type maximum has been observed before in oil shale,^{2,12-14} and tar sands⁶⁻⁸ pyrolysis.

Figure 3 also shows the majority of the hydrogen is evolving above this maximum assigned to sources other than hydrocarbon generation, and can be attributed to several reactions, depending upon the temperature and the shale. The H_2 evolving in the 500 to 650°C ranging has been assigned previously¹² to char pyrolysis reactions where the residual kerogen, and non-volatile bitumen are further decomposing yielding surface coke, H_2 , and CH_4 (see above discussion). H_2 evolving above this can have additional contributions from a variety of secondary reactions including the water-gas shift equilibrium, char gasification, and the Boudouard reaction.

Heteroatomic Compounds. Several sulfur-, nitrogen-, and oxygen-containing compounds also evolved during the pyrolysis of the oil shales. Of all these compounds, methylthiophene generally produced the most intense signal due to concentration and response of the species. Figure 4 shows the methylthiophene evolution profiles as a function of pyrolysis temperature for most of the shales studied. The profile behavior is very similar to that of the hydrocarbons, where maximum evolution occurs at temperatures of oil generation. Also listed in Figure 4 are the T_{max} for the methylthiophene. The values, in °C, for the shales not shown are: Maoming II, 454; Woodford, 437; Fushun II, 446; Brotherson A, 487; NA-13, 436; Janus did not evolve methylthiophene. In general, these values are lower than the corresponding T_{max} for total light organics generation listed in Table 2 from 4 to 32°C. However, there appears no grouping according to shale type. Excluding Brotherson A, LaLuna exhibited the smallest difference (4°C), while Wenzen exhibited the largest (32°C). Brotherson A is the exception, where T_{max} is 3°C higher than the T_{max} for total evolution. No other shale has exhibited this behavior. However, this may be due to Brotherson A being above the oil generation window. This evolution behavior for methylthiophene and other heteroatomic species has been seen before for AP-24, NA-13,⁵ Maoming,² Kimmeridge,¹ and Fushun,² oil shales, and tar sands.⁶⁻⁸

Figure 5 shows the acetic acid evolution profiles for several shales studied. The T_{max} values are also listed. The T_{max} values, in °C, for the shales not shown in the figure are: NA-13, 391; Wenzen, 431; Fushun II, 442; Maoming II, 400; Woodford, 389; Janus and Brotherson A did not evolve any acetic acid. In general, the profiles are similar to the methylthiophene and hydrocarbon profiles except the acetic acid profiles tend to be broader, and the T_{max} values are even lower than the corresponding T_{max} values for methylthiophene. The difference between T_{max} for acetic acid evolution and T_{max} for total light organics evolution was as much as 74°C (Woodford).

The T_{\max} for acetic acid suggests these compounds may not be bound in the kerogen the same way the hydrocarbons are. The most obvious choice would be binding through a carbon oxygen bond. This should have less bond strength, and therefore a lower T_{\max} . Another possibility is the acid is entrained in the matrix, but due to donor-acceptor interactions, evolves at much higher temperatures than entrapped hydrocarbons (see bimodal distribution shown in Table 3, for example). These, and other alternatives are under investigation in our laboratories.

Conclusions

1) For all shales studied, the hydrocarbon evolution behaved approximately the same. Evolution did not begin until approximately 300°C, reaching a maximum for total light organics hydrocarbon evolution ranging from 447 to 484°C (depended upon the shale), and rapidly decreasing to completion about 550°C.

2) The T_{\max} values for total light organics evolution for lacustrine shales were generally higher than for marine shale. The Maoming samples were the exceptions, acting more like marine than lacustrine shales.

3) The T_{\max} values for $C_4H_{10}^+$ ion evolution were quite similar to the T_{\max} from total light organics evolution, and exhibited similar trends with shale type.

4) The hydrocarbons, C_2H_4 , C_2H_6 , C_3H_8 , and C_4H_{10} , all exhibited individualized behavior. The T_{\max} for C_2H_4 and C_2H_6 evolution is much higher than the T_{\max} for total light organics evolution. In addition, type behavior is opposite that for total light organics evolution: lacustrine shales have T_{\max} for C_2H_4 which is lower than that for marine shales. The T_{\max} values for C_3H_8 and C_4H_{10} hydrocarbons were progressively lower in temperature for a given shale.

5) CO_2 generation divided the shales into three categories: 1) high carbonate shales, which the evolution was dominated by the high temperature decomposition due to calcite, and dolomite, 2) low carbonate mineral shales, where the CO_2 evolution exhibited no distinctive source, and 3) siderite shale which exhibited prominent CO_2 evolution in the 450 to 475°C evolution range.

6) CO evolution occurs in two regimes: 1) a minor amount in the temperature range around 400 to 450°C which corresponding to kerogen breakdown and bitumen cracking, and 2) the major amount at high temperature due to char gasification reactions and water-gas shift equilibrium.

7) Hydrogen evolution exhibited a sharp maximum concurrent with kerogen breakdown and bitumen cracking. The majority of the hydrogen evolution occurred above 500°C due to char pyrolysis and mineral decomposition induced gasification reactions.

8) Heteroatomic compound behavior was typified by methylthiophene and acetic acid evolution, where the T_{\max} values were generally lower than the corresponding T_{\max} for total light organics evolution by as much as 32°C for methylthiophene, and even lower for acetic acid. In addition, the profiles were much broader than those observed for hydrocarbon and other heteroatom compound evolution.

Acknowledgments

We thank Jack Clarkson for the Pyromat measurements and Armando Alcaraz for experimental assistance. This work was performed under the auspices of the U. S. Department of Energy by the Lawrence Livermore National Laboratory under contract number W-7405-ENG-48.

References

1. Burnham, A. K., Braun, R. L., Gregg, H. R., and Samoun, A. M. 1987. *Energy and Fuels*, 1, 452.
2. Oh, M. S., Coburn, T. T., Crawford, R. W., and Burnham, A. K. 1988. 21st Oil Shale symposium, Beijing, China, Ed.
3. Wong, C. M., Crawford, R. W., and Burnham, A. K. 1984. *Anal. Chem.*, 56, 390-395.
4. Oh, M. S., Taylor, R. W., Coburn, T. T., and Crawford, R. W. 1988. *Energy and Fuels*, 2(1), 100-106.
5. Coburn, T. T., Crawford, R. W., Gregg, H. R., and Oh, M. S. 1987. 1986 Eastern Oil Shale Symposium, KECL86-158, 291-299.
6. Reynolds, J. G., Crawford, R. W., and Coburn, T. T. 1988. 1987 Eastern Oil Shale Symposium, KECL87-175, 101-108.
7. Reynolds, J. G., and Crawford, R. W. 1989. *Fuel Sci. Tech. Int'l.* 7(5), XXX.
8. Reynolds, J. G. 1989. 1988 Eastern Oil Shale Symposium, KECL 88-YYY, XXX.
9. Burnham, A. K., Oh, M. S., Crawford, R. W., and Samoun, A. M. 1989. *Energy and Fuels*, 3, 42-55.
10. Wong, C. M., Crawford, R. W., Barton, V. C., Brand, H. R., Neufeld, K. W., and Bowman, J. E. 1983. *Rev. Sci. Instrum.*, 54(8), 996-1004.
11. Crawford, R. W., Brand, H. R., Wong, C. M., Gregg, H. R., Hoffman, P. A., and Enke, C. G. 1984. 56, 1121-1127.
12. Campbell, J. H., Koskinas, G. J., Gallegos, G., and Gregg, M. 1980. *Fuel*, 59, 718-725.
13. Coburn, T. T. 1983. *Energy Sources*, 7(2), 121.
14. Burnham, A. K., Huss, E. B., and Singleton, M. F. 1983. *Fuel*, 62, 1199-1204.
15. Huss, E. B., and Burnham, A.K. 1982. *Fuel*, 61, 1188.
16. Burnham, A. K., Clarkson, J. E., Singleton, M. F., Wong, C. M., and Crawford, R. W. *Geochim. Cosmochim., Acta*, 46, 1242 (1982).
17. Reynolds, J. G., and Crawford, R. W. unpublished results.
18. Taylor, R. W., Coburn, T. T., and Morris, C. J. 1989. 1988 Eastern Oil Shale Symposium, KECL88-XXX, YYY.
19. Reynolds, J. G., Crawford, R. W., and Alcaraz, A. 1988. ACS Div. Petrol. Chem., Preprint, Los Angeles.
20. Campbell, J. H., and Burnham, A. K. 1978. Proceedings of the 11th Shale Oil Symposium, Colorado School of Mines: 242-259.

Table 1. Oil Shale Descriptions

Shale	Country	Type	Minerals
Kimmeridge	North Sea	Marine	Quartz, Illite, Pyrite (m), Feldspar (tr), Dolomite (tr), Kaolinite (tr)
Phosphoria	Montana	Marine	Quartz, Illite (m), Siderite (tr), Pyrite (tr), Siderite (tr), Kaolinite (tr)
Teisberget	Norway	Marine	Quartz, Siderite (m), Calcite (m), Pyrite (m), Illite (m), Kaolinite (m)
NA-13	Kentucky	Marine	Quartz, Illite (m), Kaolinite (tr), Feldspar (tr), Pyrite (tr)
Janus	Norway	Terrestrial/Marine	Quartz, Illite (m), Kaolinite (tr), Pyrite (tr)
Woodford	Oklahoma	Marine	Quartz, Pyrite (tr), Kaolinite (tr), Illite (tr), Smectite (tr)
LaLuna	Venezuela	Marine	Calcite, Quartz, Kaolinite (tr)
Wenzen	West Germany	Marine	Calcite, Quartz, Kaolinite (m), Illite (tr), Pyrite (tr)
Maoming I	China	Lacustrine	Quartz, Kaolinite, Siderite (tr), Illite (tr)
Maoming II	China	Lacustrine	Quartz, Kaolinite, Siderite (m), Illite (tr)
Fushun I	China	Lacustrine	Quartz, Kaolinite, Siderite (m), (Halite), Illite (tr), Smectite (tr)
Fushun II	China	Lacustrine	Quartz, Kaolinite, Siderite (m), (Halite)
AP-24	Colorado	Lacustrine	Dolomite, Quartz, Calcite (m), Feldspar (m), Analcime (m), Pyrite (tr), Illite (tr)
Government 33-4	Utah	Lacustrine	Quartz, Dolomite (m), Calcite (m), Illite (m), Analcime (tr), Kaolinite (tr)
Brotherson A	Utah	Lacustrine	Dolomite, Quartz, Calcite, Feldspar (m), Smectite (m), Analcime (m), Illite (tr)

Minerals in {} are tentative
(m) = minor components
(tr) = trace components

Table 2

Temperatures of Maximum Evolution for Total Light Organics, C₄H₉⁺ Ions From Hydrocarbons, and Total Pyrolysate From Pyromat Micropyrolyzer

Shale	Total Light, °C Organics	C ₄ H ₉ ⁺ , °C	Pyromat, °C
Kimmeridge	454	454	442
Phosphoria	465	461	441
Teistberget	466	469	456
NA-13	447	447	443
Janus	471	471	463
Woodford	463	460	444
LaLuna	462	466	444
Wenzen	467	459	444
Maoming I	465	465	451
Maoming II	466	463	na
Fushun I	473	476	462
Fushun II	471	472	na
AP-24	452	456	459
Government 33-4	478	474	452
Brotherson A	484	487	467

na = not available

Table 3

Volatile Hydrocarbon Evolution for Selected Shales at 10°C/min Heating Rate

Shale	C ₂ H ₄ T _{max} , °C	C ₂ H ₆ T _{max} , °C	C ₃ H ₈ T _{max} , °C	C ₄ H ₁₀ T _{max} , °C
Kimmeridge	480	465 (187)	453	433
Phosphoria	500	477	463	454
Teistberget	491	474 (225)	465	462
NA 13	480 (176)	458	446	437
Janus	495	482 (192)	480	471
Woodford	495	467	458	441
LaLuna	482	474	464	455
Wenzen	482	467	459	448
Maoming I	499	472 (200)	468	451
Maoming II	487	469	459	447
Fushun I	476	473 (250)	471	462
Fushun II	473	469 (244)	471	459
AP-24	478	470	469	461
Government 33-4	484	478	473	474
Brotherson A	489	488	493	479

Table 4
CH₄ Evolution for Selected Shales at 10°C/min Heating Rate

Shale	T _{max} °C	Shoulder °C	Evolution cc/gr of TOC ^a
Kimmeridge	500	600	30.12
Phosphoria	520	588	62.24
Teist	513	610	(3.24) ^b
NA 13	500	460	60.59
Janus	509	600	(0.78) ^b
Woodford	504	584	48.54
LaLuna	512	-	55.73
Wenzen	482	600	38.40
Maoming I	500	600	30.52
Maoming II	490	582	30.46
Fushun I	487	590	39.96
Fushun II	479	590	41.06
AP-24	454	540	34.44
Government 33-4	500	620	82.46
Brotherson A	492	595	27.05

a. TOC = total organic carbon

b. cc/gr of shale

Table 5
Hydrogen Evolution Behavior for Selected Oil Shales at 10°C/Min

Shale	T _{max} , °C ^a	% Total Evolution ^b	Total Evolution cc/gr of TOC ^c
Kimmeridge	472	26.4	100.8
Phosphoria	494	16.5	137.5
Testberget	469	22.2	(9.5) ^d
NA-13	495	23.4	92.0
Janus	482	31.8	(4.26) ^d
Woodford	471	23.5	113.5
LaLuna	466	23.8	96.0
Wenzen	467	32.4	75.2
Maoming I	472	23.1	155.2
Maoming II	473	35.2	137.2
Fushun I	508	37.6	244.9
Fushun II	500	36.2	191.5
AP-24	470	36.5	117.0
Government 33-4	500	37.2	170.3
Brotherson A	515	42.1	168.0

a. T_{max} for maximum at hydrocarbon evolution

b. % of total hydrogen evolution due to primary peak at hydrocarbon evolution

c. TOC = total organic carbon

d. cc/gr of shale

Figures

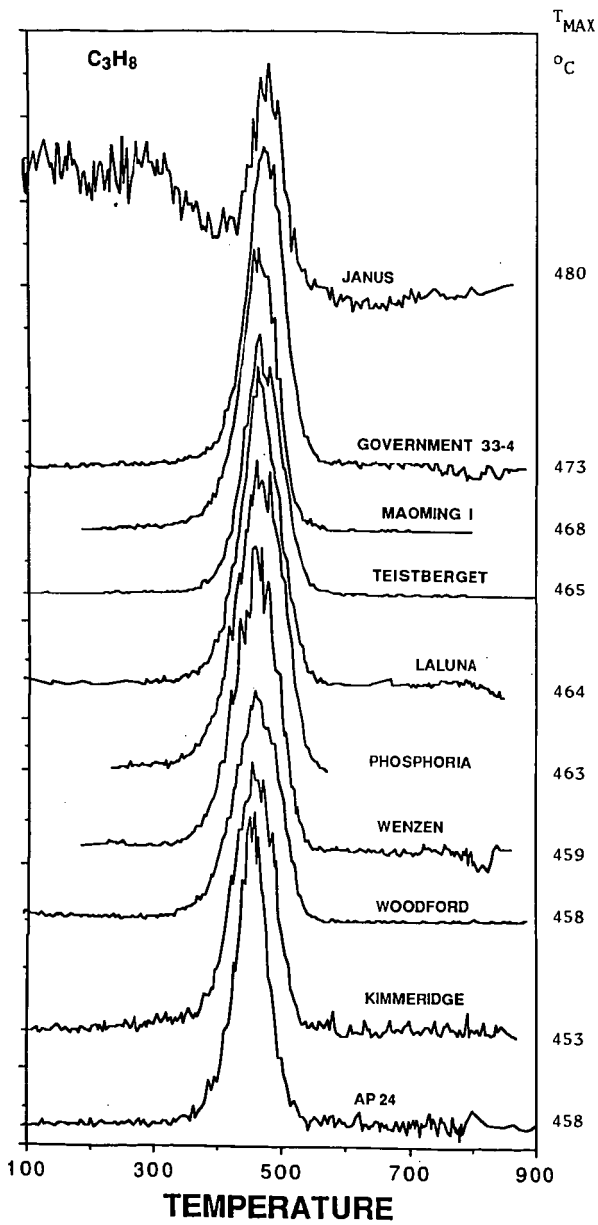
Figure 1. C_3H_8 Evolution as a Function of Pyrolysis Temperature for Selected Oil Shales at the Heating Rate of $10^\circ C/min$.

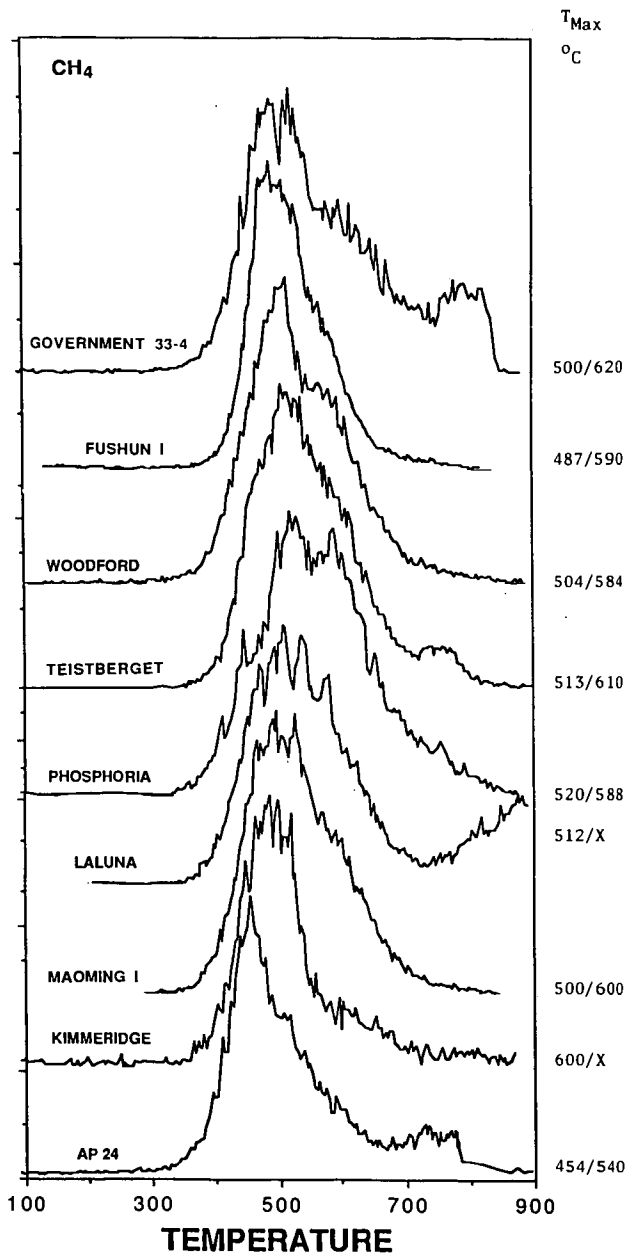
Figure 2. Methane Evolution as a Function of Pyrolysis Temperature for Selected Oil Shales at the Heating Rate of $10^\circ C/min$.

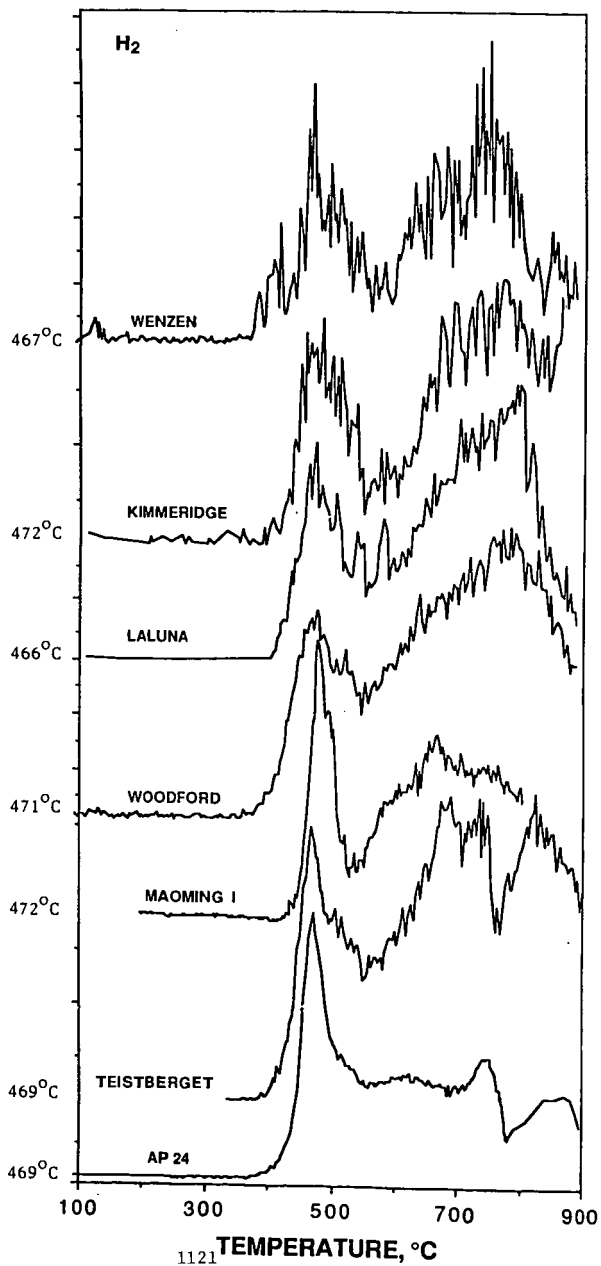
Figure 3. Hydrogen Evolution as a Function of Pyrolysis Temperature for Selected Oil Shales at the Heating Rate of $10^\circ C/min$.

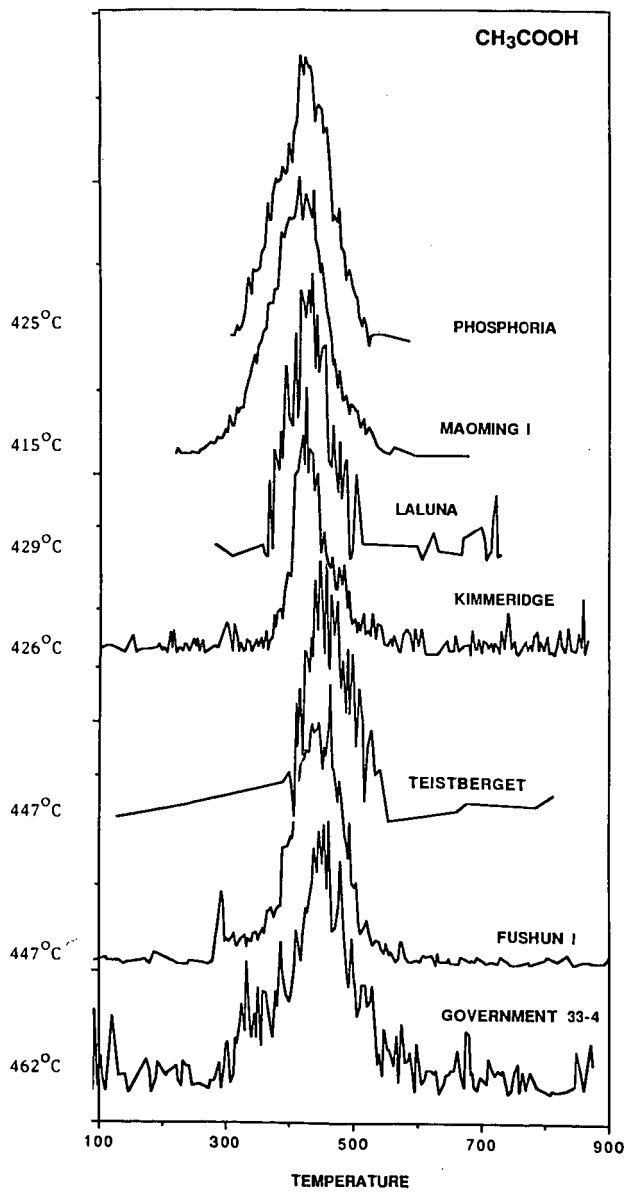
Figure 4. Methylthiophene Evolution as a Function of Pyrolysis Temperature for Selected Oil Shales at the Heating Rate of $10^\circ C/min$.

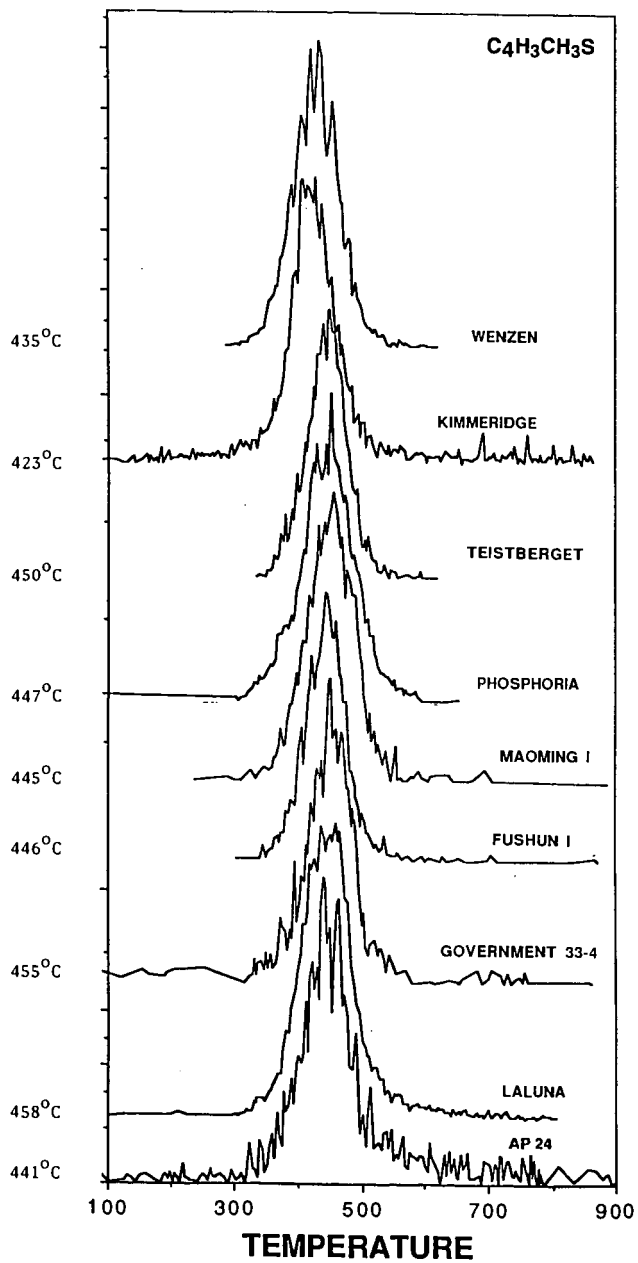
Figure 5. Acetic Acid Evolution as a Function of Pyrolysis Temperature for Selected Oil Shales at the Heating Rate of $10^\circ C/min$.











THE EFFECTS OF CARBON DIOXIDE AND CATION CONTENT
ON THE RAPID PYROLYSIS OF A LIGNITE

Robert B. Reuther
U.S. Department of Energy
Morgantown Energy Technology Center
Morgantown, WV 26507-0880

Robert G. Jenkins
College of Engineering
University of Cincinnati
Cincinnati, OH 45221-0018

INTRODUCTION

With the development of newer, more advanced technologies, especially those operating at higher pressures and under rapid heating conditions, the significance of certain variables on the pyrolysis process has been raised. The potential for developing the large deposits of low rank coals in the central regions of the United States using these technologies is leading a drive to examine these variables under conditions which simulate or approximate the technologies, especially with regard to rapid heating. Two variables of potential consequence to the processing of these low rank coals are carbon dioxide atmosphere and inherent cation content.

Until recently, the effect that the cations which are associated with certain oxygen functionalities on low rank coals have on pyrolysis has been ignored. There has been considerable interest about their effects in catalytic gasification and on combustion, especially with regard to slagging and fouling. But, with the work of Schafer (1980), Tyler and Schafer (1980), Morgan (1983), and Franklin et al. (1983), information is coming to light that removal of these species has a potentially important consequence on the yield and distribution of the products of pyrolysis. Thus, this effect also has potential repercussions on conversion processes. Ignition phenomena may be affected, for instance. It may also be possible to take advantage of this effect to produce premium products such as high density liquid fuels through a commercial pyrolysis process. The pyrolysis of a lignite is carried out in both a raw and an acid-washed state in order to confirm these findings and extend them to higher pressures.

It is well known that CO_2 reacts with coal via the Boudouard reaction. This reaction is considered unimportant on the time scale of rapid pyrolysis, however. On the other hand, CO_2 is present as a gaseous product during gasification and combustion as well as during pyrolysis. When low rank coals are pyrolyzed, the production of CO_2 can be significant through the destruction of large numbers of oxygen-containing moieties, especially carboxyl groups, present on such coals. It is hypothesized that the presence of CO_2 in the pores of a devolatilizing coal may have an impact on pyrolysis through interactions with the primary pyrolysis products. The capability of the atmospheric pressure entrained-flow reactor (APR) at Penn State to provide primary and secondary flow streams of different gas composition coupled with the high pressure capabilities of the high pressure reactor (HPR), also at Penn State, allows a unique study of the effect of CO_2 on rapid pyrolysis. This includes a focus on the interaction of CO_2 on both raw and acid-washed coal samples.

EXPERIMENTAL

Coal Sample Selection and Preparation

The coal selected for this study is PSOC-412, a lignite from the Darco seam in eastern Texas. Samples of the coal were obtained from the Penn State Coal Sample Bank. The coal was ground, sieved and resieved in order to provide a narrow size distribution, and then stored in closed containers at ambient conditions. All solid particles pyrolyzed in the experiments were collected between U.S. Standard Sieve mesh sizes 140 and 200. The mean diameter of these particles as determined by the Rosin-Rammler technique is 79 microns. Portions of the sized coal sample were used to prepare acid-washed samples according to a method used by Morgan (1983). The acid-washing is performed to remove the cations which are associated with the carboxyl group functionality on low rank coals. Portions of the acid-washed samples were then used to prepare a small amount of calcium-exchanged samples, again according to a method used by Morgan (1983). This procedure replaces the hydrogen ions on the carboxyl groups with calcium ions.

Pyrolysis Procedure

Pyrolysis experiments were conducted in the entrained-flow tube furnace systems at Penn State. The construction of these furnaces is based on a design by Badzioch and Hawksley (1970).

The APR was originally constructed by Scaroni (1979). Modifications to design and operating procedure subsequently evolved as documented by Maloney (1983) and Morgan (1983). Operation of the APR in this study follows the procedure described by Maloney (1983), except for one important difference. In these experiments, the hopper which held the solid sample prior to injection into the furnace was flushed continuously with the entraining gas. The reader is referred to Maloney (1983) for details of the operational procedure for the APR.

All the tests in the APR were conducted at atmospheric pressure and 900°C. Primary and secondary volumetric flowrates were held constant at approximately 1 and 35 standard liters per minute, respectively. Residence times were varied by placing a water-cooled collector probe coincident with the axis of the reactor at various distances from the injector tip. Residence times were determined using velocity models (see below). The solids flowrate was held constant at 1 gram per minute. The primary, or entraining, gas was He or CO₂, and the secondary gas was either N₂ or CO₂, depending on the test matrix. The Reynolds number for the total gas flow, calculated at 900°C, was in the neighborhood of 200 for N₂ and 350 for CO₂ (ignoring the small, primary gas flow of He when present).

The HPR was constructed to provide information about devolatilization studies under conditions more severe than those possible with the APR. It was designed to conduct pyrolysis at pressures to 1500 psig, temperatures to 1300°C, and in reducing atmospheres, including pure hydrogen. All experiments in the HPR were conducted at a nominal temperature of 900°C and at pressures of 200 psig. Due to the design of the HPR (and unlike the APR), the composition of the primary and secondary gas was necessarily the same for a given experiment. Pyrolysis was conducted in either He or in CO₂ atmospheres. The gas Reynolds number for the experiments in He ranged between 50 and 250. For CO₂ the gas Reynolds number varied between 500 and 2500. The solids flow rate was 1 gram per minute. As with the APR, residence times were determined using velocity models (see below). The reader is referred to Reuther (1988) for details of the pyrolysis procedure in the HPR.

Residence Time Determination

The designs of the APR and the HPR make measurement of particle velocities and residence times extremely difficult. Instead, the distances over which the particles are entrained in the hot zones of the reactors (from injector tip to collector probe entrance) are transformed into residence times using a gas velocity model coupled with a particle velocity model. The approach used is similar to that used by Morgan (1983), Maloney (1983), and Tsai and Scaroni (1984) and was originally described by Morgan (1983) for the APR. The design of the reactors and the associated pyrolysis procedures cause the gases and entrained particles to enter the reaction zone under laminar plug flow conditions with development of a parabolic flow profile following immediately. The particles are injected with a cold entraining gas (primary stream) through nozzles which are inserted down the axes of the reactors. The much larger flow of hot secondary gas flows into the reactors through the annular region created by the nozzles.

The development of the parabolic profile, created by the drag of the gas along the wall, affects the gas velocity at every point in the reactor. Also, because the gas velocity is accelerating in the region in which the particles reside, the effect this has on particle velocities must subsequently be considered. The model used for the development of the parabolic flow profile was originally described by Campbell and Slattery (1963).

The equation governing particle velocity is derived by considering the forces acting on the entrained particle (Shu, 1978). This equation is numerically solved using the fourth-order Runge-Kutta computational technique. As a consequence of the solution, one can determine the distance the particles have fallen as a function of time, thus giving a residence time for the particles in the reactor.

Discussion of Particle Temperatures

The particles are assumed to be heated primarily by the hot, secondary gas stream. That is, radiation from the walls is believed to be an important mode of heat transport under the experimental design. Thus, the gas temperature is an important parameter in determining particle temperatures. For particle diameters less than 100 microns, the particle temperature closely follows the surrounding (primary) gas temperature, and the primary gas temperature is most sensitive to conductive heating by the secondary gas. These assumptions are in general agreement with previous studies on heat transfer in such systems (see e.g., Sass, 1972; Freihaut et al., 1977; Tsai and Scaroni, 1984; Suuberg, 1987; Hajaligol, 1987). Flaxman and Hallett (1987) have subsequently confirmed these results for an entrained-flow reactor which is based on the same design and operating principles as the APR at Penn State.

Thus, the most effective way to enhance particle heating rate is to use a low heat capacity, high thermal conductivity gas (i.e., a gas with a high thermal diffusivity) as the primary (cold) gas. This is equivalent to external heat transfer control for particle heating. It follows that particle temperatures and heating rates are higher when a gas with a high thermal diffusivity, such as He, is used as the primary gas than when a gas with a lower thermal diffusivity, such as N₂, is substituted. It is argued, based on the above statements, that when a lower thermally diffusive gas is substituted for a higher in the primary stream, the particle temperature is the same or lower for a given residence time. Thus, if the weight loss is found to be higher, such increased weight loss must be due to something other than temperature. In this work, the controversy concerning the temperature of the particles during pyrolysis in a dilute-phase, entrained-flow environment is avoided as much as possible by accepting the preceding arguments and those which follow. When drawing conclusions from comparisons among pyrolysis experiments it is assumed that (1) any two experiments run under the same conditions of gas flow and composition but with different 'kinds' of solid particles (raw versus acid-washed, etc.) have equivalent particle heating rates and final temperatures and (2) when the gases are different but the particles are the same, it is pointed out which particles may have heated up faster and/or to

a final higher temperature. The overriding assumption is that particles which heat up faster and to a higher temperature lose weight more rapidly and that higher pyrolysis temperatures result in higher weight losses. It should be noted that it is not assumed that the particles pyrolyze isothermally.

Weight Loss Analysis

All char samples were subjected to a moisture analysis followed by a proximate ash analysis in order to determine weight lost during a pyrolysis run. The procedures used were slight modifications of those specified by the American Society for Testing Materials (ASTM) Test D3173-73, Moisture in the Analysis Sample of Coal and Coke, and Test D3174-73, Test for Ash in the Analysis Sample of Coal and Coke. The procedural modification in each case was to substitute approximately 0.5-gram samples for the suggested 1.0-gram sample amounts in order to conserve sample. All samples were done in duplicate. If any of the duplicate values differed significantly (i.e., outside of the recommended ASTM limits of 0.5%), further samples were ashed until the discrepancy was resolved. The amount of organic material that was devolatilized in each experiment, i.e., the weight lost, was calculated from the proximate ash values of the devolatilized sample and the undevolatilized sample using the "ash tracer" technique, as described by Scaroni (1979).

RESULTS AND DISCUSSION

Weight Loss Results

Weight loss results are presented below as a function of the presence of cations and CO₂ atmosphere.

Effect of Cations

The effect of the presence of cations on rapid pyrolysis was studied in both the APR and the HPR. Pyrolysis was performed on raw, acid-washed, and, to some extent, calcium-exchanged coal samples. The results of these experiments in various atmospheres are plotted in Figures 1, 2, 3, 4, and 5.

Figures 1, 2, and 3 are from experiments at atmospheric pressure (i.e., in the APR). Figure 1 shows the results of pyrolysis on raw, acid-washed, and calcium-exchanged coals in He/N₂. (This nomenclature (e.g., 'He/N₂') is followed throughout this discussion. The first gas listed is the primary or entraining gas, and the second gas is the secondary flow gas.) Figure 2 presents weight loss results on the same three solid samples in He/CO₂. Figure 3 displays the results of pyrolysis in CO₂/CO₂ on the raw and the acid-washed samples, only. There is a dramatic drop in weight loss for the calcium-exchanged sample in both He/N₂ (Figure 1) and He/CO₂ (Figure 2) at longer residence times. There appears to be a small drop in weight loss for the raw sample compared to the acid-washed sample in He/N₂, which is most significant at intermediate residence times. The results in He/CO₂ are similar to those in He/N₂. In CO₂/CO₂ (Figure 3), where only raw and acid-washed samples were compared, there is again a drop in weight loss in going from acid-washed to raw sample. In this case the difference appears to be more significant than in He/N₂ or He/CO₂, however, and occurs throughout the range of residence times examined.

The preliminary conclusions to be drawn from these three figures are:

1. Removal of cations appears to have had a small impact on weight loss with this coal, being most significant at intermediate to longer residence times.

2. Replacement of hydrogen ions on the carboxyl groups by calcium ions to a saturation level had a dramatic effect on weight loss.
3. The presence of CO_2 in the pores at the onset of pyrolysis has an added effect on weight loss from the acid-washed coal sample compared to the raw sample.

Figures 4 and 5 are the results of experiments in the HPR at 200 psig. Figure 4 presents the weight loss results of raw and acid-washed samples in He/He. Figure 5 shows the pyrolysis of these same two samples in CO_2/CO_2 . The weight loss of the raw sample in He/He is again reduced compared to the acid-washed sample except for the longest residence time recorded, which occurs at what appears to be an asymptotic or ultimate rapid pyrolysis yield under these conditions. When these same two samples are pyrolyzed in CO_2/CO_2 , however, only at the earlier residence times considered is there a noticeable reduction in weight loss for the raw sample compared to the acid-washed sample. At the longer residence times, as with Figure 4, weight losses are virtually identical.

Thus, as with the APR results, the presence of cations appears to reduce weight losses during the earlier periods of rapid pyrolysis in an inert atmosphere (He). The weight loss reduction is more significant at this higher pressure and may be an indication that the species which are contributing to reduced weight loss are themselves affected by mass transfer considerations. If, for example, the cations are retarding weight loss by attaching themselves to potential volatile species which, in turn, makes it more difficult for them to exit the particle under mass diffusion considerations (increased molecular weight and size), then additional constraints to mass transfer, such as increased pressure, could enhance this effect. Or, if the cations reduce weight loss via cracking reactions, then mechanisms which impede mass transfer, such as increased pressure, will allow more time for this process to occur. Both of these possible roles for cations as weight loss inhibitors are discussed by Morgan (1983) and others. What is also significant, however, is that ultimate weight loss is virtually the same in both Figures 4 and 5. This indicates that most (if not all) of the mass associated with the initially formed volatiles eventually exits the particle given enough time, although it may not have the same molecular structure as when first formed because of one or more secondary reactions. ("Initially formed volatiles" is taken to mean those species which are originally solid but which exist in the vapor state, however transiently, under the conditions of the experiment upon the initial breaking of a bond which had held it to the rest of the solid matrix.)

Finally, Figure 5 reinforces the impression that the presence of CO_2 is having an effect on weight loss. To confirm this, the pyrolysis results were replotted to show the effect of atmosphere for each coal sample (raw and acid-washed) in each reactor (APR and HPR).

Effect of Atmosphere

Figure 6 shows the results of the pyrolysis of the raw coal in the APR in He/ N_2 , He/ CO_2 , and CO_2/CO_2 atmospheres. The weight loss in He/ N_2 is less than in He/ CO_2 or in CO_2/CO_2 over most of the residence time measured. The particle temperature in He/ N_2 and in He/ CO_2 should be very nearly the same from a thermodynamic standpoint. This is because the primary gas is the same in the two cases, and the heat content of the secondary gases are identical (the volumetric flowrates and volumetric heat capacities are the same). Thus, the increased weight loss in He/ CO_2 over He/ N_2 is clearly due to some interaction of CO_2 with the devolatilizing sample. Also, heat transfer in CO_2/CO_2 should be lower than in He/ CO_2 based on the thermal diffusion arguments. Thus, it might be expected that a higher weight loss would occur in CO_2/CO_2 over He/ CO_2 on a temperature-adjusted basis at the earlier residence times.

Figure 7 shows the results of the pyrolysis of the acid-washed sample in He/ N_2 , He/ CO_2 , and CO_2/CO_2 atmospheres. Again, there is a difference in weight loss between

He/N₂ and He/CO₂ which can only be due to the interaction of CO₂ and the devolatilizing sample. Weight loss in CO₂/CO₂ exceeds even that in He/CO₂ at early residence times, but by the longest residence time measured the weight losses have converged. Weight lost from He/N₂ is still below that from the other two gas compositions for the longest residence time measured, however, which is in contrast to Figure 6.

Figures 8 and 9 show the results of experiments conducted in the HPR. Figure 8 shows pyrolysis of raw coal in He/He and CO₂/CO₂. Figure 9 shows pyrolysis of acid-washed coal in He/He and CO₂/CO₂. The pyrolysis of raw coal in He/He has significantly less weight loss than in CO₂/CO₂ over the intermediate residence times. Again, heat transfer in CO₂/CO₂ may be poorer than in He/He, thus reinforcing the weight loss differences. Again, at long residence times the weight losses converge.

Figure 9 shows a smaller difference in weight loss over intermediate times with ultimate weight losses again converging. Still, some effect of CO₂ over intermediate times even with the acid-washed sample is evident.

It is instructive to first go back to Figure 8 to explain the role of CO₂ in rapid pyrolysis. Even at the earliest recorded residence time (~76 milliseconds), weight lost in the CO₂ atmosphere exceeds weight lost in He by nearly a factor of two. By 135-140 milliseconds residence time, weight loss in CO₂ is more than twice that in He. Eventually, however, the weight losses converge at the longest residence times. Since it has been shown that the cations inhibit weight loss over this same time interval and at this pressure, the CO₂ must somehow be counteracting this effect. It is hypothesized that CO₂ could be tying up the calcium, perhaps converting CaO (calcium oxide, a known tar cracker) to CaCO₃ (calcium carbonate, inert to cracking reactions?). (The increase in char weight due to the carbonate formation is only on the order of 1% assuming all the calcium in the raw coal were carbonated. Thus, it should not significantly affect the weight loss analysis). Alternatively, the CO₂ could be enhancing weight loss by affecting active sites on the char directly. For example, active carbon sites on the pyrolysing char (created by initial bond breaking to form volatiles) could have CO₂ adsorb onto them. This would make the sites unavailable for reattachment or cracking of previously formed volatiles. Finally, CO₂ could be stabilizing reactive volatiles through the formation of carboxyl groups at the reactive sites in a Kolbe-type reaction (Morrison and Boyd, 1973, p. 804). This would allow the volatiles to more readily escape the devolatilizing char matrix. Again, it is instructive that the weight losses converge, strongly implying that all (or nearly all) of the potential volatiles exit the devolatilizing lignite given enough time, although not necessarily in the same molecular form. Also, the weight loss increase due to CO₂ is probably not due to the Boudouard reaction. More needs to be said about the second point. If the Boudouard reaction were important, it is likely that increased ultimate volatile matter would appear in CO₂ atmospheres. This is not evident. Also, most measures of the Boudouard reaction show it to be much slower than the weight loss rates considered here.

A further indication that the Boudouard reaction is not important is illustrated in Figure 9. The effect of CO₂ on acid-washed coal is not as strong as it is with raw coal. An increase in weight loss over intermediate times is apparent, however. If increased weight loss were due primarily to the Boudouard reaction, one would expect to see the differences in weight losses evident in Figure 8 as well as increased weight loss at the longest residence time. On the other hand, a comparison between Figures 8 and 9 does show that much of the effect of CO₂ in the HPR experiments is probably due to the direct effect of CO₂ on the cations.

The results of Figures 6 and 7 can thus be explained as follows. Figure 7 shows the effect of the presence of CO₂ in the absence of the complication from cations. Initial weight loss in He/CO₂ exceeds that in He/N₂ because of a stabilizing effect of CO₂ on developing active sites on the char and/or stabilization of volatiles. An additional increase in weight loss is seen in CO₂/CO₂ because of the presence of CO₂ in the pores at the onset of pyrolysis.

Figure 6 also shows that CO_2 has a strong stabilizing effect on initially formed volatiles. Additional weight loss due to the initial presence of CO_2 in the pores is masked by the inhibitory effect of cations and by (again) the somewhat scattered nature of the He/ CO_2 data from the raw coal sample.

It has been hypothesized that CO_2 may be blocking the effect of calcium to retard weight loss through formation of CaCO_3 . In the HPR the partial pressure of CO_2 is sufficient to tie up calcium as the carbonate. In the APR the equilibrium condition is not as well-defined because of the proximity of the operating condition to the calcination condition. In He/ CO_2 atmospheres there would not be enough concentration of CO_2 in the pores initially to block the effect of the cations. The indication that a CO_2 atmosphere does enhance weight loss under these conditions thus supports an argument that CO_2 must diffuse to the surface of the coal particle rather quickly and then penetrate at least part way into the macropore space where it accelerates weight loss by blocking the effect of cations and/or by stabilizing tar/char. In the CO_2/CO_2 experiments in the APR, there is probably a high enough pressure of CO_2 in the pores initially to tie up the cations, thus accelerating weight loss. In addition, there is CO_2 present for stabilization as the first bonds in the coal matrix break, thus leading to the even greater weight loss at early residence times in this atmosphere compared to He/ CO_2 , which is most clearly seen in Figure 7.

Gas Analyses

Most experiments in the HPR had gas analyses of the product gas performed using a dedicated gas chromatograph (Carle 158S Automated Gas Chromatograph). The only peaks to appear which were large enough to measure quantitatively were those associated with CO_2 , CO, CH_4 , C_2H_6 , and C_2H_4 . It was somewhat surprising that little measurable hydrogen appeared. In addition, the C_2H_4 peak was unresolvable during pyrolysis experiments in CO_2 atmospheres due to its proximity to the CO_2 peak.

The following items are noteworthy. First, the C_2H_4 content of the product gas generally increased with increased weight loss or residence time during pyrolysis of both the raw and acid-washed samples in He. There was significantly more C_2H_4 produced at similar weight losses from the raw sample than from the acid-washed sample. This is consistent with the observation that there appears to be more cracking-type reactions occurring in the presence of the cations, since C_2H_4 is often a by-product of the cracking of larger species.

Second, both the CO and the CO_2 content are higher for comparable weight losses when cations are present during pyrolysis in He. This is consistent with the observations of Schafer (1980) in again giving a role to the cations, primarily as calcium, in creating additional carbon oxides from reactions with oxygen-containing species other than carboxyl.

SUMMARY AND CONCLUSIONS

There are two likely roles that the cations could be playing to inhibit weight loss. First, they could be attaching themselves to potential volatile species, and thereby inhibiting their release by retarding mass diffusion. Second, potential volatile species could be cracked by the cations, thereby depositing at least some of the cracked material back onto the solid surface, at least temporarily. A third possibility, also suggested by Morgan (1983) in his study, is strongly discounted here. That is that the cations are inhibiting the release of volatiles by blocking pore exits. Although this could be a minor contribution, the indication that the presence of CO_2 reverses the effect of the cations argues strongly against pore blockage being a major impediment to volatiles release. This same argument also applies, although somewhat more weakly, to the supposition that cations inhibit pyrolysis via mass diffusion. In addition, gas analyses were shown to substantiate

the hypothesis that the cations affect weight loss through cracking reactions. It was also hypothesized that flooding the pores of the devolatilizing coal with CO₂ inhibited the cracking reactions by tying up the calcium ions in a nonreactive form.

It was also shown that the presence of CO₂ enhances weight loss even in the absence of cations. This is most likely due to chemical interactions between CO₂ and the developing char surface and/or between CO₂ and reactive volatile species. The CO₂ is hypothesized to stabilize reactive sites on the surface, which in turn prevents cracking of volatiles, and/or to cap reactive volatile species such as hydrogen is believed to do during hydropyrolysis.

REFERENCES

Badzioch, S. and P. G. W. Hawksley (1970), "Kinetics of Thermal Decomposition of Pulverized Coal Particles", Ind. Eng. Chem. Process Des. Dev., 9, 521-530.

Campbell, W. D. and J. C. Slattery (1963), "Flow in the Entrance of a Tube", J. Basic Eng., Trans. Am. Soc. Mech. Eng., 41-46 (March, 1963).

Flaxman, R. J. and W. L. H. Hallett (1987), "Flow and Particle Heating in an Entrained Flow Reactor", Fuel, 66(5), 607-611.

Franklin, H. D., R. G. Cosway, W. A. Peters and J. B. Howard (1983), "Effects of Cations on the Rapid Pyrolysis of a Wyodak Subbituminous Coal", Ind. Eng. Chem. Process Des. Dev., 22, 39-42.

Freihaut, J. D., A. A. Leff and F. J. Vastola (1977), "The Combined Influence of Chemical and Physical Factors Upon Coal Particle Temperature Profiles During Rapid Heating Pyrolysis", Am. Chem. Soc., Div. Fuel Chem. Prepr., 22(1), 149-157.

Hajaligol, M. R., W. A. Peters and J. B. Howard (1987), "Intraparticle Heat Transfer Effects in Coal Pyrolysis", Am. Chem. Soc., Div. Fuel Chem. Prepr., 32(3), 8-23.

Maloney, D. J. (1983), "Effects of Preoxidation on Rapid Pyrolysis Behavior and Resultant Char Structure of Caking Coals", Ph.D. Thesis, Fuel Science, The Pennsylvania State University, University Park, PA.

Morgan, M. E. (1983), "Role of Exchangeable Cations in the Pyrolysis of Lignites", Ph.D. Thesis, Fuel Science, The Pennsylvania State University, University Park, PA.

Morrison, R. T. and R. N. Boyd (1973), "Organic Chemistry", 3rd Ed., Allyn and Bacon, Boston, MA.

Reuther, R. B. (1988), "The Effects of Pressure, Carbon Dioxide, and Cation Content on the Rapid Pyrolysis of a Lignite", Ph.D. Thesis, Fuel Science, The Pennsylvania State University, University Park, PA.

Sass, A. (1972), "The Garrett Research and Development Process for the Conversion of Coal into Liquid Fuels", paper presented at the 65th Annual AIChE Meeting, New York, NY.

Scaroni, A. W. (1979), "Kinetics of Lignite Pyrolysis in Fixed-Bed and Entrained-Flow Reactors", M.S. Thesis, Fuel Science, The Pennsylvania State University, University Park, PA.

Schafer, H. N. S. (1980), "Pyrolysis of Brown Coals. 3. Effect of Cation Content on the Gaseous Products Containing Oxygen from Yallourn Coal", Fuel, 59, 295-301.

Shu, M.-T. (1978), "Concurrent Two-Phase Flow of Gas and Coal Particle Mixtures", M.S. Thesis, Drexel University, Philadelphia, PA.

Suuberg, E. M. (1987), "The Significance of Transport Effects in Determining Coal Pyrolysis Rates and Yields", Am. Chem. Soc., Div. Fuel Chem. Prepr., 32(3), 51-58.

Tsai, C. Y. and A. W. Scaroni (1984), "Pyrolysis During the Initial Stages of Pulverized Coal Combustion", Twentieth Symp. (Int.) on Combustion, The Combustion Institute, Pittsburgh, PA, 1455-1462.

Tyler, R. J. and H. N. Schafer (1980), "Flash Pyrolysis of Coals: Influence of Cations on the Devolatilization Behaviour of Brown Coals", Fuel, 59, 487-494.

ACKNOWLEDGMENTS

This work was funded in part by the U.S. Department of Energy under contract EX-76-C-01-2030.

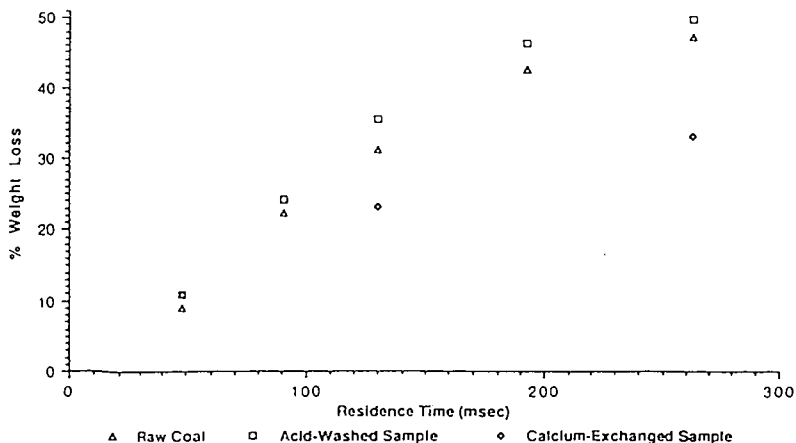


Figure 1 The Effect of Cations on Pyrolysis, P=0 psig, He/N₂ Atmosphere

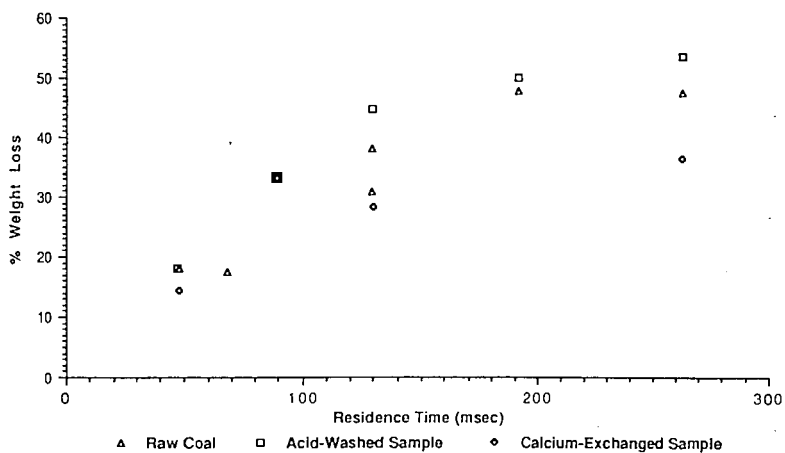


Figure 2 The Effect of Cations on Pyrolysis, P=0 psig, He/CO₂ Atmosphere

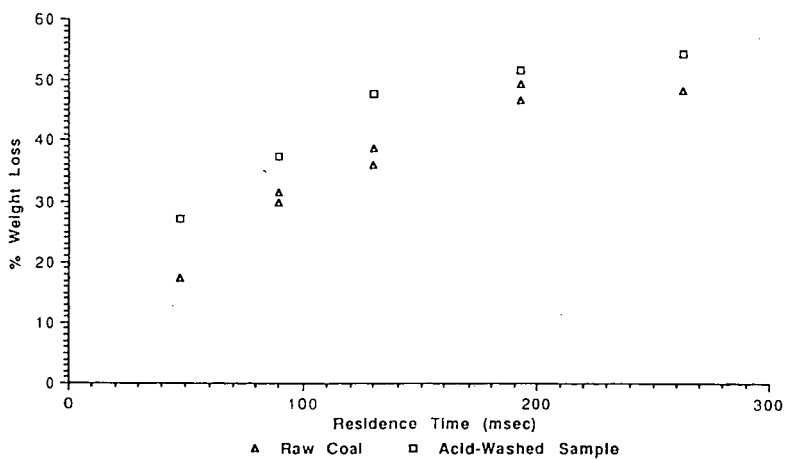


Figure 3 The Effect of Cations on Pyrolysis, P=0 psig, CO₂/CO₂ Atmosphere

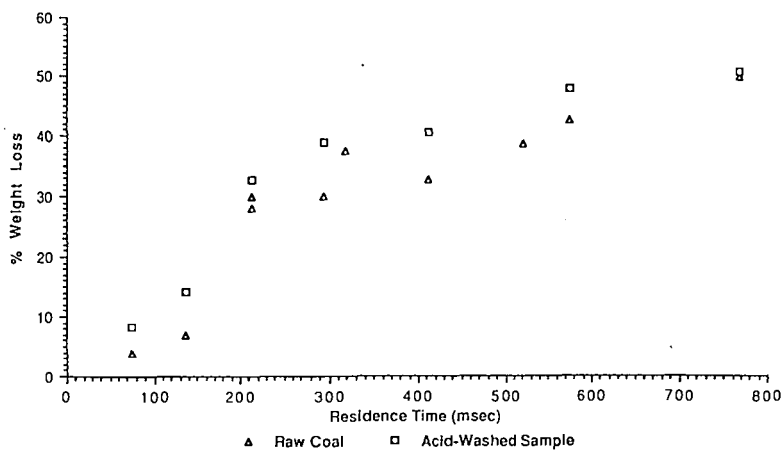


Figure 4 The Effect of Cations on Pyrolysis, P=200 psig, He/He Atmosphere

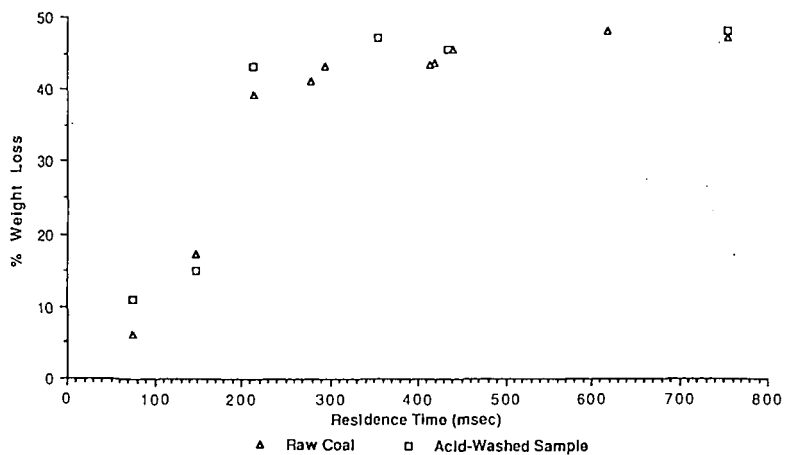


Figure 5 The Effect of Cations on Pyrolysis, P=200 psig, CO₂/CO₂ Atmosphere

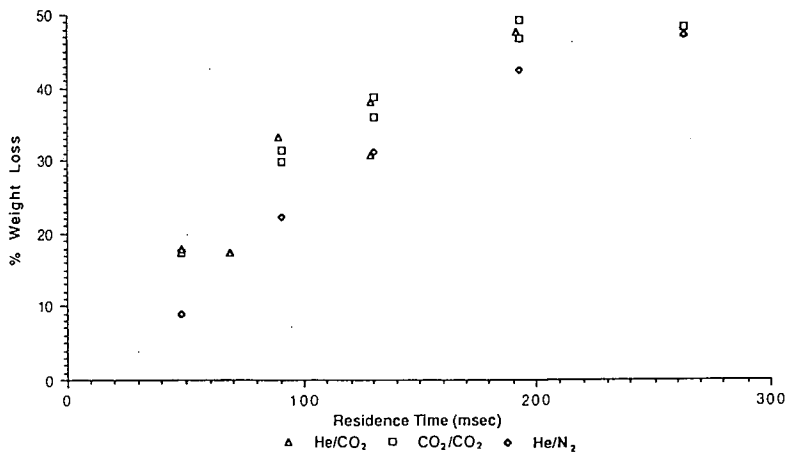


Figure 6 The Effect of Atmosphere on Pyrolysis, P=0 psig, Raw Coal

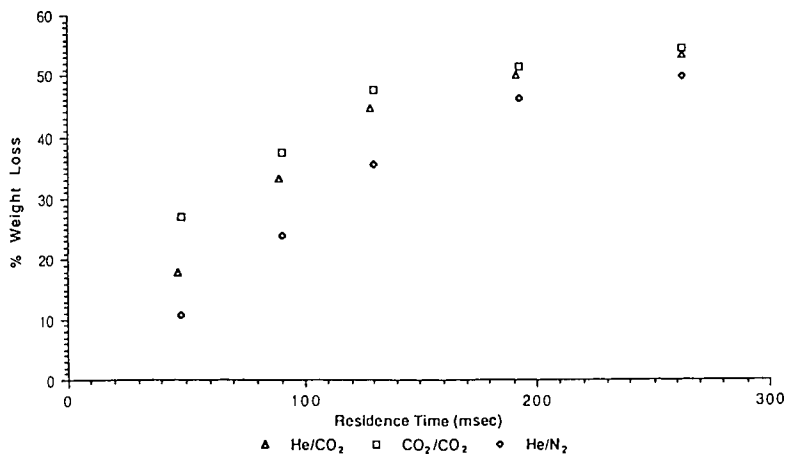


Figure 7 The Effect of Atmosphere on Pyrolysis, P=0 psig, Acid-Washed Sample

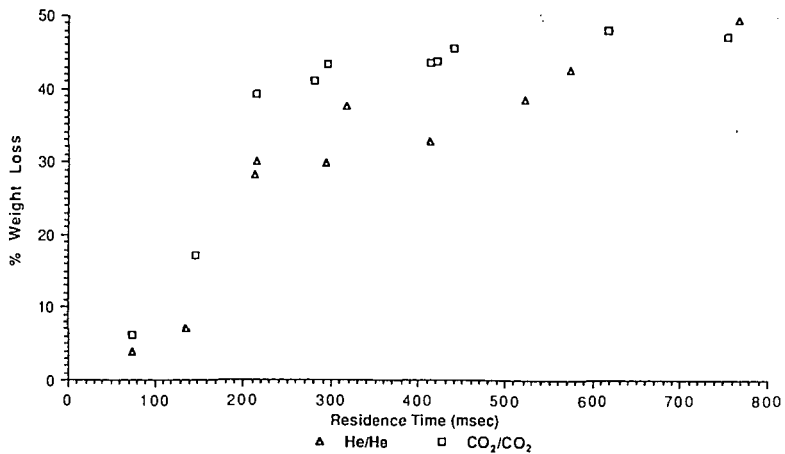


Figure 8 The Effect of Atmosphere on Pyrolysis, P=200 psig, Raw Coal

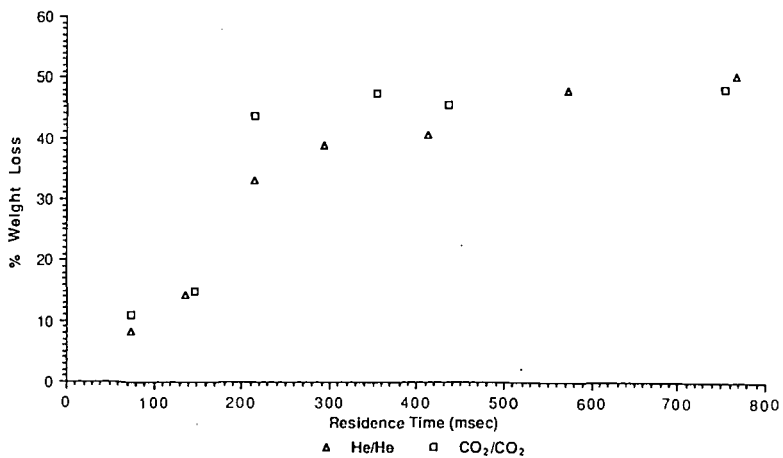


Figure 9 The Effect of Atmosphere on Pyrolysis, P=200 psig, Acid-Washed Sample

A COMPARISON OF UINTA BASIN, UTAH CRUDE OIL AND BIODEGRADED PRODUCTS

H. J. Hatcher¹, K. B. Barrett¹, K. Taghizadeh²,
D. R. Quigley¹, H. L. C. Meuzelaar²

INTRODUCTION

The Green River Formation of Wyoming, Colorado, and Utah contains a significant portion of the world's oil shale (1). In addition, the area contains large deposits of tar sands and bituminous rocks, particularly in the Uinta Basin of Utah. Commercialization of coal, oil and gas deposits are important in the economy of Utah.

The Green River Formation is considered to be rather unique in character because it has been spared extensive disruption from the forces of temperature, pressure, and fracture (2). It has probably been more thoroughly studied by organic geochemists than any other formation in the world. However, the microbiology of the formation and its relationship to hydrocarbon transformations has not been extensively investigated.

The importance of microbial activity to fossil fuel hydrocarbon transformations is widely recognized (3). The metabolic activities of the microflora over a period of time can contribute to changes in pH and redox potential which, in turn, can significantly alter the geological environment (3). These changes need not be directly involved with hydrocarbons. Sulfate-reducing anaerobic bacteria do not metabolize hydrocarbons but can, in the presence of oxygen-consuming aerobic bacteria, actively reduce sulfate to sulfide (4). A case in point is growth of anaerobic *Desulfovibrio* sp. under growth of aerobic *Beggiatoa* sp. Thiobacilli can also contribute significantly to acidification of the environment. As a consequence, sulfur and metal availability can be significantly altered thereby changing the course of subsequent hydrocarbon-generating events.

Most investigators have found that the first hydrocarbons removed from crude oil by bacteria are n-alkanes followed by alicyclics, aromatics, and acyclic isoprenoids (5). Disagreement exist regarding biodegradation of steranes and to a lesser extent hopanes. Nevertheless, it is agreed that biodegradation of a crude oil leads to another oil having a lower API gravity and greater chemical stability (6). Some evidence has been presented that suggests that paraffinic crude oils are precursors of heavy to medium-gravity naphthenic crude oils (7). Observations indicate that primary paraffinic crude oils are expelled from deep source beds. Before, during, or after a generally upward migration, the paraffinic crude is transformed microbiologically into a naphthenic crude oil. In another investigation (8) biodegradation decreased API gravities of a group of common-source crude oils and tar sands 8-fold, increased sulfur 3-fold, and metal content 6-fold. Hydrocarbon content was altered with n-alkanes, isoprenoids light aromatics, and light thiophenes completely removed (8). In

-
1. Idaho National Engineering Laboratory, Center for Bioprocessing Technology and Biotechnology Unit. P.O. Box 1625, Idaho Falls, ID 83415.
 2. Center for Micro-Analysis and Reaction Chemistry, University of Utah, Salt Lake City, Utah.

in severely degraded samples steranes were partially removed while triaromatic steranes and diasteranes were resistant to biodegradation. In a long term study of the effects of a fuel spill on the microbiology of an agricultural soil, biodegradation of the fuel was achieved (9) after three years. Coryneform bacteria and certain fungi were responsible for hydrocarbon degradation. The most active fungi in hydrocarbon degradation were Aspergillus and Penicillium sp.

EXPERIMENTAL

Sample Sources and Procedures

Samples of oil shale were collected from Hell's Hole Canyon in Utah, the C-b Tract Mine in Colorado, and the Southman Canyon area in Utah. Tar sands were collected from Asphalt Ridge in Utah. Gilsonite was collected from the Bonanza area of Utah. Petroleum samples were collected from the Red Wash Oil Field and the Altamont-Bluebell Oil Field in Utah. Solid samples were placed in plastic bags and water samples in sterile plastic tubes. The samples were transported to the Idaho National Engineering Laboratory Research Center in Idaho Falls, Idaho for microbiological studies. Samples designated for pyrolysis gas chromatography/mass spectrometry studies were sent to the Center for Micro-Analysis and Reaction Chemistry, University of Utah, Salt Lake City, Utah.

Microbial Isolation, Identification and Maintenance Procedures

Samples of solid materials were carefully cleaned and the inner surfaces exposed. The inner surfaces were scraped and the scrapings placed on trypticase-soy agar medium in petri dishes. Aqueous samples were streaked on the medium. The medium was incubated aerobically and anaerobically at about 25°C for seven to fourteen days. Colonies were examined for morphology and slides were prepared for microscopic examination. After culture purity was assured, cultures were maintained on trypticase-soy agar.

Identification of cultures was based on API Procedures (API Laboratory Products, 8114 Trans Canada Highway, Suite B, St. Laurent, Quebec H4S 1M5).

Model Compound Utilization Procedures

A basal salts medium was added to screw-cap test tubes and sterilized by autoclaving at 121°C for 20 minutes. The compound to be investigated (Table 2) was added at 0.1% concentration after sterilization. The tubes were inoculated using a pure culture and incubated at room temperature as roller tubes at about 10-20 revolutions per minute. The tubes were examined daily for growth as shown by turbidity in the tubes. Response was graded as 1+ to 4+ (poor to best).

Petroleum Utilization Studies

These were carried out much as the model compound investigation except that cultures were prepared in Erlenmeyer flasks and petroleum was added at 1% concentration. Cultures were incubated at 30°C on a rotary shaker operating at about 20 revolutions per minute.

Pyrolysis Gas Chromatography/Mass Spectrometry (Py GC/MS)

Py GC/MS analyses were carried out at the University of Utah Center for Micro-Anlysis and Reaction Chemistry, University of Utah, Salt Lake City, Utah.

A basic Curie-point Py GC/MS technique was used with a Curie-point filament temperature of 610°C(10). The gas chromatography was conducted using a Hewlett-Packard 5890 instrument with a 15 meter DB-5 column heated at 40° to 320°C, 10°C/minute. An ion-trap detector was used and a Finnigan Mass Spectrometer.

RESULTS AND DISCUSSION

Microbiological Characterization

Genera of bacteria isolated from samples are listed in Table 1. Coryneform bacteria are not listed individually because the members of this group are difficult to classify. At present it is believed that four genera are represented: Arthrobacter, Corynebacterium, Nocardia, and Rhodococcus. However verification is still pending. Only coryneform bacteria could utilize hydrocarbons and heterocyclic compounds provided as carbon sources. All coryneforms were isolated from within bitumen-containing rock and none from water associated with the rock.

Cell counts of coryneforms were at the 10^4 to 10^5 cfu/gm level. Table 2 shows the performance of the six coryneform isolates which grew best on the model substrates. Not all coryneforms could utilize these materials. In some cases, growth of the isolate was difficult to maintain and some were lost, consequently, some tests could not be completed. It is noteworthy that t-butylcyclohexane was poorly utilized. Apparently, the branched alkyl substituent on the cyclohexane ring inhibited utilization. The result is in accord with experiences with such compounds as branched alkyl benzene sulfonates, notorious in the detergent industry for resistance to biodegradation. The position of the methyl group on the alkyl chain may be significant. Isoprenoid substituents on structures such as steranes are apparently degraded.

During the course of this work, it was observed that certain differences existed between microorganisms and their capability to grow on the model compounds. The wild strains of coryneform bacteria were generally more capable of growing on the unusual substrates provided than laboratory strains obtained from commercial culture collections. The point is significant for those who would study fossil fuel degradation by microorganisms. Figure 1a compares the growth of a laboratory Arthrobacter with oil shale isolate OS-2 on pristane. Figure 1b compares laboratory Nocardia sp. with oil shale-isolate OS-2 and gilsonite-isolate G2 on the heterocyclic compound ethyl nipecotate. Growth was measured by turbidity. In Figure 2a and 2b, a laboratory strain of Arthrobacter is compared with gilsonite-isolate G2 growing on pristane. Growth was measured by oxygen consumption. OS-2, the wild strain, in these and other growth experiments, required several days of adaption before rapid growth occurred. The response suggested that enzyme induction was necessary. In contrast, G-2, also a wild strain, consistently showed immediate growth on substrates provided suggesting constitutive enzyme formation.

Petroleum Biodegradation

Figure 3a is a GC/MS chromatogram of a waxy crude oil (Bluebell Control), Figure 3b is a chromatogram of the petroleum residue of the oil after degradation by the oil shale-isolate OS-3. The residue primarily consists of isoprenoid components, with almost complete removal of n-alkanes. Figure 3c is a chromatogram of the petroleum residue after degradation by an isolate from oil shale kerogen. The residue consists of isoprenoid and triterpenoid components. Similar results for biodegradation are shown in GC/MS chromatograms for the waxy Red Wash petroleum in Figure 4a. The undegraded petroleum is primarily paraffinic in character. Degradation by the oil shale-isolate OS-3 (Figure 4b) and the gilsonite-isolate G-2 (Figure 4c) gave residue chromatograms showing primarily triterpenoid compounds remaining.

Figure 5a is a GC/MS chromatogram of an asphaltic petroleum. Degradation of the oil by the tar sand-isolate TS-8 (Figure 5b) and the oil shale-isolate OS-2 (Figure 5c) gave residues containing similar components. Pristane and phytane (shown in the 795 and 860 positions) were only partially degraded. The same is true for triterpenoids in the 1400-1600 position. The large peak in the 1760 region corresponds to perhydro- β -carotene (2). This substance seems resistant to biodegradation.

CONCLUSION

Coryneform bacteria can play a significant role in crude oil biodegradation. The capability of these bacteria for hydrocarbon degradation varies between individual bacteria and between the specific forms of hydrocarbon attacked. Tri- and tetraterpenoid compounds are resistant to degradation. Consequently, oil degraded in the laboratory tends to assume the mature character observed under natural conditions.

ACKNOWLEDGMENT

This work was supported under Contract No. DE-AC07-76ID01570 from the U.S. Department of Energy to the Idaho National Engineering Laboratory/EG&G Idaho, Inc.

REFERENCES

1. W. E. Reed. 1977. "Molecular Compositions of Weathered Petroleum and Comparison with Its Possible Source." Geochemica et Cosmochemica Acta 41:237-247.
2. M. T. Murphy, A. McCormic, G. Eglinton. 1967. "Perhydro- β -Carotene in the Green River Shale." Science 157:1040-1042.
3. J. R. Hills, G. W. Smith, E. V. Whitehead. 1970. "Hydrocarbons from Fossil Fuels and Their Relationships with Living Organisms." Journal of the Institute of Petroleum 56(549):127-137.
4. A. M. Jobson, F. D. Cook, D. W. S. Westlak. 1979. "Interaction of Aerobic and Anaerobic Bacteria in Petroleum Biodegradation." Chemical Geology 24:355-365.

5. N. S. Goodwin, P. J. D. Park, A. P. Rawlinson. 1981. "Crude Oil Biodegradation under Simulated and Natural Conditions." Advances in Organic Geochemistry. John Wiley and Sons. pp. 650-658.
6. N. J. L. Bailey, A. M. Jobson, M. A. Rogers. 1973. "Bacterial Degradation of Crude Oil: Comparison of Field and Experimental Data." Chemical Geology 11:203-221.
7. G. T. Philippi. 1965. "On the Depth, Time, and Mechanism of Petroleum Generation." Geochemica Et Cosmochemica Acta 29:1021-1049.
8. D. E. Miiller, A. G. Holba, W. B. Hughes. 1984. "Effects of Biodegradation on Crude Oils." AAPG Studies in Geology #25. Research Conference. Santa Maria, CA. October 29-November 2, 1984, pp. 233-241.
9. J. Oudot, P. Fusey, D. E. Abdelouahid, S. Haloui, M. F. Roquebert. 1987. "Capacities Degratives de Bacteries et de Champignons Isoles Contamine par un Fuel." Can. J. Microbial. 33:232-243.
10. H. L. C. Meuzelaar, W. Windig, J. H. Futrell, A. M. Harper, S. R. Larter. 1982. "Pyrolysis Mass Spectrometry and Multivariate Analysis of Several Key World Oil Shale Kerogens and Some Recent Alginites." ASTM Special Technical Publication 902. T. Aczel, Ed. pp. 81-105.

TABLE 1. IDENTIFICATION OF BACTERIAL ISOLATES

<u>Source</u>	<u>Group or Genus</u>	<u>Number of Isolates</u>
Oil shale	Coryneform, <u>Aeromonas</u> <u>Flavobacterium</u> <u>Streptomyces</u>	7
Tar sands	Coryneform	6
Gilsonite	Coryneform	3
Oil shale-Mine water	<u>Pseudomonas</u> <u>Aeromonas</u> <u>Flavobacterium</u> <u>Desulfovibrio</u> <u>Beggiatoa</u>	6

TABLE 2. MODEL COMPOUND

Isolated Bacteria (<u>Coryneform</u>)	<u>Cyclohexanol</u>	<u>Ethyl Nipeotate</u>	<u>Methyl Nipeotate</u>	<u>Ethyl-1 Nipeotate</u>	<u>Hexadecane</u>	<u>Pristane</u>	<u>Tert-butyl Cyclohexane</u>
G-2	±	4+		3+	3+	2+	-
OS-2	3+	2+		2+	3+	3+	±
OS-3	3+	ND		ND	ND	3+	ND
TS-6	3+	-		-	1+	-	1+
TS-7	2+	ND		ND	3+	2+	±
TS-8	2+	ND		ND	ND	3+	ND

ND = Culture not viable for test.

FIGURE 1a Growth Curve for Arthrobacter #15590 and OS2 + Pristane

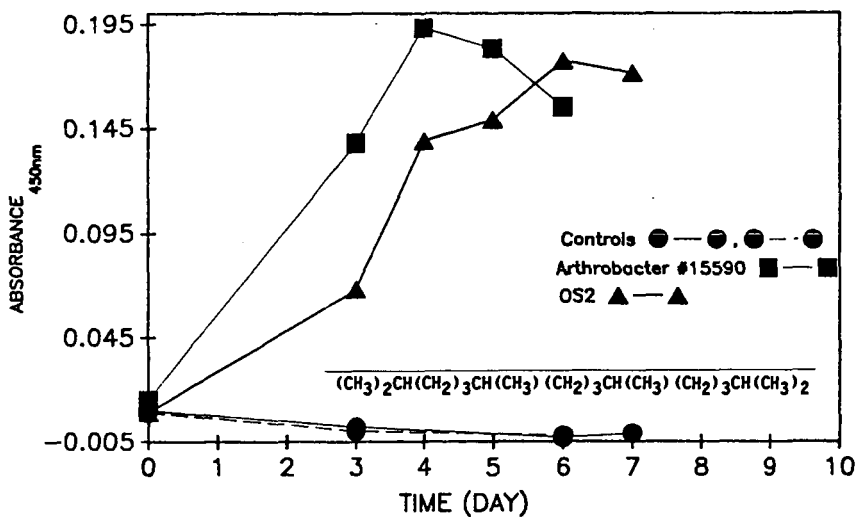
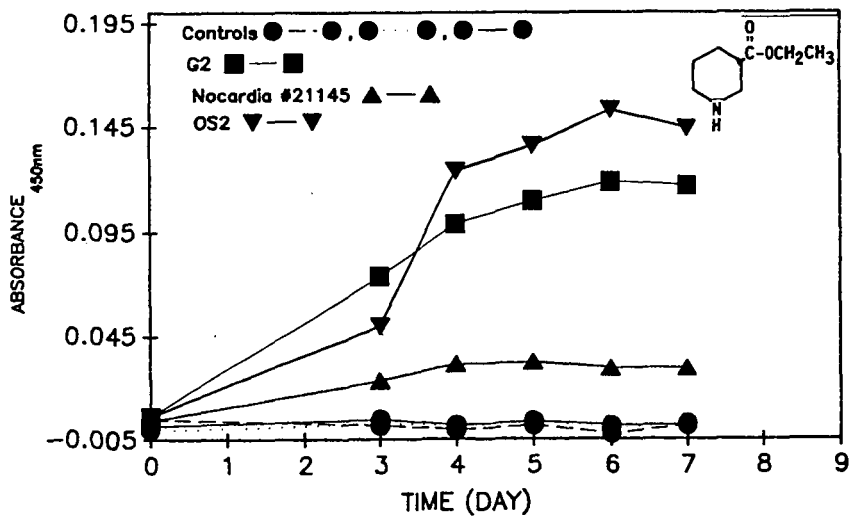


FIGURE 1b Growth curve for Nocardia #21145, G2, and OS2 + Ethyl Nipacotole



RESPIROMETER STUDIES

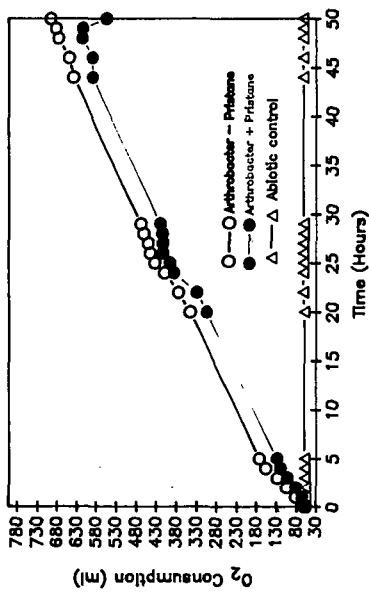


Figure 2a

RESPIROMETER STUDIES

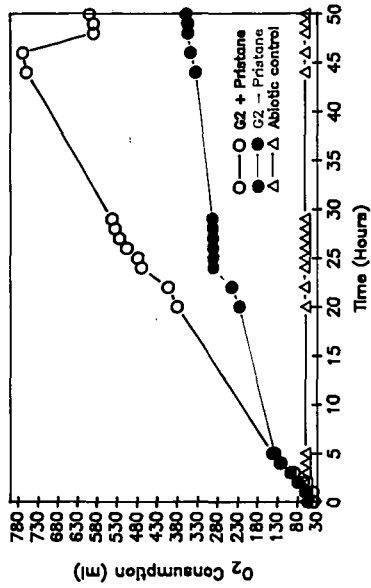


Figure 2b

FIGURE 3

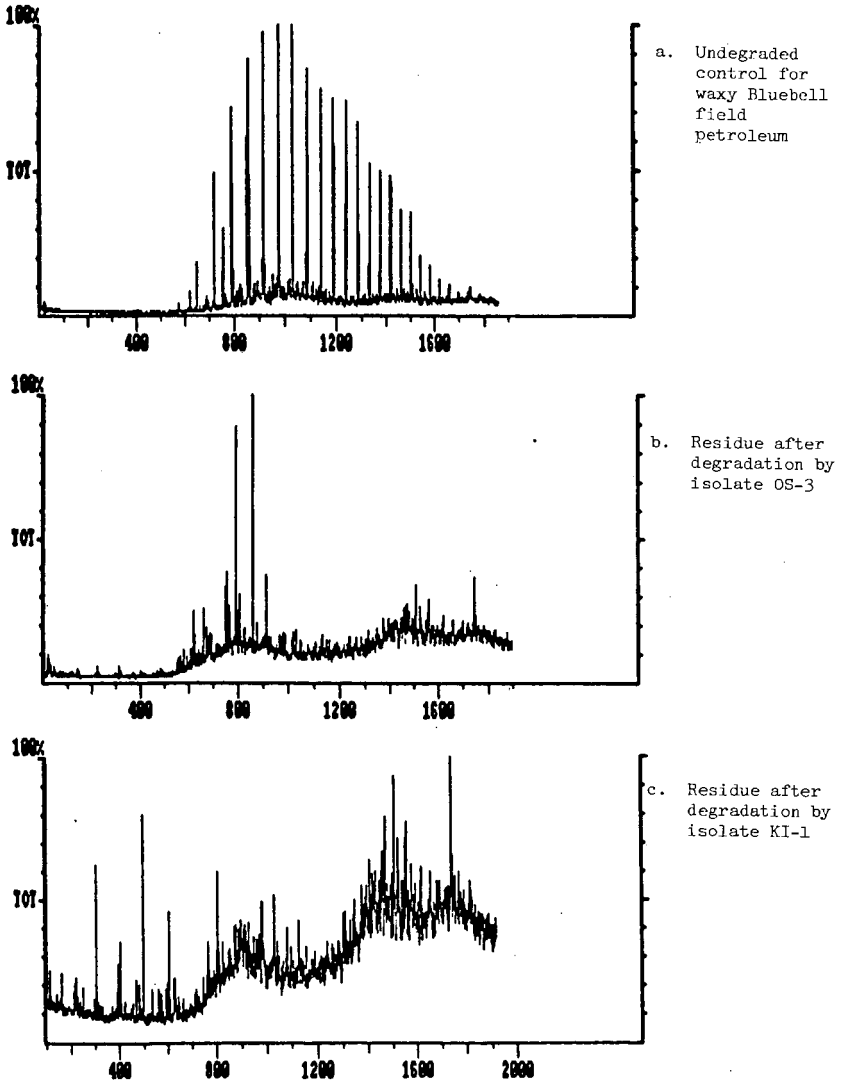


FIGURE 4

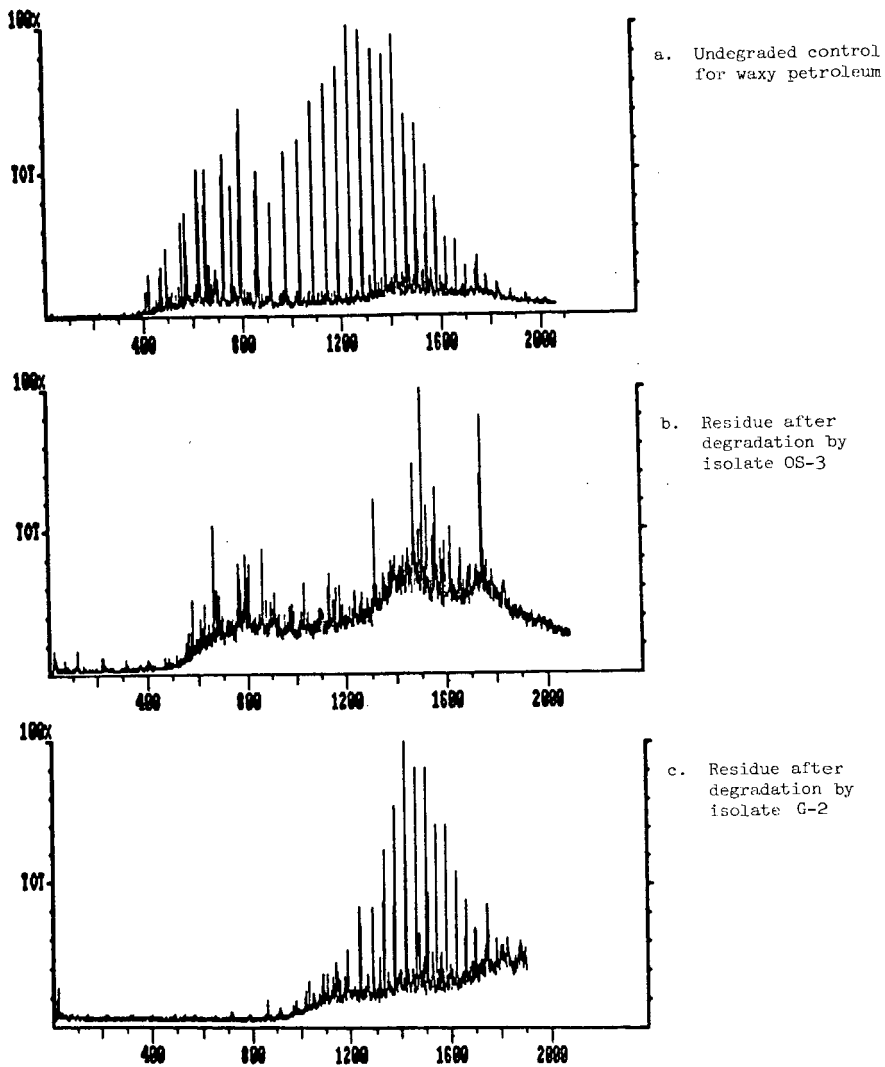
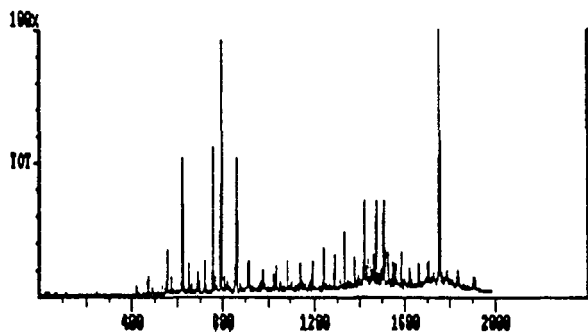
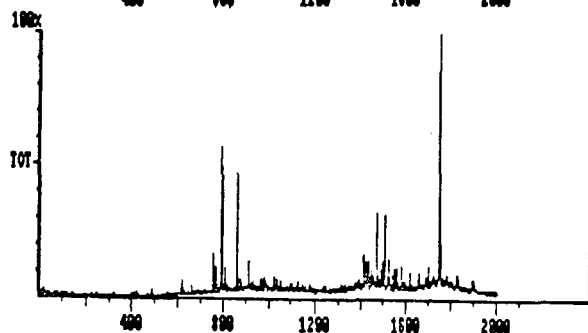


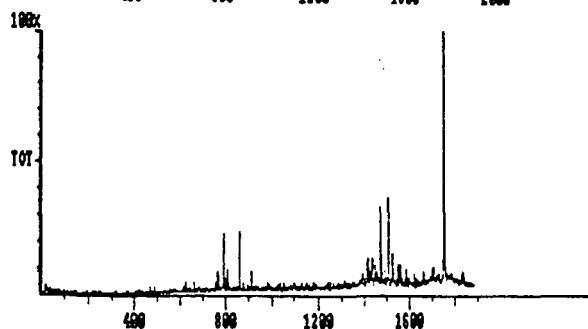
FIGURE 5



a. Undegraded control for asphaltic petroleum



b. Residue after degradation by isolate TS-8



c. Residue after degradation by isolate OS-2

**ALL-SYNTHETIC DIESEL FUEL FROM ATHABASCA BITUMEN:
PROPERTIES, TESTING AND OPERATING EXPERIENCE**

by

W.W. Almdal, R.P. Kirchen, S.N. Lau, E.C. Sanford
Syncrude Canada Limited
Box 5790, Station L, Edmonton, Alberta, Canada, T6C 4G3

and

S.J. Hinkle
Detroit Diesel Corporation
13400 Outer Drive West
Detroit, Michigan, 48239-4001

Syncrude Canada Ltd. operates an integrated oil sands plant in the Athabasca region in northern Alberta. Oil sand is extracted and the separated bitumen is upgraded by a combination of coking and hydrocracking processes. Distillates are hydrotreated to produce synthetic crude oil, which is shipped by pipeline to refineries for further processing and blending. Daily production of synthetic crude oil is approximately 23,850 m³ or 150,000 bbl (1988 daily average production).

Throughout the plant, 125,000 liters/day of diesel fuel are being consumed. Heavy haulers (170 tons, 33 units) operating in the oil sands mine are major consumers, although an appreciable amount of fuel is also used to power a variety of other units. Historically, diesel fuel was purchased from commercial sources. An opportunity to reduce operating cost by substituting the purchased fuel (45 million liters/year) with a plant derived synthetic material was identified.

Typically, during the production and refining of diesel fuel, its chemical and physical properties are modified and adjusted by blending in order to meet specifications. The blending option was not available in this case where the direct use of an existing plant stream was proposed. Although several studies and tests were reported on synthetic materials of this type, more information was needed for assuring the economical and reliable operation of a large fleet under extreme temperature conditions.

Chemical, physical and ignition properties of the all-synthetic fuel were measured and compared to conventional fuels and to diesel fuel specifications. The fuel was also tested on heavy-duty diesel engine test rigs. Following this fuel evaluation study, the fuel was approved by Syncrude for use on its equipment at its oil sands plant. The switch to all-synthetic diesel fuel took place in the spring of 1988.

Properties, test results and operating experience with Athabasca bitumen derived diesel fuel will be discussed.

Results and Discussion

Athabasca bitumen is extracted from the sand matrix by the hot water process. It is then subjected to thermal cracking in fluid cokers (1). Distillate cuts are individually hydrotreated and the hydrotreated streams are blended to form synthetic crude oil (SCO) product. This is transported by pipeline to

refineries for further processing and blending. Properties of the bitumen feedstock and of the synthetic crude oil are shown in Table 1.

The stream identified for diesel fuel use is derived from a unit which prepares naphtha needed as a diluent in the extraction process. The diluent preparation unit uses a hydrotreated distillate as feed and separates the naphtha diluent. It is the bottoms stream of this distillation which was identified as a potential diesel fuel. Although a distillation residue, this stream is quite light and highly refined, due to its prior processing. It is typically blended back into the synthetic crude oil product. Hence, the proposed fuel is readily available as part of normal plant operation (Figure 1). Properties of this stream are shown in Table 2, together with those of typical commercial diesel fuels. The corresponding boiling curves are shown in Figure 2.

The boiling curve of the all-synthetic material (Figure 2) is similar to that of commercial winter diesel fuel, which is the lighter of the three seasonal fuel blends typically used in northern Alberta (Table 2). Because this stream is, in fact, a "by-product" of an existing operating unit (diluent preparation unit), it is not practical to seasonally adjust the boiling range.

Chemical and physical properties of this stream reflect its synthetic origin and its processing history. In this list, deviations from specifications or from typical values observed for conventional fuels are indicated: + indicates an advantage for the synthetic fuel. Specifically, the following properties reflect the origin: low cloud (+) and low pour points (+), low cetane number (-) and low aniline point (-). Conversely, the following properties reflect the hydrotreating severity: low values for ash, sulfur, corrosion, acidity, carbon residue and water/sediments, good color (all +) and low viscosity (+/-).

Of these properties, two are discussed in greater detail: cetane number and viscosity.

Current Canadian diesel fuel specifications (Table 3) and minimum engine manufacturer's requirements for cetane number is 40 (ASTM D613); the measured value for the all-synthetic fuel was 31-32. However, the cetane number of a fuel can be improved by doping with an ignition improver. Typically, an alkyl nitrate is used, although other compound classes were also studied (2). Response of the all-synthetic fuel to the addition of a commercial ignition improver is shown in Figure 3. A cetane number of 40 was reached by doping the synthetic fuel with approximately 0.3% ignition improver. This is in the same range as measured in an earlier study (3) with Athabasca derived diesel fuel. The proposed "1990 Canadian specifications" (4) are met by doping with only 0.15 wt% additive.

Viscosity of a fuel is often linked to its lubricating properties or lubricity. The fuel injection system of a diesel engine relies on the fuel it is pumping for lubrication.

Viscosity of the material under investigation was low and similar to that of commercial winter fuel. Low viscosity is usually equated with low lubricity. However, there are reports (5, 6) indicating that this proportionality might only hold for fuels of similar origin, composition and processing history.

Therefore, it was desirable to obtain a direct, viscosity-independent measure of the lubricating properties of this material. This was done by using the "Ball on Cylinder Lubricity Evaluator" (BOCLE) test method (7, 8). Lubricity of the synthetic material was similar to that of commercial winter diesel fuel. Response of the synthetic fuel to the addition of lubricity improver was also

investigated. Lubricity of intermediate season fuel was reached by doping with approximately 50 ppm of commercial lubricity improver.

In summary, many of the properties of the all-synthetic fuel are similar to those of commercial diesel fuels, and in particular to winter diesel. In fact, only properties related to cetane number and lubricity are at variance. And, as shown, the fuel also responds well to the addition of additives, if this is desired. However, is the addition of additives needed, and what are the benefits obtained by doing so?

By definition, fuel specifications represent a body of chemical and physical properties that has proven sufficient to qualify a fuel. These correlations between chemical/physical data and engine performance are based on a database obtained with conventional fuels. Is the same set of chemical/physical data also sufficient (or is the full set indeed needed) to qualify a material of 100% synthetic origin? The significance of this issue can probably best be appreciated by considering the fact that even the specifications are subject to occasional review (4).

In the absence of a database covering operating experience with synthetic fuels, and to address the issue of actual engine performance, the properties of this fuel were reviewed with engine manufacturers. Based on these discussions, an engine durability test was performed at Detroit Diesel Corporation's test facility. In addition, dynamometer tests combined with emission measurements were also carried out. For the durability test, one cylinder bank of a 149 series heavy-duty engine was operated on synthetic fuel, whereas the other bank was run on conventional fuel. The engine was fully performance instrumented and was operated at various power settings, including elevated power output for more than 500 hours. Also, to obtain data truly indicative of the all-synthetic fuel, it had been agreed to run this test without any additive.

As part of the durability test, the engine was disassembled and its components were inspected. Overall, test results were definitely in favor of the all-synthetic fuel, in terms of operating parameters, as well as component wear. As indicated above, this test was run with no additives.

Eleven mode steady state emission tests revealed a measurable reduction in NO_x and CO for the all-synthetic fuel as compared to #2 diesel fuel. Further emission testing with the all-synthetic fuel and #1 diesel fuel on the U.S. Federal Transient Emission Test showed a 10% reduction in brake specific particulates. However, for this transient cycle test with the lighter #1 diesel fuel, the measurable reduction in NO_x and CO was nullified; indeed, the trend reversed itself and a slight increase in CO and NO_x was measured.

Since the all-synthetic fuel has very little sulfur content (0.01 wt %), the SO_2 emissions from engines burning the all-synthetic fuel were consistently lower and this was likely a contributor to the lower brake specific particulate measurement. Low sulfur content also has a beneficial impact on sulfur induced corrosion of engine components.

Brake specific fuel consumption (LB/BHP-HR) was moderately higher (2%) for the all-synthetic fuel relative to #1 diesel fuel. This is likely related to the fuel spray of the less viscous all-synthetic fuel. This hypothesis is supported by test runs on various internal injector components which yielded a greater sensitivity to these changes than did #1 diesel fuel or kerosene. However, addition of ignition improver additives may provide an offset for this slight performance loss.

In view of the extreme low temperatures (-40°C) measured at the plant site during winter, cold weather performance of any diesel fuel used at this location is of crucial significance. Two factors to be considered here are the fluidity and the ignition properties of the fuel at these temperatures. Good performance in both areas is typically associated with diverging trends in chemical composition. Indeed, n-alkanes which are thought to promote good ignition, tend to solidify and form wax particles at low temperatures.

As part of an earlier study, field tests at temperatures down to -28°C had been carried out. A variety of engines with power ratings from 200 to 870 HP were used. For low temperature tests, ignition improver (0.3 vol %) had been added. At temperatures above freezing no ignition improver was added. No non-starts were observed (9).

As part of the present study, additional startability tests at even lower temperatures were carried out at Detroit Diesel Corporation's test facility. One engine was equipped with an electronic fuel injection system (Detroit Diesel Corporation - DDEC II) and glow plug heads. A second engine of similar design, with flow plug heads but mechanical injector system was also tested.

It was shown that, at -46°C, the engine equipped with electronic injection started in 12 seconds when using the synthetic fuel with a small amount of ignition improver added to enhance the cetane number to 40 cetane. Without this ignition improver and at 32 cetane number, this all-synthetic fuel started at -43°C in 23 seconds. However, the other engine equipped with the mechanical injection system and using the 32 cetane synthetic fuel was unable to start at -4°C until small quantities of ether were injected. This engine was cranked in excess of 275 seconds with glow plug assist prior to the injection of the small amount of ether. Even with the ether injection, a considerable crank time (179 seconds) was required for the mechanical injection start.

These results can be interpreted as follows. Electronic fuel injection appears to play a significant role, at least under the conditions of this test. More work is still planned to investigate this observation. The nature of the synthetic fuel is definitely a strong contributing factor, considering that non-starts with conventional fuels are not unusual at these conditions. We feel that the unusually low pour point and cloud point (-66 and -61°C respectively), as well as the low viscosity of the all-synthetic fuel allow the fluidity and atomization into fine fuel droplets to be maintained even at these extreme temperatures, thereby ensuring fuel ignition. However, these fuel properties alone are not sufficient in some applications to provide ignition of the non additive added fuel (32 cetane), as shown by the tests with the engine equipped with a mechanical injection system.

In practical terms, the low temperature test results confirm that the synthetic fuel is an excellent blendstock, mainly because of its high fluidity at low temperature. Taken alone, without further blending or addition of ignition improvers, it is a good fuel at moderate temperatures for all the engines tested. However, its low temperature performance is affected by the type and design of the individual engines, particularly in the case of naturally aspirated low compression engines.

Almost all the engines at the Syncrude plant site have a mechanical injection system. Furthermore, the fleet includes low and high compression engines, as well as naturally aspirated and super/turbocharged engines.

On the basis of this fuel evaluation study, the all-synthetic fuel was approved by Syncrude for plant-wide use, on Syncrude owned equipment, at its oil sands

plant. The switch to synthetic fuel occurred in the spring of 1988. Throughout most of the year, the fuel is essentially used as it becomes available from the diluent preparation unit, without further processing.

Specifically, no ignition improver is added during this period. However, on the basis of the low temperature tests, the cetane number is raised during the winter months by the addition of cetane improver. Although this may not be required for all the engine types of the fleet, logistics are less complex when only one type of fuel is used at any time.

Government regulations require the addition of an approved dye. Furthermore, to prevent the build-up of static electricity, a conductivity additive is added. These materials are added together as a blend. Cost of these two additives is not a significant factor. Lubricity improver additive is not added.

Conclusions

Physical, chemical and ignition properties of an all-synthetic material derived from Athabasca bitumen were measured with respect to its use as a diesel fuel. This stream is readily available as part of the production of synthetic crude oil, and as such is not specially blended or processed for diesel fuel use.

Many properties of the synthetic fuel are similar to conventional diesel fuel, particularly to winter diesel. Cloud point and pour point show a significant advantage over conventional fuels and exceed requirements set by fuel specifications. Cetane number and viscosity are lower than for conventional fuels and specifications.

Fuel specifications were developed on the basis of operating experience with conventional fuels, whereas this is an all-synthetic fuel. In the absence of a similar database specifically addressing operating experience with synthetic fuels, performance and durability tests on heavy-duty diesel engine test rigs were carried out.

The synthetic fuel is being used, on Syncrude owned equipment, plant-wide at Syncrude's integrated oil sands plant. Throughout most of the year, unmodified fuel is used. Only during the winter months is a higher cetane number required, particularly for naturally aspirated low compression engines. This can be achieved by addition of ignition improver.

Further studies are in progress to optimize the low temperature performance of the fuel.

Acknowledgments

The authors would like to acknowledge the contributions of their co-workers and members of the investigating teams. We thank Syncrude Canada Ltd. and Detroit Diesel Corporation for granting permission to publish this paper.

References and Notes

1. Since this study was carried out, a 40,000 bpd hydrocracker was integrated into the primary upgrading process. Fresh bitumen is fed to this hydrocracker. Distillates are routed to the hydrotreaters, whereas hydrocracker pitch is blended into the coker feed stream.

2. Bowden, J.N., Frame, E.A., "Effect of Organic Sulfur Compounds on Cetane Number", *Ind. Eng. Chem. Prod. Res. Dev.*, v. 25, p. 156-159 (1986).
3. Cooley, J.M., Nowlan, V.J., Tan, F.O., unpublished data (1980).
4. Whyte, R.B., Gardner, L., "Update on Canadian Fuel Trends", SAE paper 841403, Fuels and Lubricants Meeting and Exposition, Baltimore, Maryland, Oct. 8-11, 1984.
5. Wei, D., Spikes, H.A. "Lubricity of Diesel Fuels", *Wear*, 111, p. 217 (1986).
6. Appeldorn, J.K., Dubek, W.G. "Lubricity of Jet Fuels", report SAE660712, 1966, Society of Automotive Engineers, Warrendale, Pennsylvania.
7. Coordinating Research Council, Inc. "Aviation Fuel Lubricity Evaluation" CRC report No. 560 (1988) Atlanta, Georgia, 30346.
8. The test was performed by Ethyl Petroleum Additives Ltd., Bracknell, U.K.
9. Houghton, R.E. "Utilization of Synthetic Duesel Fuel in Mobile Equipment: Syncrude Case History", American Society of Mechanical Engineers, Energy Resources Technical Conference, Houston, Texas, 1983, paper 83-DGP-5, 4 pp.

Bitumen

d (g/mL)	1.02
API	7.7
C (wt %)	88.3
H (wt %)	10.4
N (ppm)	5000
S (wt %)	4.5 - 5.0
Ni (ppm)	70
V (ppm)	200
Asphaltenes (C5)	17
+524°C (vol %)	59

Synthetic Crude Oil

API Gravity (API)	31.4
Total Sulfur (wt ppm)	1500
Total Nitrogen (wt ppm)	623
99% Point (°C)	516

Naptha (C5 - 177°C)

API Gravity	64.4
Total Sulfur (wt ppm)	5.0
Total Nitrogen (wt ppm)	0.9

Light Gas Oil (177 - 343°C)

API Gravity	29.8
Total Sulfur (wt ppm)	428
Total Nitrogen (wt ppm)	126

Heavy Gas Oil (343°C+)

API Gravity (API)	18.6
Total Sulfur (wt ppm)	3430
Total Nitrogen (wt ppm)	1470

Table 1: Typical Properties of Athabasca Bitumen and of Synthetic Crude Oil

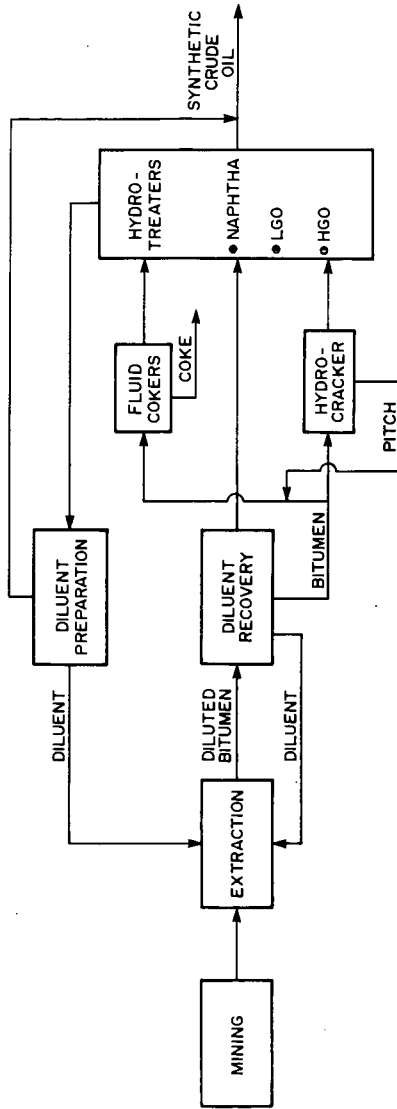
	Synthetic Diesel	Summer Diesel	Fall/Spring Diesel	Winter Diesel
d (20°C):	0.837	0.860	0.845-0.850	0.816
API:	36.8-37.8	33	35-36	42
Visc Kinemat (40°C):	1.28	2.0-4.1	1.4-2.4	1.3-2.1
Saybolt SUS (100°F):				
S wppm:	75			
Dist (D-86), IBP:	162			
10%:	174	238	215	215
50%:	199			
90%:	243	360	324	315
FBP:	278	385	338	319
Flash Point (°C):	52	45	45	45
Cloud Point (°C):	-61	0	-35	-40
Pour Point (°C):	-66	-7	-40	-45
Cetane Index:		43	43	43
Cetane Number:	31.6	40 (up to 45)	40 (up to 45)	40 (up to 45)
Aniline Point (°C):	40.6	62	57	58
Water + Sedim. (vol %):	0.00			
C-Resid, 10% bott (wt %):	0.005			
Ash (wt %):	0.00			
Copper Corrosion:	1a	0.5-1.5	0.5-1.5	0.5-1.5
Acidity (mg KOH/g):	0.00			
Color:	+14			

Table 2: Properties of Synthetic and of Commercial Diesel Fuels

Property	Fuel Type				
	Type AA	Type A	Type B	Type C	Type D
Flash point, min. °C	40	40	40	40	40
Cloud Point, max. °C	-48	-34	-23	-18	0
Pour Point, max. °C	-51	-39	-30	-24	-6
Kinematic Viscosity @ 40°C					
minimum, mm ² s ⁻¹	1.2	1.3	1.4	1.4	1.4
maximum, mm ² s ⁻¹	-	4.1	4.1	4.1	4.1
Distillation, 90% recovered max., °C	290	315	360	360	360
Water & Sediment, max. % vol.	0.05	0.05	0.05	0.05	0.05
Total Acid Number, max.	0.10	0.10	0.10	0.10	0.10
Sulfur, max. % mass	0.2	0.5	0.7	0.7	0.7
Copper Corrosion, 3 hrs at 100°C max.	#1	#1	#1	#1	#1
Carbon Residue (Ramsbottom) on 10% bottoms, max. % mass	0.15	0.15	0.20	0.20	0.20
Ash, max. % mass	0.01	0.01	0.01	0.01	0.01
Ignition Quality, Cetane No., min.	40	40	40	40	40

Table 3: Canadian Diesel Fuel Specifications (CAN 2-3.6-M81)

Figure 1. SIMPLIFIED DIAGRAM OF SYNCRUDE OIL SANDS PLANT



DIESEL FUELS

ASTM D-2887 Simulated Distillation

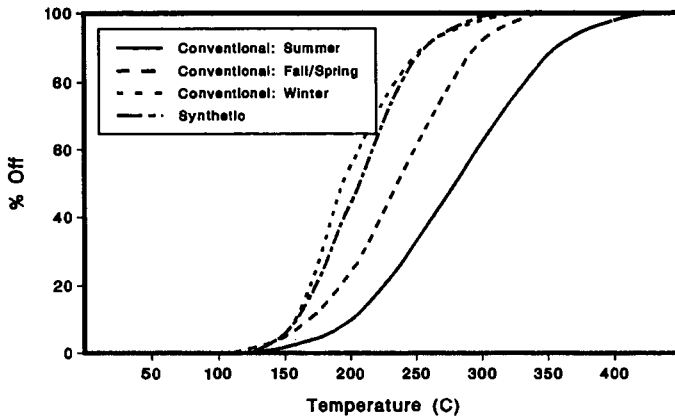


Figure 2. Boiling curves of synthetic and commercial diesel fuels.

EFFECT OF IGNITION IMPROVER

on synthetic diesel fuel

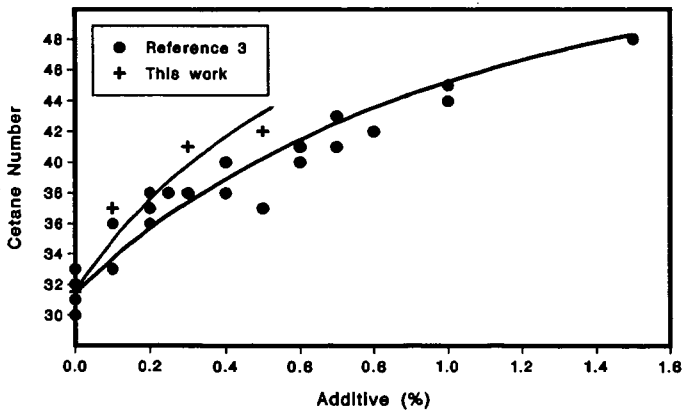


Figure 3. Effect of ignition improver on synthetic diesel fuel cetane number.

LIQUID HYDROCARBON FUELS FROM BIOMASS

Douglas C. Elliott and Gary F. Schiefelbein
Pacific Northwest Laboratory*
P. O. Box 999
Richland, WA 99352

INTRODUCTION

Renewable resources can provide a substantial energy resource for the United States. The direct production of liquid fuels from renewable resources, however, is limited to the use of biofuels. Liquids are preferred for use as transportation fuels because of their high energy density and handling ease and safety. Both biomass and municipal waste are being studied as the feedstock for production of liquid fuels [1]. Liquid fuel production from these feedstocks can be accomplished by several processes including hydrolysis and fermentation of the carbohydrates to alcohol fuels, thermal gasification and synthesis of alcohol or hydrocarbon fuels, direct extraction of biologically produced hydrocarbons such as seed oils or algae lipids, or direct thermochemical conversion of the biomass or municipal waste to liquids and catalytic upgrading to hydrocarbon fuels. This paper discusses direct thermochemical conversion to achieve biomass liquefaction.

BIOMASS LIQUEFACTION

Direct liquefaction of biomass by thermochemical means has been studied as a process for fuel production for the last twenty years. Modern development of the process can be traced to the early work at the Bureau of Mines as an extension of coal liquefaction research [2,3] and to the work on municipal waste at the Worcester Polytechnical Institute [4]. Ongoing work at universities and national laboratories in the U.S., Canada, and Scandinavia has resulted in much progress since the mid-1970's [5 and references therein]. Currently the research has focused on two general processing configurations, high-pressure liquefaction and atmospheric flash pyrolysis.

High-pressure liquefaction of biomass, shown conceptually in Figure 1, has been studied at a number of sites around the world and includes a number of process variations. The processing temperature is generally in the range of 350°C with operating pressures in excess of 1000 psig. The feedstock is generally fed as a slurry, with the nature of the slurry vehicle being a major variable in the studies. Engineering of the high-pressure feeding system is a major difficulty in the development of this type of process. The presence of added reducing gas or catalyst is another important variable. Most studies show that the operation in the presence of alkali facilitates the formation of liquids with lower oxygen contents. Product recovery is also a major issue and is highly dependent on the slurry vehicle. Various systems of centrifugation, distillation, and solvent fractionation have been tested.

The atmospheric flash pyrolysis concept, shown in Figure 2, can be traced to the ancient process of charcoal manufacture. Modern engineering methods have optimized the yield of liquid product through control of feedstock particle

*Operated for the U. S. Department of Energy by Battelle Memorial Institute under Contract DE-AC06-76RLO 1830

size, residence time, and processing temperature. Current process development utilizes short residence time, <1 second, in isothermal, fluidized- or entrained-bed reactors. The feedstock is carried by an inert gas carrier into the reactor where it thermally decomposes to tar vapors, water vapor, gases, and char solids. Recovery of the vapors as liquid product is a major difficulty for this process. Various systems for vapor quench and recovery have used complicated condensing and coalescing systems including electrostatic precipitators, cyclones, filters, and/or spray towers.

The products from the high-pressure liquefaction and atmospheric flash pyrolysis processes are vastly different from each other. The properties of the two products are summarized in Table 1. The high-pressure product is a viscous, phenolic oil. Its physical properties of high viscosity, high boiling point, and limited water solubility are readily understood as resulting from the oxygenated and aromatic character of the product components. The flash pyrolyzate is much more oxygenated and is more water soluble. As a result of the high level of dissolved water in the product, the flash pyrolyzate is much less viscous. The more oxygenated components in the product, acids and aldehydes/ethers, cause it to be more corrosive and more thermally unstable, respectively.

UPGRADING BIOMASS-DERIVED LIQUIDS

Because of the chemical differences in the two products described above, different upgrading schemes have been derived for converting the products into usable hydrocarbon fuels. Catalytic hydroprocessing is an obvious choice based on the existing knowledge of sulfur removal from petroleum products. Catalytic hydrodeoxygenation of the products has been studied in several laboratories [6,7,8]. Developments in further product refinement by catalytic cracking and hydrocracking have also been presented [9,10]. This type of processing is most directly applicable to the high-pressure liquefaction products; however, a process has been identified which allows the use of catalytic hydroprocessing of the thermally unstable pyrolyzate product [11]. Another alternative, which has been used successfully with the pyrolyzate products, is the catalytic cracking of the vapors over a zeolite catalyst without the intermediate quenching and recovery of the tars [12]. Further discussion of the products from this type of processing is not included in this paper.

Catalytic hydroprocessing of biomass-derived liquid products has been investigated at Pacific Northwest Laboratory (PNL) in a fixed-bed, continuous-feed, catalytic reactor system (shown schematically in Reference 6). Products from both high-pressure processes and flash pyrolysis processes have been upgraded [13,14]. The reactor system includes gas feed from a high-pressure (6000 psig) bottle, oil feed by positive displacement pump, a 1-liter reactor vessel containing 850 mL of alumina-supported metal sulfide catalyst (sulfided in place), pressure control by a back-pressure regulator, and product recovery in a cooled, atmospheric-pressure gas-liquid separator. Feed gas is measured by a mass flow meter; feed oil is measured in a volume flow meter; and off-gas is measured in a wet test meter. The off-gas is analyzed by gas chromatography using both a thermal conductivity detector for fixed gases and a flame ionization detector for hydrocarbon vapors up to C7.

ANALYSIS OF PRODUCTS FROM HYDROPROCESSING BIOMASS-DERIVED OILS

A range of products has been produced in the PNL hydrotreater depending on the processing conditions and the feedstock. Several representative samples are presented in Table 2. In comparison with the biomass-derived oils shown in Table 1, the hydrotreated products are significantly upgraded. The oxygen content is greatly reduced and, coincidentally, so is the density of the products. The density difference has a significant impact because, although the mass yield of the hydrotreated products is in the range of 80%, the volume yield in many cases exceeds 100%. A primary concern throughout the research has been the maintenance of the aromatic character of the biomass oil in order to minimize hydrogen consumption and to produce a higher octane gasoline blending stock. As seen in Table 2, the hydrogen-to-carbon ratio in the products is highly variable depending on the processing conditions. The extent of saturation as shown by the H/C ratio is a useful indicator of the aromatic character of the product. Saturation of the aromatic components has a strongly deleterious effect on the octane of the product. A review of the literature shows that cyclic hydrocarbons have poor octanes similar to straight-chained hydrocarbons. Our analyses also show that although the crude hydrotreated products do contain minor amounts of oxygen, water solubility in the products remains low. In addition, although sulfided catalysts are used in the hydrotreating, little incorporation of sulfur into the nearly sulfur-free biomass oils is occurring.

COMPONENT ANALYSIS IN GASOLINE-RANGE DISTILLATES

More detailed analysis of several gasoline-range distillates from the hydro-treated biomass-derived oils has been undertaken. These analyses provide additional detail on the makeup of the products and also further substantiate the relationships of the product composition to product properties. As seen in Table 3, elemental compositions can be compared with component fractionations and component analysis by instrumental methods. To fractionate the components of the distillates, we used the ASTM D 1319 method for determining hydrocarbon types by fluorescent indicator adsorption. By nuclear magnetic resonance (NMR) of carbon-13, similar component groups can be identified and quantified.

For most of the samples listed in Table 3, the D 1319 data compare quite favorably with the C-13 NMR results. The aromatic and aliphatic portions are nearly identical. The D 1319 consistently shows a small olefin fraction in the oil, while the NMR analysis detects essentially no olefinic carbon atoms. Further analysis of the fractions from the D 1319 separation was performed by gas chromatography with a mass selective detector (HP 5970). Individual components in each fraction were identified and semi-quantitatively determined by the intensity of the total ion current for each peak. Components in each of the fractions are listed in Table 4. With this analysis, the NMR results were confirmed, as the primary components of the olefin fraction were found to be bicyclic components. Some difficulty was encountered with this analysis because of the small fraction size and the contamination by the aliphatic fraction. However, no mass spectra of olefin components were confirmed, and the primary components in the fraction could be determined by comparison with the aliphatic fraction analysis.

REFERENCES

1. Thermochemical Conversion Program Annual Meeting, June 21-22, 1988. SERI/CP-231-3355, Solar Energy Research Institute, Golden, CO. July 1988.
2. Appell, H. R., Y. C. Fu, S. Friedman, P. M. Yavorsky, and I. Wender. 1971. Converting Organic Wastes to Oil: A Replenishable Energy Source. Report of Investigations 7560, Pittsburgh Energy Research Center, Pittsburgh, PA.
3. Appell, H. R., Y. C. Fu, E. G. Illig, F. W. Steffgen, and R. D. Miller. 1975. Conversion of Cellulosic Wastes to Oil. Report of Investigations 8013, Pittsburgh Energy Research Center, Pittsburgh, PA.
4. Kaufman, J. A., and A. H. Weiss. 1975. Solid Waste Conversion: Cellulose Liquefaction. PB 239 509, National Technical Information Service, Springfield, VA.
5. Beckman, D., and D. C. Elliott. 1985. "Comparisons of the Yield and Properties of the Oil Products from Direct Thermochemical Biomass Liquefaction Processes." Can. Jour. Chem. Eng. 63(1):99-104.
6. Elliott, D. C., and E. G. Baker. 1986. Catalytic Hydrotreating of Biomass Liquefaction Products to Produce Hydrocarbon Fuels: Interim Report. PNL-5844, Pacific Northwest Laboratory, Richland, WA.
7. Gevert, S. B. 1987. Upgrading of Directly Liquefied Biomass to Transportation Fuels. Chalmers University of Technology, Göteborg, Sweden.
8. Soltes, E. J., and S-C. K. Lin. 1984. "Hydroprocessing of Biomass Tars for Liquid Engine Fuels." In: Progress in Biomass Conversion, Vol. 5, p. 1. D. A. Tillman and E. C. Jahn, eds., Academic Press, New York.
9. Elliott, D. C., and E. G. Baker. 1988. "Catalytic Hydrotreating Processes for Upgrading Biocrude Oils." In: Thermochemical Conversion Program Annual Meeting, pp. 45-56. SERI/CP-231-3355, Solar Energy Research Institute, Golden, CO.
10. Gevert, S. B., and J-E. Otterstedt. 1987. "Upgrading of Directly Liquefied Biomass to Transportation Fuels - Catalytic Cracking." Biomass 14:173-183.
11. Elliott, D. C., and E. G. Baker. 1989. "Process for Upgrading Biomass Pyrolyzates." U.S. Patent #4,795,841, issued January 3, 1989.
12. Scahill, J., J. P. Diebold, and A. Power. 1988. "Engineering Aspects of Upgrading Pyrolysis Oil Using Zeolites." In: Research in Thermochemical Biomass Conversion, pp. 927-940. eds. A. V. Bridgwater and J. L. Kuester, Elsevier Science Publishers, LTD., Barking, England.
13. Baker, E. G., and D. C. Elliott. 1988. "Catalytic Hydrotreating of Biomass-Derived Oils." In: Pyrolysis Oils from Biomass: Producing, Analyzing and Upgrading - ACS Symposium Series 376, pp. 228-240. E. J. Soltes and T. A. Milne, eds., American Chemical Society, Washington, DC.
14. Baker, E. G., and D. C. Elliott. 1988. "Catalytic Upgrading of Biomass Pyrolysis Oils." In: Research in Thermochemical Biomass Conversion, pp. 883-895. A. V. Bridgwater and J. L. Kuester, eds., Elsevier Science Publishers, LTD., Barking, England.

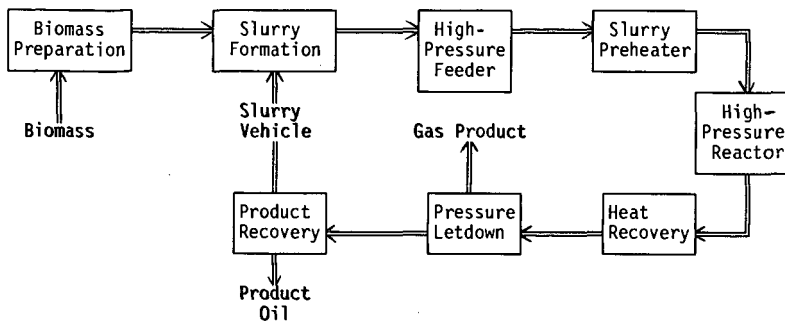


FIGURE 1. Conceptual High-Pressure Liquefaction Process

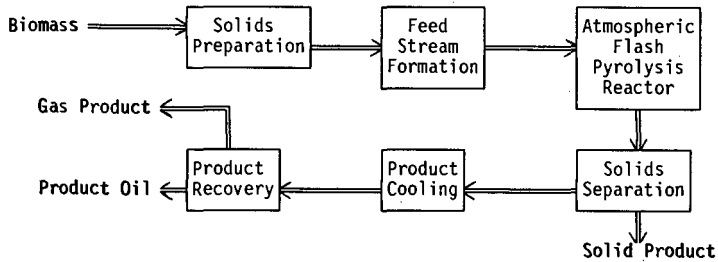


FIGURE 2. Conceptual Atmospheric-Pressure Flash Pyrolysis Process

TABLE 1. Properties of Direct Liquefaction Products from Biomass

	High-Pressure Liquefaction	Flash Pyrolysis
Elemental Analysis		
Carbon, wt%	72.6	43.5
Hydrogen, wt%	8.0	7.3
Oxygen, wt%	16.3	49.2
Sulfur, ppm	<45	29
H/C atom ratio (dry)	1.21	1.23
Density, g/mL	1.15	1.23
Moisture, wt%	5.1	24.8
HHV, Btu/lb	15,340	9,710
Viscosity, cps	15,000 @ 61°C	59 @ 40°C
Distillation Range		
IBP-225°C	8%	44%
225°C-350°C	32%	coked
350°C-EP(°C)	7%	

TABLE 2. Range of Properties of Hydrotreated Biomass Liquefaction Products

Elemental Analyses	
Carbon, wt%	85.3 - 89.2
Hydrogen, wt%	10.5 - 14.1
Oxygen, wt%	0.0 - 0.7
Sulfur, ppm	50
H/C atom ratio	1.40 - 1.97
Density, g/mL	0.796 - 0.926
Moisture, ppm	10 - 80
HHV, Btu/lb	18200 - 19500
Viscosity, cps	1.0 - 4.6 @ 23°C
Aromatic/ Aliphatic Carbon	
	38/62 - 22/78
Distillation Range	
IBP-225°C	>97% - 36%
225°C-350°C	0% - 41%
EP(°C)	188°C - 348°C

TABLE 3. Distillate Products from Hydrotreatment

ELEMENTAL ANALYSES, %				Density g/mL	HHV Btu/lb	gasoline IBP-225C	BP range	C-13 N M R			Octane Numbers		
Carbon	Hydrogen	(H/C ratio)	Oxygen					arom/ alpha	actual arom	arom/ali/olef D1319	MON	RON	R+M/2
86.6	12.1	1.66	1.3	0.844		100%	23-225C	28/72	43%	44.1/55.1/0.8	72.0	77.0	74.5
85.4	12.5	1.74	2.2	0.791		100%	68-176C	29/71	25.4%	39.5/53.6/6.9			
87.1	12.0	1.64	0.9	0.859		100%	23-225C	30/70	29.0%	47.4/48.3/4.3			
86.2	13.1	1.81	0.6	0.823	18990	100%	23-225C	24/76	32%	33.9/63.3/2.8	72.8	78.1	75.5
				0.81		100%	23-165C	20/80	28%	28.3/69.9/1.8			
86.0	12.7	1.75	1.3	0.803		100%	72-157C	22/78	29%	33.7/59.1/7.2			
84.3	13.7	1.93	1.5	0.782		100%	57-183C	12.4/87	18%	18.1/77.1/4.8			
85.6	13.3	1.84	1.2	0.802		100%	63-149C	16/84	20%	28.3/68.6/3.1			

TABLE 4. Components of D 1319 Chromatography Fractions
(within each fraction, from highest total ion current)

Saturated Hydrocarbons

ethylcyclohexane
propylcyclohexane
methylcyclohexane
methylcyclohexane
methylpropylcyclohexane
methylcyclohexane
methylpropylcyclopentane
ethylpropylcyclohexane
dimethylcyclohexane
methylcyclopentane

Aromatic Hydrocarbons

ethylmethylbenzene
methylpropylbenzene
propylbenzene
C4-alkyl-benzene
C2-alkyl-tetralin
methyltetralin
tetralin
methylindan
C5-alkyl-benzene
methylpropylbenzene

Olefinic Hydrocarbons

octahydroindene
octahydropentalene
methyloctahydropentalene

Alcohol Soluble Components

dimethylphenol
naphthalene
ethylphenol
cresol
ethylmethylphenol
cresol
methylnaphthalene
ethylmethylphenol
dimethylphenol
ethyl phenol

MILD GASIFICATION OF COAL AND HEAVY OIL MIXTURES
TO ENHANCE LIQUID YIELD/QUALITY+

M. Rashid Khan
Texaco Research Center,
Texaco Inc, P.O. Box 509, Beacon, NY 12508

F. Y. Hsieh
Oak Ridge Associated University
Morgantown Energy Technology Center
Morgantown, WV 26505

Larry Headley
U.S. Department of Energy
Morgantown Energy Technology Center
Morgantown, WV 26505

INTRODUCTION AND BACKGROUND

Our previous studies demonstrated that relatively high quality (high H/C) liquid fuels from coal can be produced by low-temperature devolatilization (1). However, the liquids produced by low-temperature pyrolysis are typically of low yield. Therefore, there is an interest to identify ways to increase the yield of the liquids produced during pyrolysis.

Coprocessing of coal and heavy petroleum residue at relatively mild conditions may provide an avenue to enhance yield. Some important advantages of coprocessing can be the following: (a) upgrading of a petroleum residue in a reaction with coal; (b) conversion of coal to synthetic crudes which can be further upgraded into premium liquid fuels. In coprocessing, the petroleum residues may serve as the "liquefaction solvent" or hydrogen donor and the aromatics present in coal liquid may serve as hydrogen "shuttlers" by efficiently transferring hydrogen to moieties where it is most deficient. Coal also can enhance the conversion of petroleum residues to lighter liquid products through the catalytic effects of the mineral matters present in the coal. Liquefaction of coal and petroleum residues are typically performed at temperatures in the range of 400° to 500°C under pressurized hydrogen atmosphere. Catalysts are generally also added for the hydroconversion of coal and petroleum residues.

Coprocessing of the coal with petroleum, heavy crudes, and petroleum residues through catalytic hydrogenation (2-7) or solvent extraction (8-10) has been extensively studied. However, relatively little has been reported in the literature regarding the coprocessing of coal with petroleum residues by simple pyrolysis (i.e., without the complicating influences of pressurized hydrogen or hydrogenation catalysts).

+This work was performed at Morgantown Energy Technology Center

Sekrieru, et al. (11), investigated copyrolysis of brown coal and petroleum products. Vikhorev, et al. (12), also investigated copyrolysis of brown coal and coal tar or petroleum residue. Both of these studies apparently noted increases in liquid yield during copyrolysis. It was suggested that the additives (coal tar and petroleum residue) can swell or weaken the coal structure leading ultimately to a higher liquid yield. Huttinger and Sperling (13) studied flash hydrocopyrolysis of coals doped with aromatics, hydroaromatics (2 percent of loading) and observed that coprocessing of coal with additives resulted in an increase in the tar yield (by 5 to 10 percent) at the expense of char yield. In contrast, Malhotra, et al. (14), pyrolyzed coal with 10 percent of coal tar and prehydrogenated coal tar at various heating rates. Their limited results show that the addition of coal tar and prehydrogenated coal tar (containing 10 to 20 percent of hydroaromatics) to coal had no beneficial effect on pyrolysis yield. However, extensive characterization data on any of the studies were not reported.

Khan, et al. (16), studied the pyrolysis of raw coal, pyridine extract and extracted coal residue by a thermogravimetric analyzer (TGA) and found that the combined weight loss of extract and extracted coal residue at 600°C is considerably lower than the weight loss obtained for the raw coal alone. Therefore, it was suggested that the presence of hydrogen-rich portions of the coal (i.e., extract) in the coal structure increases the overall weight loss for coal during pyrolysis. The extractable portion of coal may serve as the source of internal hydrogen during pyrolysis by supplying hydrogen to hydrogen deficient moieties that would otherwise undergo coking reaction (forming solid residue) rather than desirable volatiles. In other words, the extractable portion of coal, being more hydroaromatic, can serve as hydrogen-donors in partially hydrogenating the insoluble portion of coal during pyrolysis, thereby increasing the yield of volatile matter from the residue.

It is generally believed in coal liquefaction, that hydrogen-donor solvent can donate hydrogen and "cap-off" the thermally generated free radicals to form stable volatiles. The rate of coal liquefaction process apparently depends on the rate at which hydrogen can be donated from the solvent. McMillen, et al. (17), suggested a mechanism for the formation of liquid products during pyrolysis in which strong linkages (such as diarylmethane, alkylaromatic, and dialylether) are cleaved at 400°C as a result of hydrogen transfer from solvent-derived cyclohexadienyl radicals in a direct bimolecular step. Existing literature data suggest that petroleum residue may serve as an external hydrogen source by enhancing the bond-scission reactions via formation of cyclohexadienyl radicals (18) during coprocessing. It is our hypothesis in this study that copyrolysis of coal with petroleum residue at a relatively low temperature (500°C) can increase the tar yield while improving the quality of the tar perhaps by hydrogen transfer and hydrogen-transfer-promoted, bond-scission reactions. To fully test our hypothesis and to extend the data available in the literature, a copyrolysis study was initiated. The copyrolysis products were extensively characterized. Relatively little has been reported in the literature regarding the characteristics of the liquids generated by copyrolysis of coal and heavy residue (in the absence of a catalyst or high-pressure hydrogen).

EXPERIMENTAL

Feedstocks Origin and Pyrolysis Procedure: The experimental procedures for the production of pyrolysis liquids from solid fuels including reactor system, experimental procedures, and reproducibility of results have been described by Khan (1a). A fixed-bed reactor known as slow heating rate organic devolatilization reactor (SHRODR) was used to generate the pyrolysis liquids at 500°C. In addition, a thermogravimetric analysis (TGA) reactor was used for our studies. The Pittsburgh No. 8 coal (high volatile bituminous) and the Wyodak subbituminous coals were used in this study. All sample preparation and handling procedures were performed in inert atmospheres. The Kern River heavy residue was provided by the Stanford Research Institute. Additional details on the origin of these samples can be found elsewhere (1b).

RESULTS AND DISCUSSION

The proximate and ultimate analyses of Pittsburgh No. 8 coal, Wyodak coal (PSOC 1520) and Kern River heavy residue are shown in Table 1. The pyrolysis weight loss in a TGA during heat-treatment to 500°C at 20°C/min (Table 2) for the Pittsburgh No. 8 coal was 25.7 weight percent (daf) and that for the heavy residue was 80.0 weight percent (daf). The weight loss of 50/50 mixture was 62.9 weight percent (daf), which is 9.0 weight percent higher than that for the projected value (53.9 weight percent) based on the yields of the individual components. These results suggest that the presence of heavy residue increases the overall weight loss during pyrolysis of Pittsburgh No. 8 coal. The heavy residue (hydrogen-rich) may serve as hydrogen-donor providing some of the labile hydrogen to the coal (hydrogen-poor) moieties and thereby suppressing the regressive reactions during pyrolysis. Figure 1 shows the pyrolysis (derivative thermogravimetric analysis) DTG curves of Pittsburgh No. 8 coal, heavy residue, and their 50/50 mixture. There is only one major peak shown in the DTG curve for coal. Two major peaks were shown in the DTG curves of heavy residue and 50/50 mixture. The first peak in the DTG curves of heavy residue and 50/50 mixture is related to the decomposition and devolatilization of light molecules (or components), and the second peak is presumably related to the decomposition and devolatilization of original and newly formed heavy molecules (or components). As shown in Figure 1, coprolysis of coal with heavy residue slightly shifts the first peak to a lower temperature while simultaneously lowering the second peak by 40°C as compared to the pyrolysis of heavy residue alone. These findings provide credence to the concept of synergistic effects during coprolysis of coal and heavy residue.

Figure 2 presents the yield of gas, tar, and char products from pyrolysis of Wyodak coal, heavy residue, and the 50/50 mixture at 500°C in the fixed-bed reactor. The tar yield from pyrolysis of 50/50 mixture is 52.2 weight percent (daf), which is 5.1 weight percent higher than the predicted value (47.1 weight percent [daf]). This observation is consistent with the TGA coprolysis data.

Table 3 shows the ultimate analyses and heating values of tars from pyrolysis of Wyodak coal (PSOC 1520), heavy residue, and their 50/50 mixture at 500°C in the fixed-bed reactor (SHRODR). It appears that the elemental composition of tar from 50/50 mixture is similar to that for the tar from heavy residue. The tar from 50/50 mixture has higher H/C ratio, lower O/C ratio, and higher

heating value than those for the tar from coal. This confirms that copyrolysis of coal with heavy residue produces a better quality tar as compared to the pyrolysis of coal alone. Table 4 shows the elemental analyses of chars from pyrolysis of Wyodak coal, heavy residue, and the mixture. It is expected that the elemental composition of char from the mixture is similar to that for the char from Wyodak coal. The char from pyrolysis of 50/50 mixture has slightly higher heating value than that for the char from pyrolysis of coal. These results indicate that copyrolysis of coal with heavy residue upgrades the tar quality without necessarily degrading the char quality.

Figure 3 compares the composition of evolved gases from pyrolysis of Wyodak coal, heavy residue, and the mixture. It is obvious that pyrolysis of Wyodak coal resulted in a relatively high yield of CO and CO₂, which is due to the decomposition of oxygenated functional groups in Wyodak coal. Pyrolysis of heavy residue produced a relatively high yield of CH₄ and C₂H₄. This is probably due to the higher concentration of long-chain aliphatic components present in the heavy residue. Heavy residue has lower content of sulfur as compared to Wyodak coal. However, pyrolysis of heavy residue alone produces a higher yield of H₂S. This implies that the sulfur-containing compounds in heavy residue (e.g., thiol and disulfide) is more volatile than those present (e.g., thiophene, thiopyrone) in the Wyodak coal. Pyrolysis of 50/50 mixture produced lower yield of H₂S (18 percent lower) than that for the projected value. Therefore, the carbonate minerals in the Wyodak coal may also act as scavengers of hydrogen sulfide during copyrolysis of coal with heavy residue. In general, the yield of various gases for pyrolysis of the mixture ranked in the region between pyrolysis of Wyodak coal and heavy residue.

The tars from pyrolysis of coals (Wyodak coal and Pittsburgh No. 8 coal), heavy residue, and the mixture were separated by sequential elution solvent chromatography (data not shown). In general, the tars from pyrolysis of the mixture contain higher content of alkane/alkene neutral aromatics, lower content of monophenols, polyphenols, and other oxygen-containing compounds as compared to the tars from pyrolysis of coal alone. This implies that copyrolysis of coal and heavy residue upgrades the quality of coal tars.

The average structure parameters of tars from pyrolysis of Wyodak coal, heavy residue, and the mixture have been characterized by using proton NMR analysis (data not shown). The carbon aromaticity of tar from the mixture is similar to that for the tar from pyrolysis of heavy residue and much lower than that for the tar from pyrolysis of coal. The tar from the mixture contains lower content of mono-aromatics and higher content of di- and tri-aromatics than that for the tar from coal. It is interesting to note that the tar from the mixture contains higher content of naphthenic carbon and naphthenic rings/molecule than those for the tar from coal. This finding suggests that the tar from the mixture can be much easily upgraded to match the specifications of high-density jet fuel.

SUMMARY AND CONCLUSIONS

Our previous results demonstrated that relatively high-quality liquid fuel can be produced from coal by low-temperature devolatilization. Ongoing studies are aimed at producing a high-quality liquid while achieving a high yield of liquids. To better understand whether copyrolysis is a viable option to enhanced liquid yield, a coal and a heavy residue sample were copyrolyzed in a

fixed-bed reactor at a relatively low temperature and the products were characterized. Results demonstrated that there is a synergism during copyrolysis of coal and heavy residue. This synergism enhances both the yield and quality of the liquid products during copyrolysis.

In general, the tars from pyrolysis of the mixture contain higher content of alkane/alkene neutral aromatics, lower content of monophenols, polyphenols, and other oxygen-containing compounds as compared to the tars from pyrolysis of coal alone. The tars from the mixture also contain lower content of mono-aromatics and higher content of di- and tri-aromatics than that for the tar from coal. Therefore, they can be much easily upgraded to match the specifications of high-density jet fuel.

ACKNOWLEDGEMENTS

Funding for this study was provided by the U.S. Department of Energy, Assistant Secretary for Fossil Energy, Office of Coal Utilization, Advanced Conversion and Gasification. FYH acknowledges support received from U.S. DOE through the Oak Ridge Associated Universities (ORAU) Program.

REFERENCES

- 1a. Khan, M. R., Fuel Science and Technology International, 1987, 5(2), 185.
- 1b. Khan, M. R., Seshadri, K. and Kowalski, T. accepted for publication in Energy and Fuels, 1989.
2. Lenz, U, and J. Wavyzinek; Am. Chem. Soc. Div. Fuel Chem. Prepr., 1988, 33(1), 27.
- 3a. Curtis, C. W., J. A. Guin, M. C. Pass, and K. J. Tsai; Fuel Science and Technology International, 1987, 5(3), 245.
- 3b. Curtis, C. W., K. J. Tsai, and J. A. Guin; Ind. Eng. Chem. Process Des. Dev., 1985, 24, 1259.
4. Aulich, T. R., P. L. Holm, C. L. Knudson, and J. R. Ridut; Am. Chem. Soc. Div. Fuel Chem. Prepr., 1988, 33(1), 103.
5. Schwartz, M. M., and A. L. Hensley; Am. Chem. Soc. Div. Fuel Chem. Prepr., 1988, 33(1), 163.
6. Fouda, S. A., J. F. Kelly, and P. M. Rahimi; Am. Chem. Soc. Div. Fuel Chem. Prepr., 1988, 33(1), 179.
7. Oelert, H. H., R. Bloss, and P. F. Zhang; Am. Chem. Soc. Div. Fuel Chem. Prepr., 1988, 33(1), 185.
8. Mochida, I., Y. Moriguchi, Y. Korai, H. Fujitsu, and K. Takeshita; Fuel, 1981, 60, 746.
9. Moschopedis, S. E., R. W. Hawkins, J. F. Fryer, and J. G. Speight; Fuel, 1980, 59, 647.
10. Yan, T. Y., and W. F. Espenscheid; Fuel Processing Technology; 1983, 7, 121.
11. Sekriera, V. I., Z. S. Smutkina, and T. A. Titova; Solid Fuel Chemistry, 1978, 12(5), 45.
12. Vikhoven, A. A., A. M. Syroezhko, V. A. Proskuryakov, and N. A. Akhmedov; Solid Fuel Chemistry, 1987, 21(2), 78.
13. Huttlinger, K. J., and R. E. Sperling in proceedings of the 1987 International Conference on Coal Science, J. A. Moulijn, K. A. Nator, and H. A. G. Chermin, Editors; Elsevier Science Publishers B. V., Amsterdam, 1987, p. 699.

14. Malhotra, R., G. St. John, D. S. Tse, and D. F. McMillen; Am. Chem. Soc. Div. Fuel Chem. Prepr., 1988, 30(2), 257.
15. Brown, H. R., and P. L. Waters; Fuel, 1966, 45, 17.
16. Khan, M. R., R. Usmen, E. Newton, S. Beer, and W. Chisholm; Fuel, 1988, 67, 1668.
17. McMillen, D. F., R. Malhotra, G. P. Hum, and S.-J. Chang; Energy and Fuel, 1987, 1, 193.
18. McMillen, D. F., R. Malhotra, D. S. Tse, and S. E. Nigenda; Am. Chem. Soc. Div. Fuel Chem. Prepr., 1988, 33(1), 58.
19. Seshadri, K. S., and D. C. Cronauer; Fuel, 1983, 62, 1436.

TABLE 1

PROXIMATE AND ULTIMATE ANALYSES OF PITTSBURGH NO. 8 COAL, WYODAK COAL (PSOC 1520), AND KERN RIVER HEAVY RESIDUE

	Pittsburgh No. 8 Coal	Wyodak Coal	Kern River Heavy Residue
% C, daf	83.74	73.78	85.43
% H, daf	5.46	4.62	11.15
% N, daf	1.56	1.11	0.86
% S, daf	2.15	1.38	0.97
% O, daf (by difference)	7.09	19.11	1.59
<hr/>			
% Ash (as-received basis)	7.27	9.08	< 0.01
% Moisture	0.57	26.69	0
H/C Atomic (daf)	0.78	0.75	1.57
O/C Atomic (daf)	0.064	0.19	0.014

TABLE 2

TGA PYROLYSIS OF PITTSBURGH NO. 8 COAL, KERN RIVER HEAVY RESIDUE, AND 50/50 PITTSBURGH NO. 8 COAL/KERN RIVER HEAVY RESIDUE MIXTURE

Samples	Weight Loss (daf) at 500°C
Pittsburgh No. 8 Coal	25.7
Kern River Heavy Residue	80.0
50/50 Coal/Heavy Residue Mixture	62.9
Projected Weight-Loss for Mixture	53.9 ^a

^a Predicted weight loss (daf) of 50/50 mixture, assuming no synergism.

TABLE 3

ULTIMATE ANALYSES AND HEATING VALUES OF TARS FROM PYROLYSIS OF WYODAK COAL (PSOC 1520), KERN RIVER HEAVY RESIDUE AND 50/50 WYODAK COAL/KERN RIVER HEAVY RESIDUE MIXTURE AT 500°C

	Tar from Coal	Tar from Heavy Residue	Tar from 50/50 Mixture	Projected*
% C, daf	78.44	86.17	84.30	85.05
% H, daf	10.59	12.28	11.96	12.03
% N, daf	0.52	0.69	0.70	0.67
% S, daf	0.55	0.17	1.14	0.22
% O, daf	9.9	0.69	1.90	2.03
(by difference)				
H/C Atomic (daf)	1.62	1.71	1.70	1.70
O/C Atomic (daf)	0.09	0.006	0.017	0.018
Heating Value, Btu/lb	15,615	18,662	18,470	

* Projected values are calculated based on (a) the composition of individual components, and (b) their respective yield during pyrolysis. Assumes no synergism.

TABLE 4

ULTIMATE ANALYSIS AND HEATING VALUES OF CHARS FROM PYROLYSIS OF WYODAK COAL (PSOC 1520), KERN RIVER HEAVY RESIDUE, AND 50/50 WYODAK COAL/KERN RIVER HEAVY RESIDUE MIXTURE AT 500°C

	Char from Coal	Char from Heavy Residue	Char from 50/50 Mixture	Projected*
% C, daf	85.92	89.69	85.76	86.32
% H, daf	3.26	3.26	3.43	3.26
% N, daf	1.49	3.04	1.17	1.65
% S, daf	1.30	0.95	1.59	1.27
% O, daf	8.03	3.06	8.05	7.50
(by difference)				
H/C Atomic (daf)	0.46	0.44	0.48	0.45
O/C Atomic (daf)	0.07	0.026	0.07	0.065
Heating Value, Btu/lb	11,806	14,755	12,104	

* See definition of projected values on Table 3.

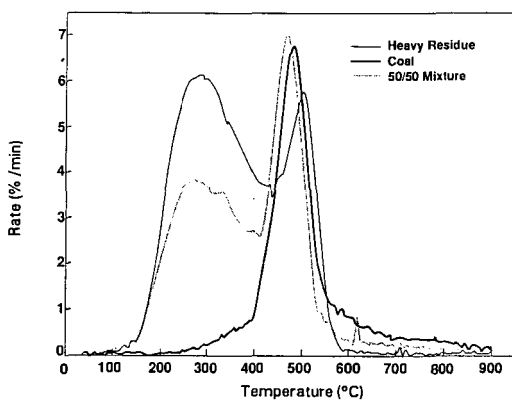


FIGURE 1 EFFECT OF CO-PROCESSING ON PYROLYSIS RATE PROFILES

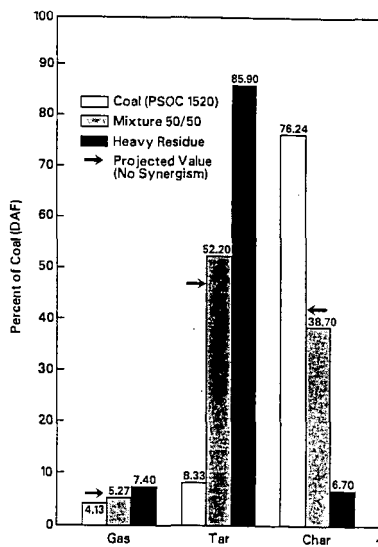


FIGURE 2 CO-PROCESSING OF COAL AND HEAVY RESIDUE

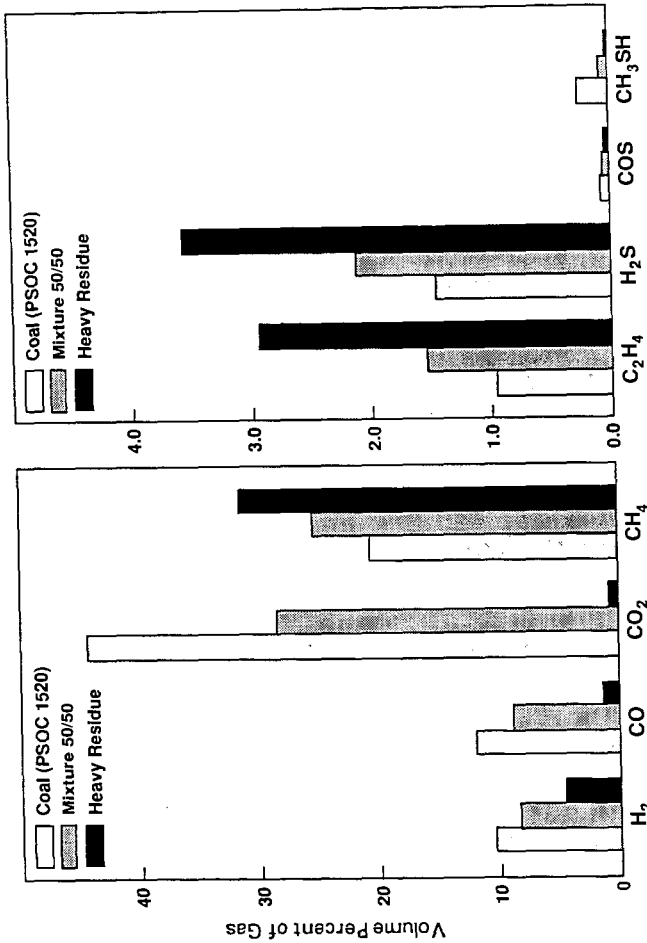


FIGURE 3 INFLUENCE OF CO-PROCESSING ON PRODUCT YIELD/COMPOSITION

FLASH PYROLYSIS OF COAL IN THE ATMOSPHERE
CONTAINING SOLVENT VAPORS

Kouichi Miura, Kazuhiro Mae, Akihiro Murata
and Kenji Hashimoto*

*Research Laboratory of Carbonaceous Resources
Conversion Technology,
Department of Chemical Engineering, Kyoto University
Kyoto 606, Japan

INTRODUCTION

We have recently presented a new coal pyrolysis method¹⁾, in which coal particles swollen by hydrogen donor solvents at around 250 °C were pyrolyzed in a Curie-point pyrolyzer. Both the conversion and the tar yield drastically increased by this pyrolysis method. The increases were brought about by the pore enlargement caused by swelling and the effective hydrogen transfer from/via the solvent to the fragments of the primary coal decomposition. This method is, however, a little complicated to be scaled up to a commercial process.

In this paper, we propose a much simpler flash pyrolysis method, in which coal particles are pyrolyzed continuously in the gas stream containing hydrogen donor solvents. It is shown that this pyrolysis method successfully increases the tar yield, and presents a possibility of an in situ control of the product distribution.

EXPERIMENTAL

The coal used was Morwell brown coal. It was ground and screened to -125 +74 μm . The properties of the coal are given in Table 1. Figure 1 shows the diagram of the entrained bed type of pyrolyzer used in this study. Reactor is a coil of stainless steel tube of 1/4 inch in outer diameter. Three different length of reactors, 0.89, 2.65 and 4.64 m, were used to change the residence time of the coal. The dried coal was fed to the reactor by a tablefeeder with nitrogen gas at the feed rate of 4 to 20 g/h. The flow rate of nitrogen was 4.0 l/min (STP). Vapor of tetralin and decalin was added to the flow of coal-nitrogen mixture at the top of reactor as shown in Figure 1. The feeding ratio of the solvent to coal was 0.12 to 0.15 by weight. Experiments without the solvent were also performed for comparison. The coal was pyrolyzed while passing the reactor, and gas, tar and char produced were led to cyclone connected to the exit of the reactor to separate the gas and tar from char. The tar and the gas were led to the condensers, where the tar was trapped. A part of the gas was collected in a gas bag.

The char and the tar yields were calculated from the changes in weight of the char collector and the tar trap, respectively. The composition of the gas was analyzed by a gaschromatograph (Shimazu GC 9A) equipped with both TCD and FID. The water in the tar was analyzed using the Karl Fischer titration (Kyoto Electronics Co., Ltd.). The tar component was also analyzed by a gaschromatograph with OV-101 column and FID. The material balance of this experiment was obtained

within 95 to 105 %. To estimate the effect of solvents on the pyrolysis of coal properly, the pyrolysis yields in the solvent vapors must be represented excluding the yields coming from solvents. So, the pyrolysis of each solvent was performed under same experimental conditions without feeding coal, and each yield in the solvent vapors, Y_i , was calculated by following equation:

$$Y_i = (\text{Yield in the solvent vapor}) - w(\text{Yield from solvent}) \quad (1)$$

where w is the feeding ratio of solvent vapor to coal.

RESULTS AND DISCUSSION

Pyrolysis in an Inert Atmosphere

To examine how we can control the product distribution of the pyrolysis of in inert atmosphere, the effects of residence time of coal and the pyrolysis temperature were examined.

Effect of Residence Time

Figure 2 shows the change of conversion, tar and gas yields with the increase of residence time (t_R) at the pyrolysis temperature of 650 °C. The conversion increased with the increase of residence time, and reached a constant value over $t_R=2$ s. The gas yield increased monotonously with the residence time. The tar yield reached a maximum at $t_R=2$ s, then decreased with increasing t_R . It indicates that the decomposition reaction of tar vapor to gas becomes significant with the increase of residence time. Figure 3 shows the similar results at the pyrolysis temperature of 800 °C. The trends of the conversion and the char yield were similar as those at 650 °C, although the final conversion level was larger than that at 650 °C. The residence time which maximizes the tar yield shifted to smaller residence time. This means that the cracking reaction rate of tar vapor at 800 °C is much faster than that at 650 °C. Figures 2 and 3 show that the primary decomposition of coal is almost completed in $t_R=2$ s.

Effect of temperature

Figure 4 shows the change of the product distribution with the pyrolysis temperature (T). The char yield decreased with temperature. On the contrary, the gas yield increased with temperature. The tar yield reached a maximum, 13.1 wt%₂₅, at 650 °C. These trends coincided with those of several researches^{2,15} using the continuous equipments. The broken lines show the yields of the flash pyrolysis performed using a Curie point pyrolyzer (CPP), in which the gas phase reaction is suppressed because only the coal is heated and the products are cooled immediately by the He flow of room temperature in CPP. The char yields of both experiments were nearly equal, indicating that the coal conversion is determined solely by the pyrolysis temperature. The gas yield of the pyrolysis in the entrained bed was larger than that of the pyrolysis in the CPP. On the other hand, the tar yield in the entrained bed was smaller than in the CPP. This indicates that the decomposition of tar is occurring in the entrained bed pyrolyzer, in which the gas stream is

also heated. Figure 5 shows the product distribution of gas component with the temperature. The yield of C_4-C_6 gas reached a maximum at 700 °C, which was 50 °C higher than the temperature for the maximum tar yield. On the other hand, the yields of H_2 and C_1-C_3 gases increased drastically with the temperature. These results also show that the gas phase reaction which decomposes tar becomes significant with the increase of temperature, and the tar yield decreased. Thus, the maximum tar yield obtained in the entrained bed pyrolyzer was 13.1 wt.% daf at $T_D=650$ °C and $t_R=2$ s. This value is 17 wt.% daf lower than that obtained in the CPP^R. The maximum tar yield attained in the entrained bed pyrolyzer will not exceed that obtained in the CPP.

Flash pyrolysis in the Vapor of solvents

Above discussion indicates that there is a limitation to increase the tar yield by controlling the temperature and the residence time as far as the pyrolysis is performed in an inert atmosphere. Then, we intended to increase the tar yield by pyrolyzing the coal in the atmosphere containing the solvent vapor. The residence time of coal was fixed as 2 s, because the primary decomposition of coal was completed in $t_R=2$ s as stated earlier.

Effect of the Kind of Solvents

Figure 6 shows the changes of tar yields of the pyrolysis in N_2 , in tetralin vapor and in decalin vapor with increasing T_D . The yields were calculated excluding the yield from solvent vapor^P by Eq. 1. The tar yield in tetralin vapor reached up to 25.2 wt.% at $T_D=750$ °C. This is twice larger than that in an inert atmosphere. Thus, the proposed pyrolysis method is found to be successful at least to increase the tar yield drastically. The effect of decalin vapor was only 2 to 3 wt.% larger than that in N_2 atmosphere at $T_D=700$ °C and 800 °C.

The Mechanism of Pyrolysis in Tetralin Vapor

Since the pyrolysis of coal in tetralin vapor was found to be effective to increase the tar yield, the mechanism of the pyrolysis was examined by comparing the yields obtained from the pyrolysis of tetralin, the pyrolysis of coal in N_2 atmosphere and the pyrolysis in tetralin vapor. The yields were all represented based on the unit weight of daf coal.

Figures 7 to 10 show the yields of char, tar, total gas, and hydrocarbon gasses, respectively. The broken line in each figure is the sum of the yield from the pyrolysis of coal in N_2 and that from the pyrolysis of tetralin. The yield in tetralin vapor coincides with the broken line if tetralin has no effect on the pyrolysis of coal.

The char yield in tetralin vapor almost coincided with the broken line as shown in Fig. 7, although it seemed to deviate at $T_D=800$ °C. This suggests that tetralin is not effective to increase the conversion. In other word, tetralin does not affect the primary

decomposition of coal. The tar yield in tetralin vapor exceeded broken line at $T_D=700$ to 800 °C, and it reached more than twice at $T_D=750$ °C as shown in Fig. 8. On the contrary, the yields of total gas and hydrocarbon gases in Figs. 9 and 10 lay far below the broken lines to compensate the increase of tar yield.

Above discussion shows that tetralin vapor contributed to the rearrangement of the product distribution of the primary decomposition of coal. The reactive radicals produced by the pyrolysis of tetralin reached mainly with light hydrocarbon gases to convert them into liquid products. The analysis of tar components, now being performed, will help us to clarify the mechanism.

CONCLUSION

A new and simple method was developed for increasing the tar yield of coal, in which coal particles were pyrolyzed in the gas stream containing the solvent vapor. The feeding rate of solvent is only around 10 wt.% of that of coal by weight. The tar yield was successfully increased up to 25 wt.% daf in the atmosphere containing the tetralin vapor from 13 wt.% daf in an inert atmosphere. This method is expected to be easily realized in a commercial scale because of its effectiveness and simplicity.

ACKNOWLEDGMENT

This work was performed in the framework of the "Priority-Area Research" and "Japan-Canada Joint Academic Research Program" which was sponsored by the Ministry of Education, Culture and Science of Japan.

REFERENCES

1. Miura, K., Mae, K., Yoshimura, T. and Hashimoto K., Proc. Div. Fuel Chem., Am. Chem. Soc. is submitted. (Miami) Sep. (1989)
2. Teo, K.C. and Watkinson, A.P., Fuel, 65, 949 (1986)
3. Tyler, R.J., Fuel, 58, 680 (1979)
4. Scaroni, A.W., Walker, P.L. and Essenhigh R.H., Fuel 60, 71 (1981)
5. Scott, D.S. and Pickorz J., Fuel Processing Technology, 13, 157 (1986)
6. Miura, K., Mae, K., Asaoka, S., Uchiyama, M. and Hashimoto, K., Proc. Int. Conf. on Coal Science is submitted. (Tokyo) Oct. (1989)

Table 1 Properties of Coal

Proximate Analysis (wt%)			Ultimate Analysis (wt% daf)				
FC	VM	ASH	C	H	N	S	O
48.2	50.3	1.5	67.1	4.9	0.6	0.3	27.1

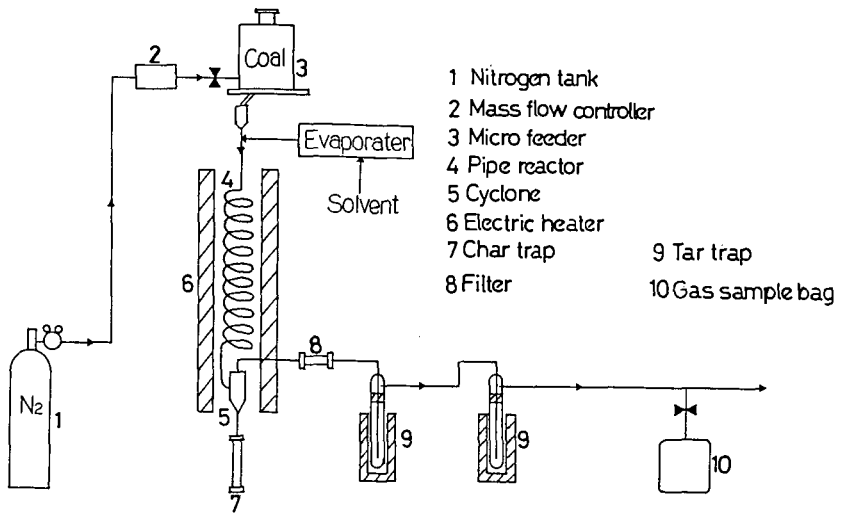


Fig.1 Schematic flow of continuous entrained bed type equipment for the pyrolysis of the coal

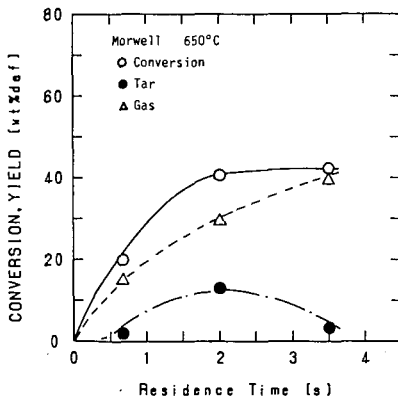


Fig.2 Effect of the residence time of coal on the product distribution ($T_p=650^\circ\text{C}$)

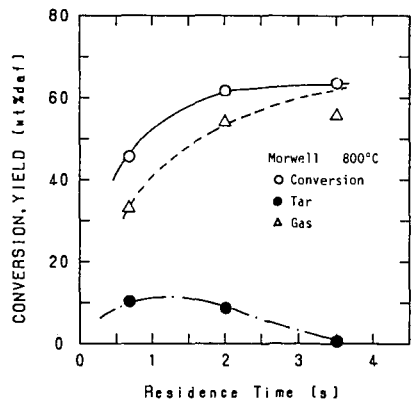


Fig.3 Effect of the residence time of coal on the product distribution ($T_p=800^\circ\text{C}$)

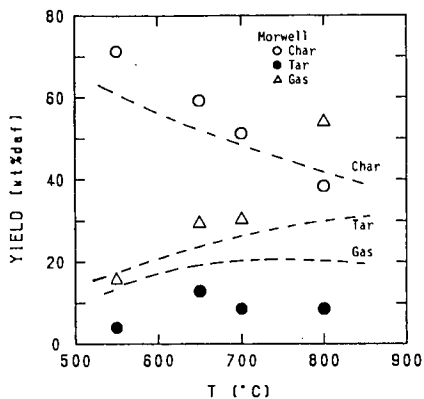


Fig. 4 Effect of the pyrolysis temperature on the product distribution ($t_p=2$ s) (broken lines: results obtained from the pyrolysis using a Curie-point pyrolyzer)

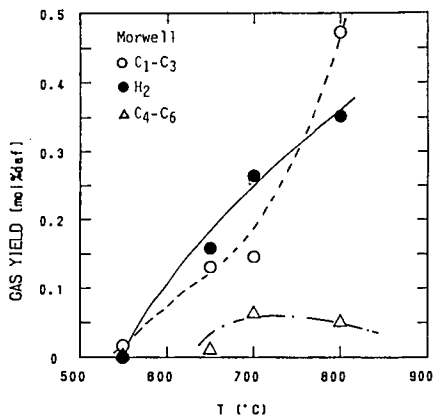


Fig. 5 Effect of the pyrolysis temperature on the gas yield

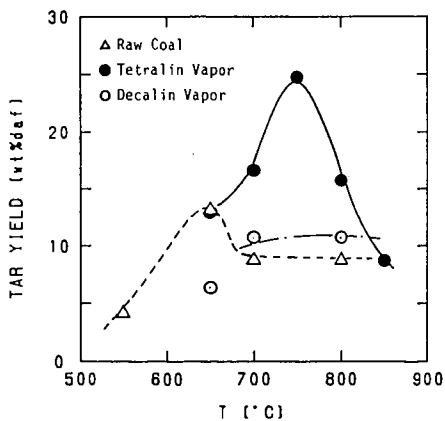


Fig. 6 Effect of the atmosphere containing solvent vapor on tar yield during the pyrolysis

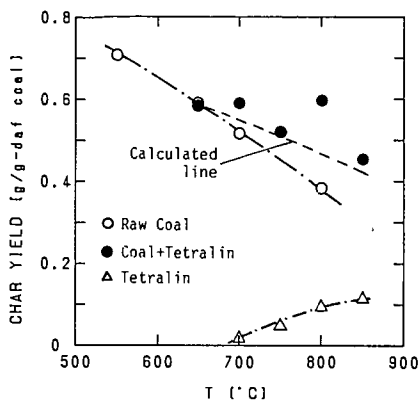


Fig. 7 Effect of the atmosphere containing tetralin vapor on char yield during the pyrolysis

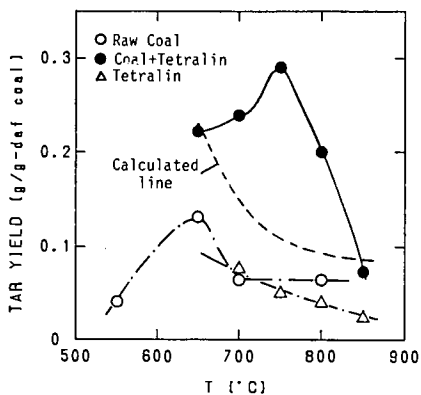


Fig. 8 Effect of the atmosphere containing tetralin vapor on tar yield during the pyrolysis

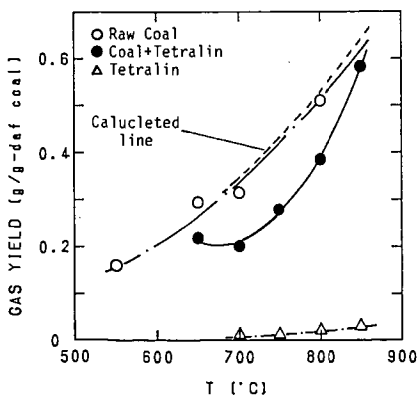


Fig. 9 Effect of the atmosphere containing tetralin vapor on gas yield during the pyrolysis

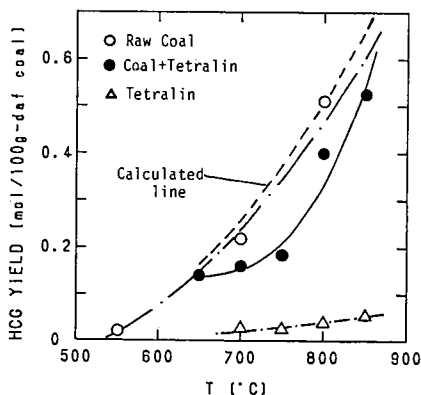


Fig. 10 Effect of the atmosphere containing tetralin vapor on HCG yield during the pyrolysis

PREDICTION OF HYDROGEN CONSUMPTION FOR
UPGRADING OF PYROLYSIS LIQUIDS¹

Clint Williford
University of Mississippi,
University, MS 38677

M. Rashid Khan²
Texaco Research Center
Texaco Inc, P.O. Box 509, Beacon, NY 12508

H. F. Bauer
U.S. Department of Energy
Morgantown Energy Technology Center
Morgantown, WV 26505

INTRODUCTION AND BACKGROUND

High performance aircraft require fuels with maximum heat of combustion per unit volume to achieve their maximum performance. A special class of hydrocarbon liquids can offer a relatively high energy density, fuel stability, high boiling point, and low viscosity. These fuels include bicyclic compounds composed of five- and six-ring structures such as decalin and biphenyl. Their heats of combustion range from 8800 to 9600 cal/ml versus 8000 cal/ml for JP-6 (Letort, 1962). On a volume basis such fuels would thus increase an aircraft's traveling range by 10-20%. Production of such fuels from petroleum (much of which is imported) derivatives appears to be relatively expensive. In contrast, coal liquids produced from low temperature pyrolysis or "mild gasification" may provide a rich source of aromatic bicyclics. These occur predominantly in the naphthalene or "heart-cut" of about 220-350°C boiling range (Hawk et al., 1965; Letort, 1962). Use of coal liquids however does require substantial upgrading to meet product specifications. Full boiling range liquids contain on the order of 60-75+% aromatics, 1.6-10% oxygen, 0.5-3.0% sulfur, and 0.3-2.0% nitrogen (Gray et al., 1983; Hawk et al., 1965; Khan, 1986, 1987). Resulting jet fuels should meet specifications approximating those shown in Table 1.

Recent investigation at Naval Propulsion Center indicated that hydrogen content can serve as the decisive specification for aviation fuel quality (Moses et al., 1984; Masters et al., 1987). Investigators concentrated on combustion

¹ A portion of the work was done at Morgantown Energy Technology Center.

² Adjunct Professor of Chemical Engineering, University of Mississippi, University, MS 38677.

properties such as burning with minimal soot formation. They found that engines could operate satisfactorily on fuels with a hydrogen content below a reference of 13.8 wt%. Most engines could operate without adverse effects with fuels having a hydrogen content down to 13.3 wt%; and some, to 12.8 wt% of hydrogen. Likewise, Sullivan (1987) reported that fuels hydrotreated to meet combustion specifications should meet other specifications such as viscosity or freezing point.

A typical strategy for upgrading would include distillation of a heart-cut about 220-350°C. Severe hydroprocessing can be applied e.g., about 400°C and 2500 psig with a suitable nickel-containing catalyst. In some cases, it may be preferable to desulfurize first with a Co/Mo catalyst to improve the efficiency of the hydrogenation stage (Hawk et al., 1965). In addition it would be beneficial to hydrocrack 3-ring structures, phenanthrene, to 2-ring structure while limiting cracking of bicyclics.

Certain general observations can be made for the hydrogenation of a naphthalene heart-cut to low aromatics. First, the severe conditions noted above will essentially remove heterocyclic compounds from the products well before the <20 LV% aromatics specification is met. Therefore, there is no need to calculate incremental hydrogen consumption, but only a total consumption for given heteroatom content (Hawk et al., 1965; Eisen and Tice, 1977). Second, saturated and partially saturated bicyclics will dominate product composition. The degree of hydrogenation thus represents the extent of aromatic rings within a fairly stable, predictable molecular environment.

The objective of this study was to predict hydrogen consumption for conversion of a defined coal derived liquid to usable high density fuels. Literature on hydrogen consumption for upgrading coal derived liquids is extremely sparse. Many investigators do not determine hydrogen consumption in their studies. An excellent article published by Letort (1962) gave a clear picture of feed and product compositions and material balanced yields. The paper also reported hydrogen consumption for production of a high density jet fuel meeting JP-5 specification. Sullivan (1983) performed an extensive hydrotreating studies on upgrading a variety of coal derived liquids and determined the hydrogen consumption and jet fuel properties. Our analysis and subsequent predictions of hydrogen consumption are based on Letort's results with appropriate supporting data from Sullivan and others. This approach should be quite realistic for potential upgrading of bicyclic-rich coal derived heart-cuts.

EXPERIMENTAL

The analysis presented in this study is based almost entirely on literature data, primarily reported by Letort. Letort (1962) performed a series of hydrogenation experiments on 230-310°C coal liquid distillate cut. The liquids were generated presumably in a commercial coal carbonization process. Hydrogenation experiments were performed in lab-pilot plant and commercial scale equipment. Calculations on hydrogen requirement were also performed based on the in-house data generated using a fixed-bed reactor. Detailed description of the reactor unit has been previously presented (Khan, 1987).

RESULTS AND DISCUSSION

Upgrading mild gasification liquids into high quality fuels (e.g., high energy liquids) requires that the liquids be further treated to remove sulfur and nitrogen and to increase hydrogen content. This can be done by reacting the liquids with hydrogen gas. Ideally, the hydrogen required would be a product of the mild gasification process. While the amount of hydrogen required (approximately 2,000 SCF/bbl of liquids) is relatively low for the mild gasification process liquids, it is greater than the 10-20 volume percent (hydrogen) normally present in the mild gasification product gas. Typically, any additional required hydrogen is produced by gasifying the product char which adds process complexity; however, a preliminary experiment indicates that a calcium oxide bed can produce sufficient hydrogen by cracking methane and other hydrocarbon in the pyrolysis off-gas. In this experiment the gas products from coal pyrolyzed at 500°C were cracked over a bed of calcium oxide at 800°C. The product gas from the calcium oxide bed contained 50 percent hydrogen, which could be sufficient to totally upgrade the mild gasification liquids. Additionally, the hydrogen sulfide in the off-gas was greatly reduced by reaction with the calcium oxide. As an alternative, carbon monoxide and methane present in the product gas can be shifted and reformed to provide additional hydrogen.

Two approaches were used for hydrogen consumption calculation: (1) a simple approach using the H/C ratio of the feed and product streams; and (2) a more complex approach using molecular types in the feed.

In the simplified approach, hydrogen requirements for converting tars from different coals into usable liquids with H/C of 2. Table 2 presents the yields and analyses of tars from various coals from the fixed-bed reactor. Hydrogen consumption for upgrading the tars from fixed-bed reactor is compared to those from fluidized-bed reactor (Tyler, 1980; and Yeboah, 1980), from heated-grid reactor (Suuberg, 1979). Results on the hydrogen requirements (in gm of hydrogen needed to upgrade 100 g of raw pyrolysis liquids to a product with H/C of 2.0), from this comparison are plotted against the H/C in tars and coals as shown in Figure 1. It is noted from Figure 1 that an increase in hydrogen consumption occur with the decrease of H/C ratio of the raw tars. Figure 1 data also demonstrates that the liquids from the high heating rate processes such as fluidized bed and heated grid, have a smaller H/C ratio than those from a fixed bed reactor, which is a slow heating process.

Hydrogen consumption was also determined for a 180-280°C coal tar cut (Hawk et al., 1965) using this simplified approach. By material balance on the hydrogen content in the feed, product gas and product streams, hydrogen consumption of 5.16 SCF/100 lb of feed is estimated. This is in general consistent with the reported values.

In the second approach, the molecular structure and content for a 230-310°C coal tar distillate cut drawn from Letort's data were shown in Table 3. In this analysis the composition reported in Table 3 were taken as representative of the aromatic portion of a feedstock. For simplicity we are using this 100% aromatic-heteroatomic blend. In effect we are assuming that the saturated materials are carried through any given process as a diluent. Therefore one would use the methods presented here to calculate hydrogen consumption of the aromatic-heteroatomic portion and adjust results to reflect overall hydrogen

consumption on a "total barrel" basis. Table 4 shows expected reactions for hydrogenation and cracking of feedstock components. Note that phenanthrene is effectively converted to decalin.

In our analysis we have used the given feed, product compositions, yields, and reaction types outlined in Tables 3 and 4 to construct Tables 5a and 5b. This gives the distribution of products from each feed component upon upgrading. A number of modest assumptions were made regarding the material balancing of various ring structures. Table 6 summarizes hydrogen consumption calculations for the original base case from Letort (1962) leading to 19.82 LV% aromatic in the jet fuel cut.

In our analysis we have combined several pieces of information from Letort (1962). Letort hydrogenated a feed of the Table 3 composition to 10.2 LV% aromatics. He also reported a product component distribution. Using this product distribution as a guide we have estimated product distribution for a case of about 20 LV% product aromatics. (This aromatic content would be more in line with jet fuel specifications.) Essentially we assumed that the ring structure and degree of cracking between the two cases would be very similar with the main difference lying in a quantitative difference in the content of aromatic molecules. Working directly from the product distribution reported by Letort we doubled the content of aromatic products and accordingly decreased the amount of saturated product components. We then performed a lb mole balance analysis for the conversion of feed components to product components. This appears in Table 5a. We then determined the lb moles of H₂ consumption to convert each lb mole of feed component to the respective product components. We present the hydrogen consumption for each product component in Table 5b.

In more detail, Table 5a presents an estimated product distribution for the hydrogenation of 100 lb of an aromatic feed described in Table 3 (Letort, 1962). Along each row are product components resulting from the hydrogenation of each feed component, listed on the left. For example, 0.328 lb moles of naphthalenes and alkyl naphthalenes enter as feed, of which 0.214 lb moles are converted to decalins; 0.0168 lb moles, to alky lindanes; and so forth. The total product components in each row equals the lb moles of feed, except where the feed molecule cracks into two molecules as noted by "x2" below the product amount.

From the product distribution estimates in Table 5a we calculated hydrogen consumption as presented in Table 5b. Values shown are estimated lb moles H₂ consumed to convert feed components listed in the left hand column to the product components listed along each row. H₂ consumption was estimated by multiplying the lb moles for each product component in Table 5a by the lb moles H₂ required to convert the feed component (left hand column) to the product component in the same row. For example 0.328 lb moles naphthalenes/alkyl naphthalenes enter as feed and 0.214 lb moles are converted to decalins with 5 lb moles H₂ required for each lb mole converted. Multiplying 0.214 X 5 = 1.07 lb moles H₂ consumed, listed under the column labeled "Decalins."

We also applied this estimation technique to Letort's data. We estimated a hydrogen consumption of 16.19 SCF/lb feed at 10.2 LV% product aromatics and a

product density (based on component densities) of 0.8696 g/cc. Letort (1962) reported 15.8 SCF/lb feed and 0.886 g/cc.

In order to estimate incremental hydrogen consumption we started with the initial case of 19.82 LV% aromatic in the product. The hydrogen consumption was then calculated for a case of 10.2 LV% product aromatics and the difference was calculated. Dividing by the change in aromatics gave an average incremental hydrogen consumption per LV% aromatics in the range of interest.

The average incremental hydrogen consumption, calculated is about 32 SCF/LV% aromatics/bbl in the 10-20 LV% range. This is comparable to the "rule of thumb" value (25 SCF/LV%aromatic/bbl) applied to petroleum distillate fractions. Note that once the fuel has been hydrogenated to about 20 LV% aromatics the hydrogen consumption for heteroatom removal approaches zero. Also note that in the original case much of the biphenyl cracks to a light cut (B.pt.<150°C) or gas. This is undesirable due to hydrogen consumption and destruction of a fuel component. The saturated dicyclohexyl has a heating value/ml about 12% higher than that for JP-6 (Letort, 1962).

It is very likely that satisfactory hydrogenation can be achieved with much less cracking. Hawk et al. (1965) hydrogenated comparable liquids with only 1.7 wt% loss to gases versus about 10% by Letort (1962). Sullivan (1983) reported losses to C₄ of less than 0.5%. Thus an optimum process should promote cracking of 3- to 2-ring species but suppress as much as possible the cracking of biphenyl. The benefits are threefold: (1) hydrogen consumption is lower than the other cases, (2) aromatics are lower, at 16.8 LV%, and (3) fuel cut yield is higher, at about 100 lb versus 85.5 lb for the two previous cases that exhibited the relatively large extent of cracking consistent with Letort's observation. Hydrogen consumption for three cases was considered by Letort, representing hydrogen consumption for a 100% aromatics feed to low product aromatics concentration of 10-20 LV%. On a barrel basis this would amount to about 5,000 SCF/bbl, a very high value. Sullivan (1983) gave more representative values, i.e. from 700-2,550 SCF/bbl, for a number of coal liquids hydrogenated to 20 LV% aromatics.

One should recognize that hydrogenation to about 20 LV% aromatics and consequently about 0 LV% heteroatoms is literally a given requirement. Further hydrogenation would be used to meet the remaining specifications, e.g., smoke point. Excessive hydrogenation must be minimized to conserve hydrogen and because hydrogenation generally reduces density.

The relationship between aromatic saturation and liquid properties is an interesting topic. Letort (1962) reported that his fuels ranged from 0-11 wt% aromatics and met freezing point and viscosity specifications for JP-5. Results from Eisen and Tice (1977) who used syncrudes from Utah and west Kentucky coals reveal the impact of percent aromatics on properties such as freezing, flash, and smoke points.

Comparing the data for each coal in the two aromatics ranges shows little change in physical properties below 25 LV% aromatics. Only smoke point and density change modestly. What this shows is that hydrogenation alone can be used to meet aromatics LV% and smoke point specifications. However, once aromatics have been reduced to about 20 LV%, properties such as flash or

freezing point will depend on more subtle characteristics of the mixture of molecular structures.

SUMMARY AND CONCLUSIONS

Based on a review of literature it appears that specific information on hydrogen consumption appears to be limited for upgrading of pyrolysis liquids. The appropriate tar fraction for upgrading to jet fuel is the 220-350°C cut which is composed of mainly aromatics with 2-ring structures with a minor amount of phenanthrene.

To achieve about 20 LV% product aromatics results in almost total heteroatom removal during the hydrogenation of aromatics.

For a 100% aromatic feed stream hydrogen consumption will be approximately 15.33/lb feed to yield 20 LV% product aromatics. However, typical values for actual coal liquids will range from 70-2,500 SCF/bbl. Suppression of cracking, perhaps through catalyst choice, could potentially reduce hydrogen consumption by 10-20% and improve product yields.

Incremental hydrogen consumption is about 30-32 SCF/bbl/LV% aromatics in the 10-20 LV% product aromatics range.

Additional aromatic saturation in the 10-20 LV% product aromatic range affects transport properties little, but does modestly affect smoke point and density.

Excessive hydrogenation must be avoided through choice of process conditions and catalysts because it wastes hydrogen and decreases density. Hydrogen content (12.8-13.3 wt%) may serve as the decisive specification for jet fuel quality.

It is important to crack phenanthrene to meet product specifications, e.g., viscosity, but biphenyl cracking should be suppressed. This conserves hydrogen and increases product yields with the saturated bicyclohexyl form, a high density fuel component.

ACKNOWLEDGEMENT: A portion of this study was performed at the US Department of Energy, Morgantown Energy Technology Center (by MRK, see ref 5).

REFERENCES

1. Antoine, A. C., and J. P. Gallagher. 1977. "Jet Fuels from Synthetic Crudes," Coal Processing Technology, vol. 3, P.107-114.
2. Arnold, M. St. J., and P. F. M. Paul. 1980. "Aviation Fuels from Coal," Journal of the Institute of Energy, June:55-62.
3. Eisen, F. S., and J. D. Tice. 1977. "Gas Turbine Engine Fuel from Synthetic Crude," Coal Processing Technology, vol. 3, P.115-121.
4. Hawk, C. O., and others. 1965. Hydrorefining Coal-Oils to Fuel for Supersonic Aircraft. U.S. Bureau of Mines, Rep. Invest. No. 6655.
5. Khan, M. R., March 1986. Production of a High-Quality Liquid Fuel from Coal by Mild Pyrolysis of Coal-Lime Mixtures. 13 pp. DOE/METC/86-4060. NTIS/DE86006603. Also, Khan, M. R., 1987, Fuel Science and Technology International, 5(2).

6. Letort, M. 1962. "Now-Make Jet Fuels from Coal," Hydrocarbon Processing and Petroleum Refiner 41(7):83-88.
7. Masters, A. I. and others. March 1987. Additional Development of the Alternate Test Procedure for Navy Aircraft Fuels, Final Report for Naval Air Propulsion Center, Trenton, N.J., NAPC-PE 160C.
8. Moses, C. A. and others. August 1984. An Alternate Test Procedure to Qualify Fuels for Navy Aircraft. Phase II, Final Report for Naval Air Propulsion Center, Trenton, N.J. NAPC-PE-145.
9. Stein, T. R., S. E. Voltz, and R. B. Callen. 1977. "Upgrading Coal Liquids to Gas Turbine Fuels. 3. Exploratory Process Studies," Industrial and Engineering Chemistry Product Research and Development 16(1):61-68.
10. Suuberg, E. M. W. Peters, and J. Howard. 1979. Combustion Symposium (International), The Combustion Institute, p.117.
11. Sullivan, R. F. November 16-17, 1983. "Refining of Syncrude from Direct Coal Liquefaction Processes," Paper Presented at DOE Direct Liquefaction Contractors Project Review Conference, Pittsburgh, PA.
12. Sullivan, R. F. April 5-10, 1987. "High-Density Jet Fuels from Coal Syncrudes," Paper Presented at Symposium on Structure of Future Jet Fuels, ACS Meeting, Division of Petroleum Chemistry, Denver, CO.
13. Tyler, R. 1980. Fuel, 59, 218.
14. Tamas, J. 1986. "Determining Physical Properties for Multicomponent Hydrocarbon Mixtures," Chemical Engineering September:103-108.
15. Yeboah, Y. D. and others. 1980. Industrial and Engineering Chemistry Process Design and Development, 19(4), pp. 646-653.

Table 1
JP-5 Specifications
(Eisen and Tice, 1977)

Distillation, °F:		
10%.....	400	max
E.P.....	550	max
Gravity, °API.....	36-48	
Freezing Point, °F.....	-51	max
Aromatics, Vol.%.....	25	
Smoke Point, mm.....	19.0	min
Flash Point, °F.....	140	min
Viscosity, cSt -30°F.....	16.5	max

Calculated hydrogen requirements for converting coal pyrolysis tars into usable liquids (with H/C = 2) presented as a function of tar H/C and feedstock H/C. Pyramids: Fixed-bed (this study) of tar H/C and feedstock H/C. Star: Tyler, fluidized bed (600°C) reactor tar (500°C). Square: Suuberg, heated grid (540°C) bed (540° and 650°C). Club: Yeaboah, fluidized

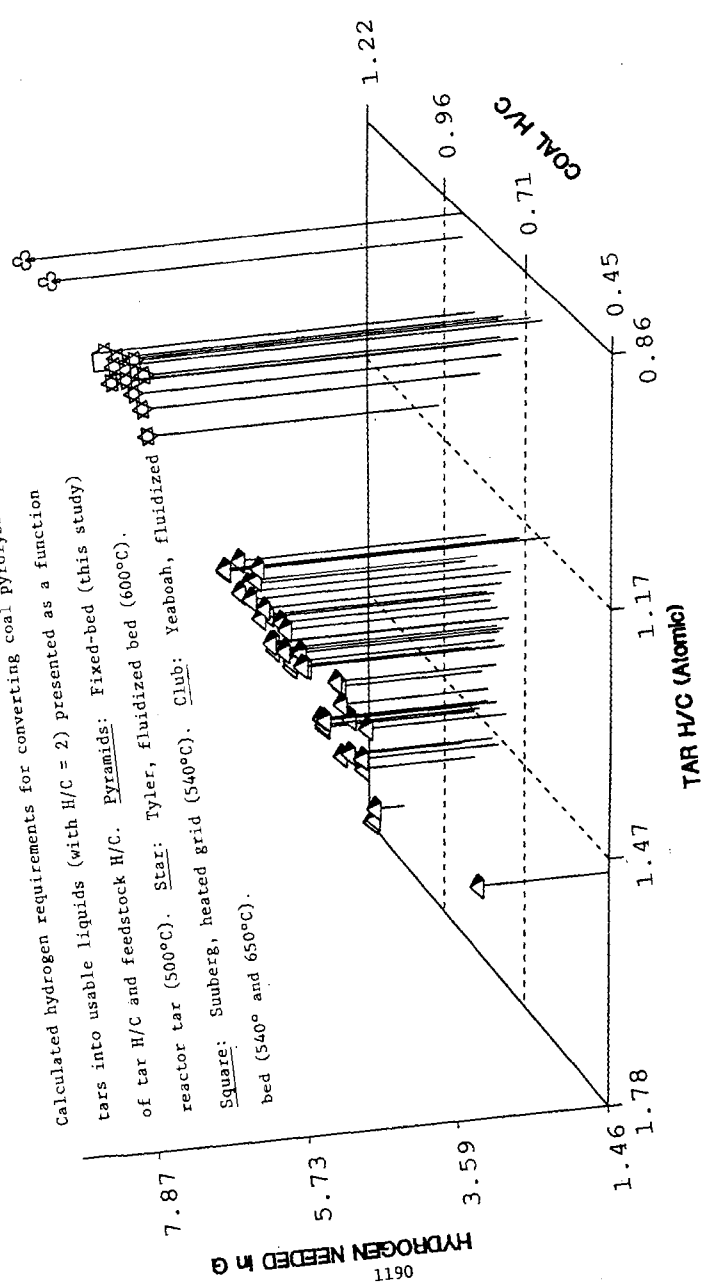


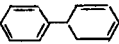
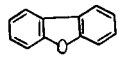
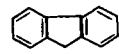
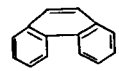
FIGURE 1

TABLE 2
Yield and Analyses of Liquids Generated from Various Coal
in the Fixed-Bed Reactor

OBS	Sample	Rank	Tar*	Gas (L)	Char*	Tar H	Tar C	H/C
1	PSOC 123	hvAb	14.8	6.04	75.2	10.19	84.89	1.44
2	PSOC 181	Sub A	13.8	7.90	81.9	9.36	83.01	1.35
3	PSOC 267	hvA	14.3	7.02	75.4	8.90	85.09	1.26
4	PSOC 275	hvAb	12.6	5.58	73.6	9.58	82.38	1.40
5	PSOC 296	hvAb	15.4	6.34	76.7	9.38	83.89	1.34
6	PSOC 306	hvAb	10.3	5.88	78.1	8.66	80.32	1.29
7	PSOC 355	hvAb	12.2	7.78	75.8	8.81	81.12	1.30
8	PSOC 375	hvAb	15.2	7.04	75.3	8.66	79.37	1.31
9	PSOC 1109	hvCb	25.0	9.29	56.6	11.66	78.70	1.78
10	PSOC 1313	mbv	5.5	6.02	84.7	8.59	85.91	1.20
11	PSOC 1323	hvBb	14.9	9.30	71.5	8.59	73.10	1.41
12	PSOC 1443	Sub C	10.5	9.80	66.6	10.33	80.93	1.53
13	PSOC 1445	hvC	14.1	9.80	69.5	10.78	84.51	1.53
14	PSOC 1448	hvAb	15.7	7.10	76.5	10.41	84.93	1.47
15	PSOC 1449	hvAb	23.6	7.12	62.3	11.06	78.04	1.70
16	PSOC 1451	hvA	14.1	3.10	80.5	8.70	82.01	1.27
17	PSOC 1469	hvAb	8.4	6.48	83.0	9.07	84.01	1.30
18	PSOC 1470	hvAb	9.2	3.82	76.8	8.22	80.08	1.23
19	PSOC 1471	hvAb	16.1	7.00	74.7	8.69	79.66	1.31
20	PSOC 1472	hvAb	14.8	8.06	76.2	9.37	86.03	1.31
21	PSOC 1473	hvAb	18.8	5.78	70.4	9.52	85.75	1.33
22	PSOC 1475	hvAb	15.8	7.84	75.1	10.08	84.58	1.43
23	PSOC 1481	hvAb	15.3	6.54	73.1	8.91	74.68	1.43
24	PSOC 1492	hvCb	13.7	7.90	70.5	8.60	74.67	1.38
25	PSOC 1499	hvAb	15.4	8.34	69.6	10.32	83.56	1.48
26	PSOC 1502	hvCb	12.7	8.40	69.9	10.01	81.07	1.48
27	PSOC 1504	hvAb	14.9	7.68	72.4	10.33	84.82	1.46
28	PSOC 1508	lv	3.2	5.50	91.0	--	--	--
29	PSOC 1516	lv	6.9	5.50	95.2	7.74	80.53	1.15
30	PSOC 1517	hvAb	14.2	8.60	75.3	8.88	79.73	1.34
31	PSOC 1520	Sub C	7.9	8.42	53.8	9.75	78.57	1.49
32	PSOC 1523	hvAb	12.7	6.30	80.5	9.25	83.66	1.33
33	PSOC 1524	hvAb	11.9	7.20	78.1	9.17	81.75	1.35
34	Pitts No. 8	hvAb	17.7	7.00	75.3	9.10	80.70	1.35
35	Ill. No. 6	hvCb	14.0	7.60	76.7	9.05	76.22	1.42
36	Ohio No. 6	hvCb	12.9	5.60	71.7	8.32	78.52	1.27
37	Wellmore No. 8	hvAb	14.2	7.00	75.6	8.76	84.30	1.25
38	AMAX	hvAb	14.1	7.70	77.1	8.53	85.86	1.19
39	N.D. Lignite	lig	4.0	11.40	64.1	9.14	75.04	1.46
40	Miss. Lignite	lig	21.3	13.00	54.2	11.40	77.80	1.76

* Tar and char yield in weight percent (dry-basis)

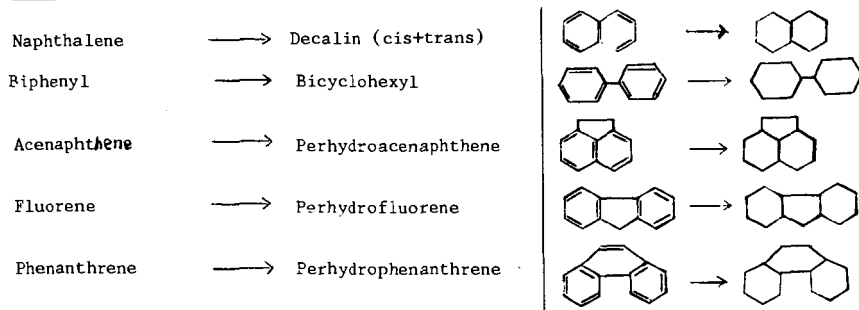
TABLE 3
 REPRESENTATIVE FEED COMPOSITION FOR COAL LIQUID AROMATICS

Formulas	Constituents	Weight %
	Light Constituents	1.1
	Naphthalene	10.3
	Quinolines	1.8 (0.2% Nitrogen)
	Alkyl Naphthalenes	38.7
	Biphenyl	5.4
	Acenaphthene	14.6
	Dibenzofuran	16.7 (1.6% Oxygen)
	Fluorene	6.9
	Phenanthrene	11
	Various Alkyl-biphenyls Alkyl-fluorenes	3.4
		<u>100.0</u>

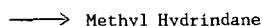
Tar fraction boiling between 230 and 310°C contains ring compounds in the quantities shown. Letort (1962).

TABLE 4
TYPICAL REACTIONS FOR COAL LIQUID UPGRADING TO JET FUEL

RING SATURATION

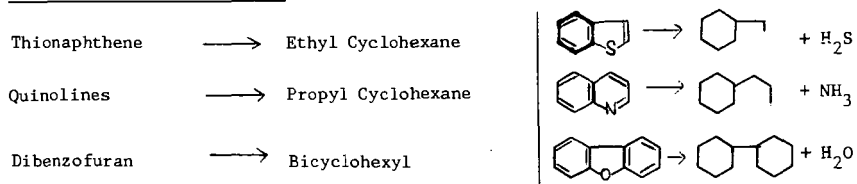


Isomerization
Decalin



Ring saturation and isomerization reactions take these forms.

ELIMINATION OF HETERO ATOMS



CRACKING

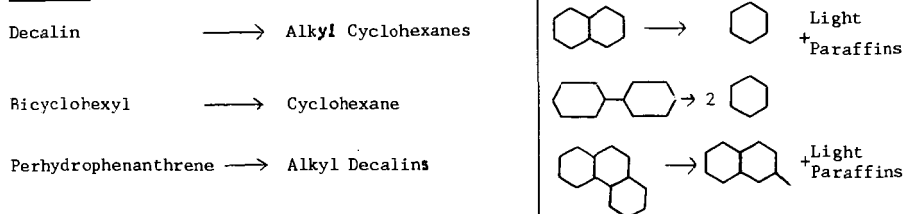


TABLE 5a

ESTIMATED PRODUCT DISTRIBUTION FROM
HYDROGENATION/CRACKING OF COAL TAR

(Values are feed, product lb moles on a 100 lb liquid feed basis)

Product Components	Feed	Alkylcyclohexanes	Decalins	Dicyclohexyl	Perhydro- acenaphthene	Fluorene	Alkylbenzene	Alkylindanes	Tetra- lins	Cyclohexyl- benzene	Tetrahydro- acenaphthene	Hydrindanes	Phenanthrene
Light Constituents	.012	.008					.004						
Naphthalenes and Alkyl-naphthalenes	.328		.214					.0168	.048			.05	
Quinolines	.014	.008					.006						
Biphenyl, Alkylbiphenyl, and Dibenzofuran	.144	.0005 x2	.026				.013 x2		.01				
Acenaphthene	.095		.041	.039				.0012	.0068		.003	.004	
Fluorene and Alkylfluorene	.051	.023 x2	.0033			.0066		.003	.0032			.007	
Phenanthrene	.062		.0375					.003	.008			.009	.004
Product Totals		.063	.3008	.026	.039	.0066	.036	.024	.066	.01	.003	.07	.004

19.8 LV% Product
Aromatics

Product Components
Feed Components

presented here is an estimated product distribution for the hydrogenation of 100 lb of an aromatic feed described in Table 3 (Letort, 1962). Along each row, are product components resulting from the hydrogenation of the feed. The total product amount from the hydrogenation of 100 lb moles of naphthalenes and alkyl-naphthalenes is 0.328 lb moles, of which 0.214 lb moles are converted to decalines; 0.0168 lb moles, to alkylindanes; and so forth. The total product components in each row equals the lb moles of feed, except where the feed molecule cracks into two molecules as noted by "x2" below the product amount.

We derived the product distribution shown here for about 20 LV% aromatics from Letort's work in which he hydrogenated the given feed to 10.2 LV% product aromatics. For the estimate we doubled the product aromatics to give the product aromatics shown above. The amount of saturated products so as to material balance with the feed component in each row. We assumed that the extent of ring opening and other cracking reactions would remain little changed between the two cases.

TABLE 5b

ESTIMATED HYDROGEN CONSUMPTION FOR PRODUCTION OF PRODUCT DISTRIBUTION IN TABLE 5a

(Values are lb moles H₂ consumed on a 100 lb feed basis)

19.8 LV% product

Aromatics

Product Components ↑

Feed Components ↓

	HDS, HDN, HDO	Alkyl-cyclohexanes	Decalins	Dicyclohexyl	Perhydro-acephthene	Fluorene	Alkylbenzene	Alkylindanes	Tetralins	Cyclohexyl-benzene	Tetrahydro-acephthene	Hydrindanes	Perhydro-phenanthrene
Light Constituents	.024						0						
Naphthalene and Alkyl-naphthalenes		1.07						.0326	.096			.35	
Quinolines	.042	.032					.006						
Biphenyl and Alkylbiphenyl	.0035			.1296			.026			.03			
Dibenzofuran	.2												
Acenaphthene			.082		.156			.0048	.0272		.006	.028	
Fluorene and Alkylfluorene	.184		.0664			.0396		.015	.016			.056	
Phenanthrene			.3375					.018	.048			.081	.028

Values shown are estimated lb moles H₂ consumed to convert feed and the product components listed along each row. Product components are listed in Table 5a. H₂ consumption was estimated by multiplying the lb moles of each product component in Table 5a by the lb moles H₂ required to convert the feed component (left hand column) to the product component in the same row.

For example 0.328 lb moles naphthalenes/alkyl-naphthalenes enter as feed and 0.214 lb moles are converted to decalines. The 0.114 lb moles H₂ required for each lb mole of naphthalene (0.214 x 5.3) is subtracted from the 0.328 lb moles H₂ consumed listed under the column labeled "decalines".

TABLE 6
SUMMARY OF HYDROGEN CONSUMPTION TO PRODUCE
PRODUCT WITH 20 LV% AROMATICS
(From feed described in Table 3)

Description of Hydrogen Consumption	H ₂ Consumed
Aromatics Saturation	2.894 lb moles
Heteroatom Removal	0.242 lb moles
Production of Light Cut (<150°C)	0.365 lb moles
Production of Gases	<u>0.770 lb moles</u>
TOTAL:	4.271 lb moles H ₂ /100 lb feed
	or 15.33 SCF/lb feed

**HIGH ENERGY DENSITY MILITARY FUELS
BY HYDROPROCESSING OF COAL PYROLYZATES**

Marvin Greene, Steven Huang, Vincent Strangio, James Reilly
LUMMUS CREST INC
Bloomfield, NJ 07003

INTRODUCTION

Lummus Crest Inc. (LCI), a subsidiary of Combustion Engineering Inc., successfully responded to a DOE-Morgantown Energy Technology Center (METC) solicitation for development of high energy density fuels from mild gasification coal liquids and other selected synfuels and is currently carrying out a multi-year test program at its Engineering Development Center. With Amoco Oil Company as a major subcontractor, LCI's program is directed towards the determination of the minimum processing requirements to produce high energy density distillate fuels for use in military aircraft and/or diesel-powered vehicles.

The specific objectives of the program are:

- o Conduct a technical and economic assessment of promising processing and upgrading methods to convert raw liquid products from mild coal gasification and other selected synfuel processes into advanced high volumetric energy density test fuels;
- o Conduct screening tests of alternative processing methods; and
- o Generate test quantities, ca., 100 gallons each, of two advanced fuels from mild coal gasification liquids and from Colorado shale oils provided by DOE contractors for a Phase I program and from two additional synfuels to be specified for an optional Phase II program.

BACKGROUND AND STATEMENT OF PROBLEM

METC has recently been reassessing the technologies for best utilizing our domestic coal resources to provide for the future demand for transportation fuels and generation of clean power. Much of the technological strategies has been unidimensional, i.e., development and marketing of coal utilization technologies that produce a main product such as liquid boiler fuel, refinery syncrude, desulfurized clean coal, etc.

As part of its assessment, METC has concluded that there is a technology type, referred to as Mild Coal Gasification (MCG), which has the potential to simultaneously satisfy the transportation and power generation fuel needs in a most cost-effective manner. MCG is based on low temperature pyrolysis, a technique known to the coal conversion community for over a century. Most past pyrolysis developments were aimed at maximizing the liquids yield which results in a low quality tarry product requiring significant and capital intensive upgrading.

By properly tailoring the pyrolysis severity to control the liquid yield-liquid quality relationship, it has been found that a higher quality distillate-boiling liquid can be readily "skimmed" from the coal. The resultant liquids have a much higher H/C ratio than conventional pyrolytic tars and therefore can be

hydroprocessed at lower cost. These liquids are also extremely enriched in 1-, 2-, and 3-ring aromatics. The co-product char material can be used in place of coal as a pulverized fuel (pf) for power generation in a coal combustor. In this situation where the original coal has a high sulfur content, the MCG process can be practiced with a coal-lime mixture and the calcium values retained on the char can tie up the unconverted coal sulfur upon pf combustion of the char. Lime has also been shown to improve the yield and quality of the MCG liquids.

Aviation turbine fuels represent less than 10 percent of the refinery production in the U.S. The growing scarcity of light sweet petroleum crude could impact the future availability of a minor refinery product such as jet fuel. Thus, alternate feedstocks such as coal liquids, shale oils and tar sands bitumen, may eventually be utilized as feedstocks for distillate fuels.

Future aircraft, military as well as commercial, may need to meet certain performance criteria such as extended flying range or need to fly at supersonic or hypersonic speeds. Similarly, future military land vehicles may need to have extended ranges between fuel reloading. With the exception of selected relatively low volume refinery streams (e.g., rerun reformates, pyrolysis gas oils), the bulk of petroleum-derived turbine fuels contains a significant concentration of aliphatic materials. These paraffinic compounds do not possess the desirable specific gravity-calorific value or the endothermic (dehydrogenation ability) characteristics of those of cyclic compounds. These latter cyclic or naphthenic materials, whose precursors can be single or multi-ring aromatics, are the only known and practical hydrocarbons that meet the high energy volumetric density and/or endothermic properties required for the advanced High Energy Density Fuels, hereinafter referred to collectively as HEDF.

Thus, there is a beneficial synergism between the distillable aromatics-rich liquids produced by mild gasification and the production of advanced HEDF.

While the MCG liquids are enriched in the HEDF precursors, namely, 1-, 2-, and 3-ring aromatics, they must be processed in such a manner as to generate a product meeting all environmental and technical specifications for HEDF aviation turbine and diesel fuels. LCI, as a process technology firm, has developed a whole family of hydrogenation processes for hydroprocessing various refinery and petrochemical streams from C₄'s all the way to vacuum residua, utilizing both fixed-bed and expanded-bed hydroprocessing reaction systems. The latter system is of special importance for feedstocks contaminated with trash metals and/or for reactions requiring critical heat removal due to the severe exothermicity of the hydroprocessing reactions. LCI's general approach consists of a combination of mid-distillate hydrotreatment; atmospheric resid or VGO hydrocracking; delayed coking of the atmospheric resid portion of the synfuel liquids. Selection of the optimal processing routes will be identified by use of Amoco's refinery linear programming models.

The MCG liquids contain significant heteroatom content in the form of phenols, aromatic sulfur compounds, pyridines and other organic nitrogen compounds. These materials have to be processed in such a way as to remove the heteroatoms without dearomatizing the ring structure and at conditions that will minimize hydrogen consumption. Although it may be possible to utilize one catalyst having all the required functionalities, i.e., HDN, HDS, HDO and ring saturation, and charged in a single reaction system, an overall loss in selectivity and activity will probably result. It may therefore be more cost effective to segregate the process

functions into separate stages thereby allowing the utilization of more selective and active catalysts for the heteroatom removal and the aromatic ring saturation steps.

The proposed technical approach for the distillate hydrotreating step is to identify the optimal reaction conditions for each step of the two-step process (heteroatom removal followed by ring saturation). The identification of the preferred catalysts in each stage is a key component of the program. Focus will be placed on determining the minimum processing steps including necessary separation or recycle systems to produce the advanced HEDF.

HIGH ENERGY DENSITY FUELS

Three advanced HEDF types have been defined for the program by the DOE:

Category I - Aviation Turbine Fuel

This advanced fuel is defined as one having a Lower Heating Value (LHV) in excess of 130,000 Btu/gal and having high thermal stability. For comparison, conventional JP-4 turbine fuel has an LHV of only 119,400 Btu/gal and typical kerosene has a value of about 123,000. Decalin, an unsubstituted 2-ring cycloparaffin, has an LHV of 135,400 Btu/gal and an alkylated decalin has an LHV of 134,950 Btu/gal. This Category I advanced fuel must conform to the operational requirements reflected in the DOD fuel specifications for JP-4 and JP-8 but with necessary chemical composition variations required to achieve the desired higher volumetric energy densities and/or to reduce the required processing severity.

Category II - Endothermic Turbine Fuel

This advanced fuel must have a high energy density value but also must have those properties to make it a satisfactory fuel for use in advanced hypersonic aircraft. At hypersonic speeds, significant thermal problems arise due to the effect of stagnation temperature, the latter being the resultant temperature due to the resistance of the air molecules impeding the motion of the vehicle. Heat can be removed by either a mechanical refrigeration system; a non-combustible coolant; or by the fuel itself, the latter being the most preferred. Three types of endothermic processes can be used depending upon fuel type: a) catalytic dehydrogenation of naphthenes; b) thermal cracking of various hydrocarbons; and c) depolymerization of polymers. All of these systems have varying heat sink limits and the prior R&D reported in the literature (1) has pinpointed the naphtha dehydrogenation route as a preferred endothermic mechanism. Typical compounds having good heat sinks include methylcyclohexane(MCH), methycyclopentane(MCP), decalin, dicyclohexyl, etc. Compounds of these types or their unsaturated precursors might exist in the Mild Coal Gasification liquids at some appreciable concentrations to result in the production of a reasonable yield of the Category II advanced fuel.

Category III - High Energy Diesel Fuel

This advanced fuel must meet DOD's diesel spec VV-F-800D and have an energy density comparable to that of the Category I turbine fuel thus allowing extended driving range for military vehicles such as tanks. This spec has no volumetric energy density limitation per se, but the Cetane No. spec can be affected by hydrocarbon type, in particular, aromatics, and the latter will affect the

resultant energy density of the fuel. The three grades of VV-F-800D diesel fuel, namely, DF-A, DF-1 and DF-2, have varying operability characteristics pursuant to the climactic specification. Grade DF-A, Arctic grade, has the lowest viscosity requirement and distillation end point limit. Back-end diesel cut blending to achieve the desired high volumetric energy density will have to be balanced against front-end blending to insure that the Distillation End Point, Viscosity and Carbon Residue specifications are not violated.

PROGRAM METHODOLOGY

Eight contract work tasks were defined with the bulk of the experimental testing consolidated into Tasks 3 and 5. Task 3 consists of a screening program to collect process operating data for each of the candidate processes over a relatively wide range of conditions. These data will be used as the input to the Task 4 modeling studies being performed by Amoco for the purpose of identifying the near optimal commercial processing sequences. Based on the latter, the Task 5 pilot plant program will be carried out to produce 100-gal each of two types of advanced HEDF fuel for each candidate synfuel feedstock. Resultant samples as well as liter quantities of test samples produced during the screening task will be delivered to DOE contractors for further evaluation.

Two feedstocks have been identified for the Phase I program: a mild coal gasification liquid and a Colorado shale oil. These liquids were required in 1000-gal quantities and therefore they had to be obtained from relatively large scale pilot or commercial plants. Since MCG technology is currently being scaled up from the laboratory or bench scales, DOE elected to provide a commercially available material having properties comparable to those anticipated for the MCG process. The resultant MCG liquid provided to LCI was derived from the British COALITE Process. The latter is a low temperature carbonization process developed in the early 1900's (2) based on the use of a vertical retort. A COALITE plant built in 1936 at the Bolsover Works of Coalite and Chemical Products Ltd. is still in operation and the 1000-gal sample was procured and delivered to LCI by United Coal Company Research Corporation under a separate DOE-METC contract. Table 1 is a summary of the properties of the whole range COALITE and the nominal 300-650F mid-distillate fraction which served as the feedstock for fixed-bed hydrotreating. The COALITE was produced from a medium coking British coal and is expected to have properties similar to those of U.S. Eastern bituminous coals. The balance of this paper will review the process variables scan testing of the fixed-bed hydrotreatment of the 350-650F COALITE mid-distillates.

The fixed-bed hydrotreating unit consists of a two-stage, close-coupled, fixed-bed reactor system equipped with high pressure liquid and gaseous (hydrogen) feed systems and a product recovery system. Each reactor contains about 100-150 cc of catalyst and both reactors can be operated in series or the second reactor can be bypassed with only the first reactor in use. To date, three catalyst types are being evaluated: a nickel tungsten; a promoted nickel tungsten; and a nickel moly.

The major technical challenge to achieving the minimum energy density specification is the addition of hydrogen to the mid-distillates in such a way that the rate of decrease in specific gravity upon hydrogenation does not exceed the rate of increase of gravimetric heat content. Otherwise, the net volumetric energy density will deviate from the target. Catalysis and operating severity must be controlled to minimize ring opening as well as to minimize hydrogen-consuming gas forming reactions.

In evaluating the process screening data, we found good correlations between the Refractive Index (R.I.) and the other HEDF fuel properties of interest, namely, volumetric energy content, API gravity, hydrogen content, Smoke Point, Cetane Index, Luminometer No., aromatics content, etc. Figure 1 maps the interaction of the API gravity-R.I. relationship vs. the predicted volumetric energy density expressed as lower heating value (LHV). Upon interchanging the API and the R.I. axes (Figure 2), we can see the extent of the hydrogenation on the whole distillate LHV for a series of hydrotreating tests made with the nickel tungsten catalyst. The slope of the regressed data is slightly skewed to the lines of constant LHV. It would appear that at hydrogenation severities resulting in whole distillate product R.I.'s below about 1.49, continued hydrogenation to reduce heteroatoms and smoke-forming aromatics results in excursions away from the LHV target of 130,000 Btu/gal.

However, it is important to appreciate that other jet and diesel properties besides energy density need to be met, such as for example, flash point and freeze (or pour) point, if the HEDF fuel is to be successfully implemented. The original test distillate feedstock was arbitrarily defined as a nominal 350-650F fraction. During hydrotreatment, the heteroatoms, in particular, phenolics and cresylics, are hydrogenated to their cyclic hydrocarbon counterparts and these materials (e.g., cyclohexane, methylcyclohexane). These have boiling points below those in the 350-650F starting material and adversely affect the flash point properties. Furthermore, the selected end point of 650F was apparently too high because it resulted in high freeze points for the whole distillate product. Accordingly, a post-hydrotreating fractionation operation is required to top and tail the material in order to meet the volatility and freeze point properties of HEDF fuels.

Table 2 shows the properties of distillate products recovered from the topping and tailing of the hydrotreated 350-650F COALITE distillates. Even though the whole hydrotreated distillate products from these runs had energy densities some 2.2 to 2.8% below the target, the removal of portions of the front-end and back-end by distillation resulted in a net increase in the LHV to within 0.7 to 1.3% of the 130,000 Btu/gal target. While the removal of the lighter front-end for flash point adjustment increases the LHV to above the target, the simultaneous removal of the heavier back-end for freeze point adjustment reduces the specific gravity with a resultant net LHV fractionally below the target. In tailing the two products shown in Table 2, we apparently removed too much of the back-end causing freeze points (-54 to -57F) better than the -40F spec. Easing off on the tailing operation should increase the LHV to within less than 0.5% of the target. We also are investigating other hydrotreating catalysts that have the potential for further improvements in selectivity towards the desirable 2-ring cyclics in order to meet and/or exceed the 130,000 Btu/gal LHV target.

ON-GOING AND FUTURE WORK

Nominal 350-650F distillates derived from the expanded-bed hydrocracking via LC-Finingsm of the 650F+ residual fraction of the COALITE were produced and subjected to fixed-bed hydrotreatment. Noticeable differences in severities to achieve HEDF specs were observed for the LC-Finates in comparison to the raw

(sm) LC-Fining is a service mark of LCI for engineering, marketing and technical services relating to hydrocracking and hydrodesulfurization processes for reduced crudes and residual oils.

hydrotreated distillates, with the LC-Finates being more reactive. Similar testing was carried out with coker distillates derived from delayed coking of the 650F+ COALITE. The process scanning program is also being carried out for the Colorado shale oil sample supplied to LCI by Western Research Institute. The Colorado shale oil is not as aromatic as the MCG liquids and therefore the degree of hydrogen addition is not as severe as for the case of the COALITE. However, tailoring the catalyst functionality to produce the proper mix of cyclics and aliphatics in the hydrotreated shale oil distillates is a technical challenge and is being addressed in this program.

ACKNOWLEDGEMENTS

This work is being supported by the Department of Energy under DOE Contract No. DE-AC21-88MC25020. LCI would like to acknowledge the technical and management support of Charles Byrer and Jim Burchfield of METC. We would also like to acknowledge the efforts of Lou Senario, LCI's pilot plant supervisor, and Sam Mikhail, LCI's analytical services supervisor. Supporting technical consulting by Joe Masin and Dave Soderberg of Amoco has also been beneficial to the program.

REFERENCES

- (1) Lander, H. and Nixon, A.C., "Endothermic Fuels for Hypersonic Vehicles", 15th Annual AIAA Meeting, Philadelphia (October 21-24, 1968).
- (2) G.S. Pound, "The Production of Chemicals From Low Temperature Tar", J.Inst. Fuels, Coke & Gas, (October 1952).

Table 1. Summary of Properties of Whole Range and 350-650F COALITE Distillate

	<u>WHOLE DEWATERED COALITE</u>	<u>350-650F DISTILLATE</u>
<u>Elementals, wt%</u>		
Carbon	83.56	84.00
Hydrogen	8.55	9.26
Nitrogen	1.10	0.81
Sulfur	0.85	0.73
Oxygen	5.94	5.20
H/C Atomic Ratio	1.23	1.32
Specific Gravity @ 60F	1.039	0.9923
R.I. @ 20C	-	1.5469
VLHV, Btu/gal	133,100(est.)	132,741
Con Carbon Residue, %	3.52	<0.1
<u>TYPE ANALYSIS, 1vol%</u>		
Saturates	-	24.3
Olefins	-	14.6
Aromatics	-	61.1
<u>Distillation, F</u>		
10% distilled	D-1160	D-86
30% distilled	415	422
50% distilled	543	460
70% distilled	655	504
90% distilled	771	552
End Point	-	616
	958 (87%)	652

Table 2. Summary of Analytical Inspections of Finished COALITE-derived HEDF⁽¹⁾

<u>Source</u>	<u>Test FB-47</u>	<u>Test FB-48</u>
LHV, Btu/gal	129,095 ⁽²⁾	128,295 ⁽³⁾
Aromatics, %	4.3	17.1
Specific Gravity @ 60F	0.8388	0.8504
Refractive Index @ 20C	1.4570	1.4640
Viscosity @ -4F, cs	7.5	7.0
Freeze Point, F	-54	-57
Flash Point, F	115	115
Aniline Point, F	136	116
Diesel Index	50.6	40.5
Smoke Point, mm	30	20
Luminometer No.	82	66
Existent Gum, mg/100 ml	4	10
Accelerated Stability, mg/100 ml	<0.1	2.0
<u>D-86 Distillation, F</u>		
IBP	311	315
10% distilled	347	352
30% distilled	390	393
50% distilled	412	415
70% distilled	448	449
90% distilled	486	486
EP	540	534

- (1) Promoters such as oxidation inhibitors, corrosion inhibitors and deicing agents are not reflected in the analyses of these samples.
- (2) Increases to an estimated 129,775 Btu/gal if Freeze Pt. is relaxed to the equivalent of a -40F max. spec.
- (3) Increases to an estimated 129,275 Btu/gal if Freeze Pt. is relaxed to the equivalent of a -40F max. spec.

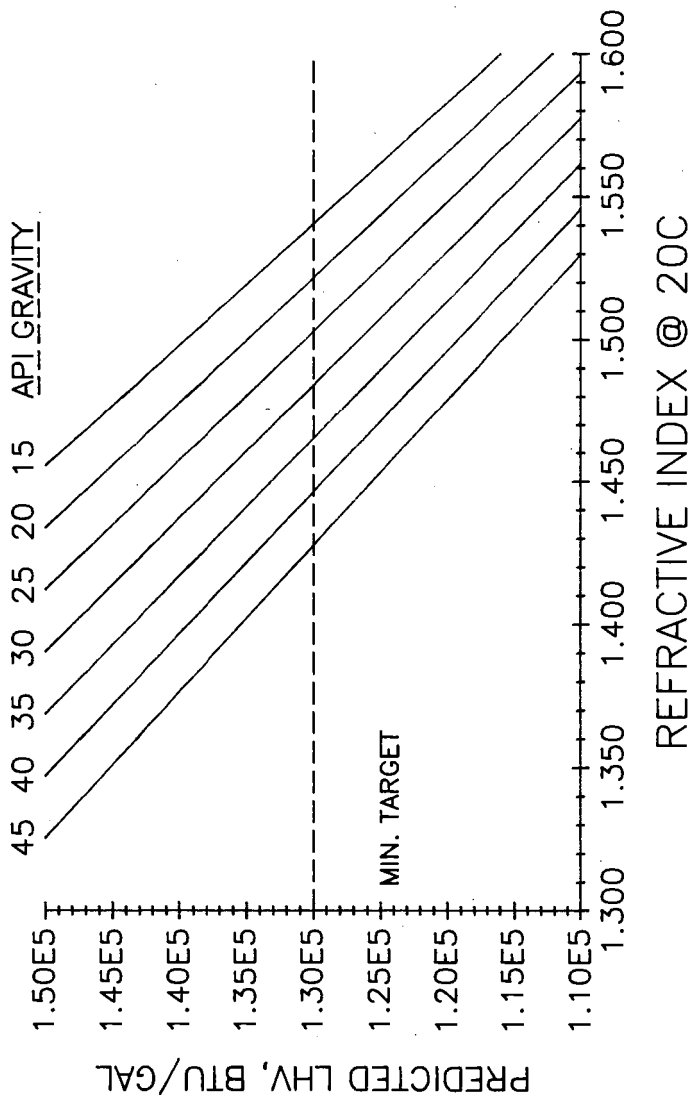


Figure 1. Predicted LHV of Hydrotreated 350-650F COALITE Distillates

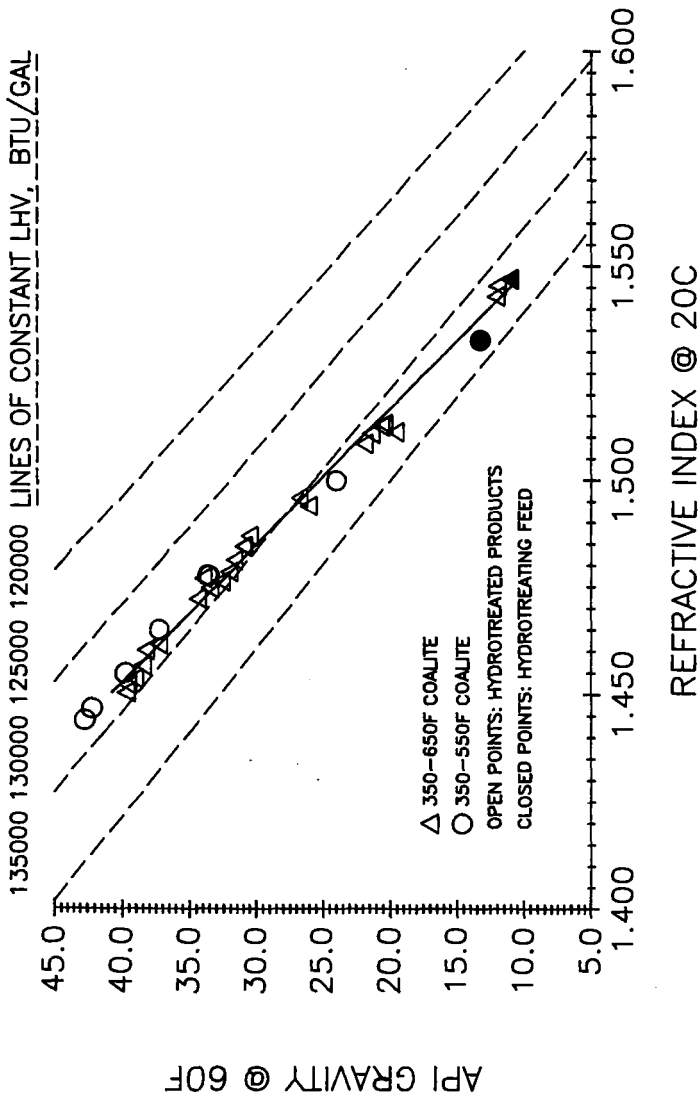


Figure 2. LHV-R.I.-API Relationships For Whole Hydrotreated COALITE Distillates

SYMPOSIUM ON PYROLYSIS PRODUCTS DERIVED FROM COAL,
OIL SHALE, TAR SANDS, BIOMASS, AND HEAVY OIL

Presented Before the
Fuel Chemistry Division
American Chemical Society
Miami Beach, Florida

September 10-15, 1989

STATUS OF THE CHARACTERIZATION OF JET
FUELS FROM COAL LIQUIDS

by

M.B. Perry, G.W. Pukanic, and J.A. Ruether
U.S. Department of Energy
Pittsburgh Energy Technology Center
P.O. Box 10940
Pittsburgh, Pennsylvania 15236

INTRODUCTION

In the future, jet fuels will need higher densities and higher heat contents. These fuels will increase the range of aircraft and/or permit heavier payloads to be transported. Furthermore, these fuels will also be required to function as heat exchange fluids to remove heat from leading edges and vital engine parts. Very stringent specifications are placed on the composition, physical and chemical properties, thermal stability, and stability upon storage of fuels for commercial and military jet engines. Of the three basic hydrocarbon types -- paraffins, naphthenes (cycloparaffins), and aromatics -- naphthenes have the most desirable properties for jet fuels. One potential source of such a fuel is coal. Many of the compounds in coal are aromatic, and coal liquefaction products are likewise highly aromatic. Coal liquids can be further hydrotreated to produce naphthenes.

Many studies have involved the production of conventional and high-density jet fuels from coal liquids [1-21]. Sullivan et al., at Chevron Research Company, Richmond, California, conducted a number of studies for the Department of Energy to assess the feasibility of refining synthetic coal liquid feedstocks to distillate fuels, such as high-density jet fuels [5-14,22-24]. The upgrading of products from single-stage processes, such as SRC-II [5,8], H-Coal [6,8,14], and EDS [7-8], and from two-stage coal liquefaction processes, such as the Lummus Crest Integrated Two-Stage Liquefaction Process (ITSL) [9-11,13-14] and the HRI Catalytic Two-Stage Liquefaction Process (CTSL) [12-14], has been carried out. "Key factors that determine how easy or difficult a particular syncrude is to refine are EP [endpoint], boiling range, hydrogen content, and heteroatom content [14]."

In September 1986, the Fuels Branch of the Aero Propulsion Laboratory at Wright-Patterson Air Force Base, Ohio, began an investigation of the potential for production of jet fuel from the liquid by-product streams produced by the gasification of lignite at the Great Plains Gasification Plant located in Beulah, North Dakota. Funding was provided to the Department of Energy (DOE) from the Air

Force to administer the experimental portion of the effort. The Morgantown Energy Technology Center administered the effort (DOE Contract Number DE-FC21-86MC11076) at Western Research Institute, which studied the potential of the liquid by-product streams for the production of jet fuels [25]. The Pittsburgh Energy Technology Center (PETC) administered the effort (DOE Contract Number DE-AC22-87PC90016) at the University of North Dakota Energy and Mineral Research Center, which characterized these liquid by-product streams [26]. The PETC also administered the effort (DOE Contract Number DE-AC22-87PC90015) of Amoco Oil Company and Lummus Crest, which conducted a preliminary analysis of upgrading alternatives for the production of aviation turbine fuels from the Great Plains liquid product streams [27]. A small research effort was also conducted in-house at PETC.

The in-house research effort at PETC sought to further characterize jet fuels produced at Chevron and the coal-derived syncrudes from which they were prepared. While some of the characterization data may replicate the work of Sullivan et al. [9,10,12,22-24], the nuclear magnetic resonance data (NMR), the low-voltage high-resolution mass spectrometric (LVHRMS) data, and the test of "fit" to correlations previously developed at PETC for narrow-boiling range coal distillates are supplemental to and amplify the characterizations performed at Chevron. Furthermore, in-house characterization of the properties of the Great Plains tar oil was carried out, including NMR and LVHRMS analyses. The tar oil was distilled and the bottoms were hydrotreated. The overhead and bottoms (before and after hydro-treatment) were similarly characterized.

Interest in the properties of these materials and of similar materials derived from tar sands and oil shale culminated in a symposium on the structure of future jet fuels presented before the Division of Petroleum Chemistry at the American Chemical Society Meeting in Denver, April 5-10, 1987. At that symposium, Sullivan gave a summary report on this investigation related to high-density fuels from coal [24]. It was also at that meeting that Knudson et al. presented results of their evaluation of jet fuels from tar oil obtained from the Great Plains Gasification Plant (GPGP) at Beulah, North Dakota [28].

The present report will compare results of analyses and correlations of properties carried out on samples of high-density fuels from the ITSL process. These samples were produced at Chevron. We will also describe in part those investigations carried out on GPGP tar oil.

EXPERIMENTAL

Samples that have been characterized at the PETC from the ITSL process include three wide-boiling-range coal-derived syncrudes and four jet-boiling-range products produced at Chevron. The syncrudes include an Illinois No. 6 coal-derived oil, and a light and heavy oil derived from Wyodak. The jet-boiling-range products include hydrotreated Wyodak light and heavy oils, and hydrotreated and hydrocracked Illinois No. 6 oils. Procedures used for upgrading the syncrudes have been reported [9-10]. Other samples that have been characterized include the GPGP tar oil stream, as well as the overhead and bottoms from distillation of the tar oil and the hydrotreated distillation bottoms of the tar oil; the North Dakota lignite used to produce the tar was also characterized.

Chemical and physical property measurements were carried out at PETC and at Huffman Laboratories (Wheatridge, Colorado); and numerous property measurements were reported by Sullivan [9-10,12,22-24]. Characterizations include simulated

distillation by gas chromatography (ASTM D2887) for boiling-point-range determination [29], CHONS elemental analysis [30-32], Karl Fischer determination of water [33], molecular weight [32], refractive index [34], specific gravity [32], viscosity [35], Carbon-13 and proton NMR [36], IR [37], low-resolution mass spectrometry with an ionizing voltage of 70 eV (ASTM D2789 type analysis was used to calculate the compound classes), and LVHRMS [38-39]. Detailed results of these analyses are the subject of an in-house report in preparation [40]. The data relevant to this report are summarized in Tables 1 through 6. Additionally, correlations developed at PETC for narrow-boiling-range coal liquid distillates [41] were applied to these samples.

The Great Plains Gasification Plant operated by the ANG Coal Gasification Company for the Department of Energy produces 150 million scf of substitute natural gas per day [26]. Three by-product hydrocarbon liquid streams -- tar oils, crude phenols, and naphtha -- are also produced. Of the three liquid streams, the tar oil stream (produced at the rate of 2900 bbl/day [27]) is thought the most appropriate for conversion to jet fuel [26]. The tar oil from the GPGP had a boiling range of 107°C to 524°C. About 20 liters of the tar oil were vacuum distilled to an atmospheric equivalent cut point of 350°C at the University of Pittsburgh Applied Research Center. About 66% of the tar oil was found in the overhead, and 34% in the vacuum bottoms. A 300-g portion of the 350°C+ bottoms was hydrotreated in a 1-liter batch autoclave at 350°C under 13.6 MPa H₂ (3 scf/hr) using a presulfided Shell 324 catalyst for one hour. Five runs were made and a total of 1500 g of product hydrotreated.

RESULTS AND DISCUSSION

Coal liquids derived from two-stage processes were lower in oxygen and nitrogen, and for a given boiling range, Sullivan found these liquids easier to upgrade than products from single-stage processes [14]. The properties of jet-fuel products, consisting mostly of cyclic hydrocarbons, were virtually the same from both the single-stage and two-stage processes. For all processes evaluated at Chevron, the jet-fuel products had high densities and high volumetric energy contents. The Wyodak CTSL light oil [12] was easier to upgrade than the other syncrudes, apparently because of its low-boiling-point end point, higher hydrogen content, and lower heteroatom content [14]. For syncrudes with a high-boiling-point end point, a successful upgrading procedure was developed that consisted of a two-step process: (1) hydrotreatment for heteroatom removal and (2) low-temperature hydrogenation for aromatic saturation [9,13,14].

The hydrotreatment process that produces the jet-boiling-range products from the coal-derived syncrudes removes heteroatoms, breaks down heavy paraffins into lighter paraffins, and hydrogenates aromatic rings, creating cyclic aliphatic functionalities. This is observed in the characterization data. The hydrogen contents of the hydrotreated products are greater than those of the syncrudes; and proton NMR, as well as carbon-13 NMR, confirms the predominance of aliphatics over aromatics in the hydrotreated product versus the predominance of aromatics in the syncrude. Results from LVHRMS and low-resolution mass spectrometry indicate a larger amount of the desirable lighter cyclic hydrocarbons in the jet-boiling-range products than in the corresponding syncrudes.

Table 3 compares properties of the four jet-fuel products prepared and characterized by Sullivan [9,10,12], and further characterized and studied here, to those of a Jet A specification fuel [13] and a high-density fuel [42]. The coal-derived jet-fuel products meet most of the Jet A and high-density fuel speci-

cations. The Illinois ITSL hydrocracked product exceeds the minimum for flash point, and the distribution of hydrocarbon types does not quite meet the specifications, although a high concentration of naphthenes is desirable. The four jet-fuel products do exceed the API gravity specifications, that is, they have higher densities than the specification fuels. This specification, however, is probably not necessary for aircraft with modern fuel-flow controllers [14]. There were previously no jet-fuel products with an API gravity below 37 that have met the other specifications [13]. The higher densities would probably be an advantage, since the fuel would have a higher volumetric energy content. These four products otherwise meet most of the jet-fuel specifications and have the desirable high naphthenic content and thus have potential for serious consideration as aviation jet fuels.

Franck et al. [43] recently concluded that two- or three-ring cycloparaffins with molecular weights in the range of 120 to 200 give the best performance in describing the different properties of jet fuels. Of the compound types that they studied, these cycloparaffins were the only ones to show simultaneously the following properties [13]:

- o high heating value by volume
- o satisfactory heating value by weight
- o excellent thermal stability
- o very low freezing point
- o low volatility, high flash point
- o acceptable low-temperature viscosity
- o acceptable flame characteristics (smoke point, etc.)

"No other hydrocarbons in the jet-boiling-range have all of these properties [13]." Analyses of the four ITSL jet-boiling-range products at PETC (Table 4) confirm that the predominant compounds classes are indeed 1-, 2-, and 3-ring cycloparaffins, and the molecular weights (Table 1) are slightly below 200. Analysis of the Wyodak Light ITSL Syncrude by LVHRMS required 31 compound types in the range C₅-C₂₁ to account for the sample, while the same analysis of the Wyodak light ITSL hydrotreated product required only 13 compound types in the range C₆ to C₁₆ to account for the sample [41]. Thus, hydrotreating this syncrude resulted in a less complex sample. Part of this loss in diversity can be accounted for by the fact that a certain distillate range was selected for the product, but in part, the diversity is lower because of heteroatom removal. Conceivably, a processing mode could be developed that would result in a product consisting of only a few compounds. The GPGP tar oil and overhead both fall in the molecular weight range of jet products, but only the overhead has the right boiling range. The GPGP overhead, however, has a high heteroatom content (37.81% C₆-C₁₂ hydroxybenzenes), as measured by LVHRMS (Table 5). The phenolic oxygen in the tar bottoms is less than half of that in the overhead (Table 2).

The GPGP tar oil, as well as the 350°C overhead and 350°C+ bottoms, is clearly very different (see Tables 1 and 2) from the coal liquefaction syncrudes evaluated by Sullivan. The twelve predominant compound types (from LVHRMS) found in the tar, the distillate overheads, and the bottoms are given in Table 5. The tar oil contains 33% of C₆-C₁₂ hydroxybenzenes, and the overheads contain almost 38%. The bottoms contain no large quantities of any compound types. The differences are most obvious in the NMR data (Table 2). Aromatic hydrogen and aromatic carbon are significantly higher in the GPGP tar oil samples. The weight percent oxygen as phenols (Table 2) is also higher in the GPGP samples. Surprisingly, the hydrotreated GPGP 350°C+ bottoms have properties very similar to the

Wyodak heavy ITSL syncrude. Presumably, this material could be further processed to produce a jet-fuel fraction that would have properties similar to the jet fraction produced by hydrotreating the Wyodak heavy ITSL syncrude. Similarly, the overheads could be hydrotreated to produce a jet-fuel-like distillate product. However, the oxygen content of the overhead fraction would require efficient heteroatom removal because oxygen functionalities have been implicated in problems with stability upon storage.

Correlations developed for narrow-boiling-range coal liquids [41] were successfully applied to the GPGP tar oil products as well as to the syncrudes and jet-boiling-range products. The results are reported in Table 6. The Illinois ITSL hydrocracked product gave the largest error when correlations were used to estimate molecular weight (15.93%) and refractive index (4.26%). An error of 7.8% resulted from estimation of the molecular weight of the tar oil, and an error of 1.32% resulted from estimation of the refractive index of the Wyodak heavy ITSL hydrotreated product. It is unclear why the hydrocracked product properties are difficult to estimate, but if this product is eliminated from the set, the average error in the estimated molecular weight is 2.37%, and the average error in the estimated refractive index is 0.49%. Khan recently reported successful applications of correlations based on refractive index to other liquids produced by coal pyrolysis [44].

Finally, bench-scale experiments conducted by Amoco have provided the basis for a process plan, established pilot-plant conditions, and produced small amounts of JP-8, JP-8X, and JP-4 jet fuels from GPGP tar oil [27]. With clay treatment and antioxidant additives, the JP-4 product was expected to meet all specifications except heating value, and the JP-8 and JP-8X were expected to meet all specifications except flash point. Two barrels of JP-8 jet fuel were jointly produced by Amoco and Lummus for evaluation by the Air Force.

CONCLUSIONS

Jet fuels can be prepared from a wide range of coal liquids produced in single-stage and two-stage liquefaction processes, as well as from by-product streams of gasification processes. The high aromaticity of coal, the very property that makes it an excellent candidate as a feedstock for high-density fuels, exacts a heavy penalty, however, in hydrogen consumption. The high heteroatom content not only consumes large amounts of hydrogen to produce mostly NH_3 , H_2S , and H_2O , but the remaining nitrogen tends to poison catalysts, and the nitrogen in jet fuel is blamed for gum formation. Oxygen compounds have been implicated in oxidative coupling reactions resulting in degradation of fuels upon storage.

In the future, with the decline in production of high-quality crudes, refiners will be pressed to process lower quality petroleum crudes. At some point then, production of jet fuels from coal will become an attractive and viable alternative. In the near term, there is still time to perform the requisite research yet remaining.

ACKNOWLEDGMENTS

The authors are grateful to Karl Waldner for assistance in the laboratory throughout this work. We gratefully acknowledge Chuck Schmidt for performing the mass spectrometry experiments; Dick Lett, Richard Sprecher, Marjorie Hough, and Paula Flenory for the nuclear magnetic resonance analyses; Adam Vayda for the distillation of the Great Plains gasifier tar oils; and Richard Hlasnik for con-

ducting the high-pressure hydrotreatment runs. We are also grateful to Gary Stiegel for copies of the contractor reports on investigations of Great Plains gasifier tar oils and for the trip to Wright Patterson Air Force Base, where we met in a planning session with the principal investigators at WRI, UNDERMC, and the Air Force.

DISCLAIMER

Reference in this paper to any specific commercial product, process, or service is to facilitate understanding and does not necessarily imply its endorsement or favoring by the United States Department of Energy.

BIBLIOGRAPHY

1. Fraser, Malcolm D., Proceedings of Third Annual Pittsburgh Coal Conference, September 1986.
2. Hibbard, R.R., and W.T. Olson, Proceedings of Conference on Fuels and New Propellants, 1964.
3. Refining Synthetic Liquids from Coal and Shale, National Academy Press, Final Report of the Panel on R&D Needs in Refining of Coal and Shale Liquids, Washington, D.C., 1980.
4. Kalfadelis, C.D., H. Shaw, and W.F. Taylor, A Preliminary Engineering Assessment of Jet Fuel Production from Domestic Coal and Shale Derived Oils, Government Research Laboratories, Exxon Research and Engineering Company, 11th IECEC.
5. Sullivan, R.F., and H.A. Frumkin, Third Interim Report, Processing of SRC-II Syncrude, March 1980, FE-2315-47.
6. Sullivan, R.F., D.J. O'Rear, and H.A. Frumkin, Fifth Interim Report, Processing of H-Coal Syncrude, September 1981, FE-2315-61.
7. Sullivan, R.F., D.J. O'Rear, and H.A. Frumkin, Ninth Interim Report, Processing of Texas-Lignite EDS Syncrude, June 1984, DOE/ET/10532-T19.
8. Frumkin, H.A., Tenth Interim Report, Revised Stock Balances and Updated Cost Estimates, May 1985, DOE/ET/10532-T23, FE-2315-115.
9. Sullivan, R.F., Eleventh Interim Report, Processing of Illinois ITSL Oil: Experimental Studies, May 1985, DOE/ET/10532-T25.
10. Sullivan, R.F., Twelfth Interim Report, Processing of Wyodak and Illinois ITSL Oil: Experimental Studies, November 1985, DOE/ET/10532-T28.
11. Frumkin, H.A., Thirteenth Interim Report, Processing of 750°F End Point Illinois ITSL Oil: Engineering Design Studies and Estimated Processing Costs, August 1986, DOE/ET/10532-T31.
12. Sullivan, R.F., Fourteenth Interim Report, Processing of Wyodak CTSL Oil and Related Experimental Studies, DOE/ET/10532-T32, August 1986.

13. Sullivan, R.F., American Chemical Society, Division of Petroleum Chemistry, Chicago Meeting, September 8-13, Preprints, Vol. 30, No. 3, pp. 503-512, 1985.
14. Sullivan, R.F., Transportation Fuels from Two-Stage Liquefaction Products, Chevron Research Company, Richmond, California; American Chemical Society, Division of Fuel Chemistry, Anaheim, Sept. 7-12, Vol. 31, No. 4, pp. 280-293, 1986.
15. Nowack, C.J., J. Solash, and R.J. Delfosse, Coal Processing Technology, Vol. 3, 1977.
16. Eisen, F.S., and J.D. Tice, Coal Processing Technology, Vol. 3, 1977.
17. Gallagher, J.P., and A.C. Antoine, Coal Processing Technology, Vol. 3, 1977.
18. Arnold, M. St. J., and P.F.M. Paul, Journal of the Institute of Energy, June 1980.
19. Hawk, C.O., M.D. Schlesinger, P. Dobransky, and R.W. Hiteshue, ROI-6655, 1964.
20. Schlesinger, M.D., and R.W. Hiteshue, ROI-5902, 1961.
21. Providing R&D Test Fuels from Alternate Energy Sources, An Assessment of Options, National Academy Press, Washington, D.C., 1983.
22. Sullivan, R.F., and H.A. Frumkin, American Chemical Society, Division of Fuel Chemistry Preprints, April 13-18, New York, 31(2), 325-339, 1986.
23. Sullivan, R.F., U.S. DOE Direct Liquefaction Contractors' Review Meeting, October 20-22, 1986, Abstracts, p. 5, Marriott Monroeville, Pittsburgh, Pennsylvania.
24. Sullivan, R.F., American Chemical Society, Division of Petroleum Chemistry Preprints, April 5-10, Denver, 32(2), 584-590, 1987.
25. Smith, E.B., F.D. Guffey, and L.G. Nickerson, AFWAL-TR-87-2042, Vol. III, May 1988.
26. Knudson, C.L., AFWAL-TR-87-2042, Vol. II, May 1988.
27. Furlong, M.W., Draft Final Report: Tasks 2 and 3 Results of Bench-Scale and Pilot-Plant Testing, Mail Station H-4, Naperville, IL 60566.
28. Knudson, C.L., W.G. Wilson, D.J. Miller, R.O. Ness, Jr., and A. Ruud, American Chemical Society, Division of Petroleum Chemistry Preprints, April 5-10, Denver, 32(2), 591-594, 1987.
29. ASTM Method D-2887-73 (1978), Standard Method of Test for Boiling Range Distribution of Petroleum Fractions by Gas Chromatography, Annual Book of ASTM Standards, Volume 05.02 (1982).
30. Houde, M., J. Champy, and R. Furminieux, J. Micro Chem., 24, 300-309 (1979).

31. Merz, W., Fresenius Z. Anal. Chem., 237, 272-279 (1968).
32. Schmidt, C.E., M.B. Perry, C.M. White, G.A. Gibbon, and H.L. Retcofsky, DOE/PETC/TR-87/4 (DE87002513), October 1986.
33. Mitchell, J., Jr., and D.M. Smith, Aquametry, 2nd Ed. Part III, 5, 107-136 (1980).
34. ASTM Method D-1218-61 (1977), Test for Refractive Index and Refractive Dispersion of Hydrocarbon Liquids, Annual Book of ASTM Standards, Volume 05.02, 10.03 (1984).
35. ASTM Method D-2170, Standard Method of Test for Kinematic Viscosity of Asphalts, Annual Book of ASTM Standards, Volume 04.03 (1984).
36. Brown, J.K., and W.R. Ladner, Fuel 39, 87 (1960).
37. Lett, R.G., C.E. Schmidt, D.H. Finseth, and H.L. Retcofsky, Appendix 2. Qualitative Determination of N-H and O-H Functional Groups in Coal-Derived Asphaltene via Near-Infrared Spectroscopy. DOE/PETC/TR-82/13, July 1982.
38. Johnson, B.H., and T. Aczel, Anal. Chem., 39, 682 (1967).
39. Schmidt, C.E., R.F. Sprecher, and B.D. Batts, Anal. Chem., 39, 2027 (1987).
40. Pukanic, G.W., M.B. Perry, and J.A. Ruether, Technical Report in Preparation.
41. White, C.M., M.B. Perry, C.E. Schmidt, and L.J. Douglas, Energy and Fuels, 1, 99-105 (1987).
42. Production of Jet Fuel from Coal-Derived Liquids, Request for Proposal Number DE-RP22-87PC90015, September 1986.
43. Franck, J.P., J.F. LePage, G. de Gaudemaris, and P. Bonnifay, Hydrocarbon Processing, 56(13), 287-289 (1977).
44. Khan, M. Rashid, Energy and Fuels, 2, 834 (1988).

Table 1. Inspection Properties of Coal-Derived Jet-Boiling-Range Products, Syncrudes, and GFCP Tar Oil, Overhead, and Bottoms.

Sample	Boiling Range of 1-5-95%	T _b mid, °F	MW	RI	Specific Gravity	Density
Illinois ITSL Hydrotreated	302-561	462	185	1.4741	0.8750	0.8742
Illinois ITSL Hydrocracked	261-545	403	192	1.4600	0.8504	0.8497
Wyodak Heavy ITSL Hydrotreated	302-566	454	187	1.4679	0.8596	0.8589
Wyodak Light ITSL Hydrotreated	359-567	484	188	1.4772	0.8840	0.8832
Illinois ITSL Syncrude	212-731	546	201	1.5314	0.9513	0.9505
Wyodak Heavy ITSL Syncrude	347-850	652	229	1.5733	1.0074	1.0065
Wyodak Light ITSL Syncrude	331-713	575	205	1.5360	0.9596	0.9588
Great Plains Tar Oil	287-873	545	187	1.5700	ND	1.0193
GFCP Tar Overhead	274-665	472	155	1.5471	ND	0.9674
GFCP Tar Bottoms	652-967	776	355	ND	ND	1.0990
GFCP Tar Bottoms Hydrotreated	517-956	738	ND	ND	ND	ND

ND means not determined.

Table 2. NMR and IR Characterization of Coal-Derived Product

Sample	H-Aromatic Fraction	H _α	H _β	H _γ	C		wt% Oxygen as Phenols
					Aromatic	C	
Illinois ITSL Hydrotreated	0.02	0.03	0.69	0.26	0.04	0.04	ND
Illinois ITSL Hydrocracked	0.01	0.02	0.61	0.36	0.00	0.00	ND
Wyodak Heavy ITSL Hydrotreated	0.01	0.01	0.69	0.29	0.03	0.03	ND
Wyodak Light ITSL Hydrocracked	0.01	0.01	0.70	0.28	0.02	0.02	ND
Illinois ITSL Syncrude	0.14	0.16	0.53	0.17	0.38	0.38	0.1
Wyodak Heavy ITSL Syncrude	0.19	0.21	0.47	0.13	0.49	0.49	0.1
Wyodak Light ITSL Syncrude	0.14	0.15	0.53	0.18	0.35	0.35	0.1
Great Plains Tar Oil	0.24	0.32	0.35	0.09	0.69	0.69	2.4
GFCP Tar Overhead	0.26	0.36	0.30	0.08	0.64	0.64	3.2
GFCP Tar Bottoms	0.22	0.22	0.45	0.11	0.66	0.66	1.5
GFCP Tar Bottoms Hydrotreated	0.15	0.23	0.48	0.14	0.49	0.49	ND

ND means not determined.

Table 3. Properties of Jet Fuel Products

Sample	Illinois ITSL		Wyodak Heavy ITSL Hydrocracked ^a		Wyodak Light ITSL Hydrocracked ^c		Jet A ^d Specification		High-Density Fuel Specification	
	Hydrocracked ^a	Hydrocracked ^a	Hydrocracked ^b	Hydrocracked ^b	Hydrocracked ^c	Hydrocracked ^c	Specification	Specification	Specification	Specification
Gravity, API	29	34	32	28	17	20	37 Min.	35 Min.		
Smoke Point, mm	19	21	21	17	20	20	20 Max.	-47 Max.		
Freeze Point, °F	<-94	<-94	<-94	<-94	100	100	40 Max.	122 Min.		
Flash Point, °F	128	107					100 Min.			
Paraffins, LV %	1	2	7	5				0-10		
Naphthenes, LV %	91	96	82	86				70-90		
Aromatics, LV %	8	2	11	9				10-30		
Viscosity at -40°F, cSt	10.2	6.2					20 Max.	12 Max.		
							8 Max.			

^aReference 9; ^bReference 12; ^cReference 10; ^dReference 13; and ^eReference 42.

Table 4. Analysis of Jet-Boiling-Range Products by Mass Spectrometry

Compound Classes, Percent	Illinois ITSL		Illinois ITSL		Wyodak Heavy ITSL		Wyodak Light ITSL	
	Hydrocracked	Hydrocracked	Hydrocracked	Hydrocracked	Hydrocracked	Hydrocracked	Hydrocracked	Hydrocracked
Paraffins	4.16	2.59	8.26	5.95				
Monocycloparaffins	20.54	53.29	39.44	35.88				
Dicycloparaffins	53.23	27.64	30.45	33.83				
Tricycloparaffins	12.92	11.88	13.27	15.80				
Benzenes	6.45	4.33	3.99	5.21				
Naphthalenes	0.31	0.14	0.23	2.76				
Indans	2.39	0.13	4.37	0.53				

NOTE: These analyses were obtained at low resolution with an ionizing voltage of 70 eV. The ASTM D2789 type analysis was used to calculate the compound classes.

Table 5. Analysis of Great Plains Tar Oil, 350°C Overheads, and 350°C+ Bottoms by LVHRMS
(Twelve Major Constituents)

Tar Oil	Overheads <350°C	Bottoms >350°C
33.00% C ₆ -C ₁₂ hydroxybenzenes	37.81% C ₆ -C ₁₂ hydroxybenzenes	7.05% C ₅ -C ₉ diolefins/cycloalkenes
11.71% C ₁₀ -C ₁₈ naphthalenes	14.72% C ₁₀ -C ₁₆ naphthalenes	6.98% C ₁₆ -C ₂₂ pyrenes
8.81% C ₆ -C ₁₅ benzenes	10.15% C ₆ -C ₁₅ benzenes	5.74% C ₁₄ -C ₂₁ phenanthrenes
4.78% C ₈ -C ₁₅ indans/tetralins	4.00% C ₅ -C ₁₀ pyridines	5.68% C ₅ -C ₉ olefins/cycloalkenes
3.70% C ₅ -C ₁₀ pyridines	3.98% C ₉ -C ₁₄ indans/tetralins	4.83% C ₁₃ -C ₂₀ hydroxyace- naphthalenes/hydroxyfluorenes
3.41% C ₈ -C ₁₄ hydroxyindenes	3.69% C ₈ -C ₁₄ hydroxyindenes	4.56% C ₁₄ -C ₂₀ hydroxyphenanthrenes
3.33% C ₁₀ -C ₁₇ hydroxynaphthalenes	3.03% C ₁₀ -C ₁₅ hydroxynaphthalenes	4.31% C ₁₆ -C ₂₂ hydroxypyrenes
3.32% C ₉ -C ₁₄ indenes	3.53% C ₉ -C ₁₄ indenes	4.40% C ₆ -C ₁₁ benzenes
2.68% C ₁₄ -C ₂₀ phenanthrenes	2.10% C ₅ -C ₉ diolefins/cycloalkenes	3.50% C ₁₂ -C ₁₈ hydroxybenzofurans/ dihydroxyfluorenes
2.33% C ₆ -C ₁₀ diolefins/cycloalkenes	1.80% C ₁₂ -C ₁₇ acenaphthylenes/ fluorenes	2.97% C ₁₀ -C ₁₅ naphthalenes
2.32% C ₅ -C ₉ olefins/cycloalkenes	1.64% C ₈ -C ₁₂ hydroxyindans/ hydroxytetralins	2.97% C ₁₈ -C ₂₄ chrysenes
2.20% C ₁₂ -C ₁₈ acenaphthylenes/ fluorenes	1.61% C ₁₄ -C ₁₈ phenanthrenes	2.85% C ₁₅ -C ₂₂ cyclopenta[def] phenanthrene/dihydropyrene

LVHRMS data taken from reference 40.

Table 6. Test of Fit to Existing Correlations Between Refractive Index, Molecular Weight, and Density

Sample	Refractive Index, n_D		Molecular Weight, M_w	
	Experimental	Calculated	% Error	
Illinois ITSL Hydrotreated	1.4741	1.4625	0.79	185
Illinois ITSL Hydrocracked	1.4600	1.3978	4.26	192
Wyodak Heavy ITSL Hydrotreated	1.4679	1.4486	1.32	187
Wyodak Light ITSL Hydrotreated	1.4772	1.4784	0.08	188
Illinois ITSL Syncrude	1.5314	1.5168	0.96	201
Wyodak Heavy ITSL Syncrude	1.5733	1.5814	0.52	229
Wyodak Light ITSL Syncrude	1.5360	1.5381	0.14	205
Great Plains Tar Oil Feed	1.5700	1.5676	0.15	187
Great Plains Overhead	1.5471	1.5466	0.03	155

^aCalculated using Equations 1 and 2 of reference 41.

^bCalculated using Equation 5 of reference 41.

Towards a deeper understanding of coal-tar pitch structure and its relation to thermally induced pitch reactivity

M. Zander
Rütgerswerke AG, D-4620 Castrop-Rauxel, FRG

Coal-tar pitch is the residue of the technical distillation of high-temperature coal-tar; it is obtained in 50 % yield, relative to crude coal-tar. Pitch serves predominantly as an important raw material for the manufacture of electrodes for electrochemical and electrothermal metallurgy (1). Moreover, it can be used for manufacturing pitch-based carbon fibres (2).

Since the appearance of the fundamental work of Brooks and Taylor (3) in 1965 of an intermediate mesophase state in the carbonization of pitches interest in pitch research has grown tremendously. It became also increasingly evident that a deeper understanding of the structure and the thermally induced (carbonization) chemistry of coal-tar pitch is of high interest from both the industrial and scientific point of view.

1. The toluene-soluble fraction of coal-tar pitch / molecular weight range and chemical structure principles

The toluene-soluble fraction ("TS-fraction") of pitch typically amounts to ca. 75 % per weight, relative to the entire pitch.

As follows from gas chromatography/mass spectrometry examination the smallest molecules present in the TS-fraction (in very low concentrations) have molecular weights of about 200 Dalton. Typical examples are: fluorene, phenanthrene, anthracene, carbazole, pyrene and fluoranthene. However, molecular mass of TS-fraction constituents cover a wide range; for example, TS-subfractions with mean molecular masses up to approximately 2200 Dalton have been isolated by a chemical method (Charge-Transfer Fractionation, see below). ¹H nmr spectroscopy revealed that these fractions are highly aromatic in nature. This leads to an important and interesting question: Are the higher-molecular TS-fraction constituents large monomeric polycyclic systems or rather oligomeric systems where medium-sized aromatic units are connected by e.g. C-C single bonds (oligo-aryl type), -CH₂-groups, ether bridges, etc.? The two possible structure models of the higher molecular TS-fraction constituents are schematically depicted in Fig.1. The circles symbolize aromatic units of different size, the lines C-C single bonds between aromatic units and -X- denotes bridging functions.

Experimental findings obtained with the higher-molecular weight TS-subfractions indicate that the oligomeric structure model is much more likely:

- Solubility in organic solvents: In spite of their high molecular weights, the materials are surprisingly readily soluble in organic solvents. The non-planar (twisted) arrangement of the aryl/heteroaryl units, due to steric hindrance, explains in known fashion the relatively good solubility of the oligomeric systems.
- Clathration ability with respect to smaller aromatic molecules: It has been observed that the higher-molecular TS-subfractions contain smaller molecules e.g., fluoranthene, pyrene, benzopyrenes, and others which in spite of their good solubility in organic solvents cannot easily be removed by extraction with e.g., toluene at boiling temperature (4). It must therefore be concluded that these smaller "guest" molecules are relatively strongly bonded to the higher-molecular

components which act as "host" molecules. Again an oligomeric structure model of the host molecules provides a much more obvious explanation of their clathration ability than a monomeric structure model can do. For an oligomeric structure it can be assumed that it contains three-dimensional "cages" which can act as traps captivating the smaller guest molecules.

- nmr spectroscopy: As discussed elsewhere (5, 6) ^1H and ^{13}C nmr spectra also support strongly the oligomeric structure model.

2. The basic character of the higher-molecular portion of the TS-fraction

Assuming a statistical distribution of nitrogen among pitch constituents it has to be concluded that the probability for finding a nitrogen containing molecule in a pitch fraction increases with increasing molecular mass of the fraction. On this assumption and in spite of the rather low nitrogen content (typically 1 %) of the TS-fraction, the higher-molecular portion of the TS-fraction may be expected to contain a relatively large amount of nitrogen-containing compounds. By treatment of a toluene solution of coal-tar pitch with gaseous HCl (at room or boiling temperature) a precipitate of hydrochlorides of organic bases is obtained in 27 % yield, relative to TS-fraction (26 % calc. for the Cl-free fraction). It has been shown by model experiments that under the experimental conditions used only basic nitrogen-containing compounds form insoluble hydrochlorides while polycyclic aromatic hydrocarbons, carbazoles, and oxygen containing compounds do not (4). As found by GC/MS approximately 90 % of the basic TS-subfraction consists of molecules with molecular weight > 300 Dalton. The higher-molecular mass portion of the basic TS-subfraction shows the properties of an oligomeric system as described in section 1. With regard to a further specification of our model of the higher-molecular portion of the TS-fraction we can now conclude that most of the oligomeric molecules contain at least 1 basic nitrogen atom. Besides that other N functions (carbazole structures) as well as O and S containing functions are present as follows from elemental analyses.

The basic TS-subfraction can be further separated by a chemical-method that has been termed "Charge-Transfer Fractionation" (CTF) (4,5,6). The first step in the CTF of pitches or pitch fractions is to prepare a solution in a suitable solvent; the solvents most widely used in CTF are toluene and chloroform. An electron acceptor species (picric acid or elementary iodine) is then added to the solution at room temperature. Immediately after the acceptor has been added a mixture of charge-transfer complexes of pitch constituents precipitates from the solution and is isolated by filtration. It has been shown that the nitrogen-containing basic pitch constituents are the compounds that predominantly form CT complexes (4). Decomposition of the CT complexes allows the recovery of the uncomplexed (electron donor) pitch molecules. The most important experimental parameter in the CTF of pitches is R, the ratio per weight of electron acceptor to pitch (or pitch fraction) dissolved (7). With decreasing R the yield of CT complexes obtained decreases. The same applies to the amount of electron acceptor present in the complexes. The nitrogen content of the uncomplexed donor material (obtained after decomposition of the complexes) also decreases with decreasing R while the mean molecular mass of the material increases. Clearly CTF fractionates the basic TS-constituents according to molecular mass. An example of the relation between R and the mean molecular mass of basic TS-subfractions obtained by CTF (electron acceptor: picric acid) is given in Fig.2a. Similarly Fig.2b shows the relation between R and the nitrogen content of the fractions obtained, while Fig.2c gives the relation between mean molecular mass and nitrogen content of these fractions.

3. Do pitches contain very large monomeric polycyclic aromatics ?

The idea that the higher-molecular portion of the TS-fraction consists predominantly of oligomeric systems where medium-sized aromatic/heteroaromatic units are connected by C-C single bonds and bridging functions, does, of course, not exclude the possibility that pitches also contain very large monomeric polycyclic aromatic systems.

The presence of such systems may be particularly suspected in those pitch fractions that are only sparingly soluble in organic solvents. This applies to e.g., the toluene and the chloroform insoluble fractions. Electrical measurements, in fact, indicate that these fractions rather consist of very large monomeric aromatics than of oligomeric systems.

It is well established that polycyclic aromatic hydrocarbons, after addition of small amounts of iodine, are electrical semiconductors. Fig.3a shows the exponential dependence of the electrical resistance on molecular size for the polyacenes (after addition of 1 % iodine). Electrical resistance decreases with increasing molecular size. For theoretical reasons this must apply to all topologies. In Fig.3b the yield of chloroform-insoluble material of various coal-tar pitches is plotted against the logarithm of the electrical resistance (measured after addition of 1 % iodine) of the chloroform-insoluble fractions. An exponential decrease of electrical resistance with increasing yield of chloroform-insoluble material is observed (8). The preliminary though most likely interpretation of this result includes the assumptions that (i) the yield of the chloroform-insoluble fraction increases with increasing mean molecular weight of the fraction and (ii) (by analogy with the result obtained for the acenes) the size of the fully-conjugated aromatic systems present increases regularly with molecular weight. To fit the latter assumption with the oligomeric structure model additional assumptions on the structure of the systems would be necessary.

4. Carbonization chemistry of medium-sized polycyclic aromatic pitch constituents

The reaction types characteristic of the thermal chemistry of medium-sized pitch constituents were examined taking by way of example perylene (I) (Fig.4) as the model substance (9). The thermolysis experiments were carried out in isothermal conditions at 450 °C in an argon atmosphere. After a reaction time of 20 h perylene conversion amounted to 42 %. The compounds identified from the liquid phase thermolysis of perylene are shown in Fig.4. The yield of products formed by condensation through loss of hydrogen ("aromatic growth"), i.e., biaryls IV, V, and VI, higher-molecular peri-condensed systems II and III and semicoke-like material was found to amount to 85 % in total, related to converted starting material. In addition fragmentation products (compounds VII - X) were formed in approximately 5 % yield. Formation of fragmentation products occurs by hydrogen transfer to intact perylene molecules and subsequent splitting of C-C single bonds initially formed. Due to fragmentation reactions methyl and ethyl hydrocarbon radicals are also formed that lead to alkylated products (compounds XI - XV) of the parent hydrocarbon.

Whereas in terms of quality the thermal chemistry of polycyclic aromatic hydrocarbons and structurally related heterocyclic systems is extensively independent of the structure of the reactants, in terms of quantity a heavy reactant depend-

ence is evident, i.e., in thermolytic reactions the conversion rate of hydrocarbons and heterocycles varies greatly with their size and topology. Carbonization rates of the polycyclic aromatic hydrocarbons listed in Fig.5 have been measured (10). Highly purified samples of each hydrocarbon were isothermally treated in sealed glass tubes at 430°C, i.e., above the melting points of the compounds, for 4 h. The conversion rates were determined by uv/vis spectroscopy and high-pressure liquid chromatography. Dependent on size and topology of the systems conversion rates range from 9 to 99 %, related to starting material. A linear free energy relation between the logarithms of conversion rates and a reactivity index (lowest Dewar localization energy) derived from MO theory has also been observed (10).

5. Carbonization chemistry of coal-tar pitch fractions/role of mean molecular weight, structure and nitrogen content

Carbonization experiments in liquid phase (430°C) clearly revealed that the higher-molecular basic TS-subfraction obtained with gaseous HCl (see section 2) is much more reactive than the corresponding lower-molecular non-basic material obtained from the mother liquor of HCl treatment. Similarly TS-subfractions obtained by CTF (section 2) are more reactive than the TS-fraction itself or the entire pitch. This follows unambiguously from formation rates of toluene-insoluble material (TI), relative rates of mesophase formation as well as from activation energies of TI and QI formation (QI = quinoline insoluble material). For example, activation energy of QI formation from the entire pitch amounts to 36 kcal/mol but to 17 kcal/mol from a CT fraction obtained with picric acid as the electron acceptor ($R = 0.05$, see section 2) (6, 11).

The thermally more reactive materials are distinguished from the less reactive ones by: (1) higher mean molecular weight, (2) probably an oligomeric structure (as opposed to the assumed monomeric structure of the less reactive material) and (3) by slightly higher nitrogen contents.

For all topologies of polycyclic aromatic systems reactivity increases with molecular size. Therefore an increase of thermal reactivity of pitch fractions with mean molecular weight is not unexpected. An oligomeric structure of the reacting material is particularly suited for intramolecular cyclization reactions. The drastic reduction in solubility following thermal treatment of the reactive pitch fractions can be easily explained with the formation of large planar aromatic systems. As is known from numerous examples planar aromatic compounds are much less soluble in organic solvents compared to non-planar ones with the same molecular size. There is some experimental evidence (7, 12) that nitrogen containing constituents enhance the thermal reactivity of pitch fractions. The effect, however, has been shown to be rather small (13). It cannot quantitatively explain the pronounced thermal reactivity of pitch fractions obtained by e.g., CTF (14).

In summary, the higher thermal reactivity of pitch fractions obtained by CTF or by treatment of the TS-fraction with gaseous HCl compared to that of the entire TS-material can be explained with the higher molecular weights of these fractions and particularly with their proposed oligomeric structure.

6. Role of free radicals and their precursor molecules in pitch carbonization

Although it is controversial whether free radicals play a dominant role in the **primary** step of the thermally induced polymerization of polycyclic aromatic hydrocarbons (15, 16), the importance of free radical formation in pitch carbonization has been unambiguously proven (17). Because of their much longer lifetimes π -radicals are more relevant than σ -radicals (15). The most important π -radical precursor molecules present in pitch are dihydro aromatics of the 9,10-dihydroanthracene type, amines, and phenols. The π -radicals are formed by thermally induced cleavage of the CH, OH, and NH bonds, respectively. Thermally abstractable hydrogen from CH, OH and NH groups amounts in total to approximately $6 \cdot 10^{-2}$ % H, relative to the entire pitch (6).

References

1. Stadelhofer, J.W.; Marrett, R.; Gemmeke, W. *Fuel* **1981**, 60 877.
2. Singer, L.S. *Fuel* **1981**, 60, 839.
3. Brooks, J.D.; Taylor, G.H. in *Chemistry and Physics of Carbon*, vol.4, p.243, Walker, P.L.; Thrower, P.A., Eds.; Marcel Dekker: New York 1968.
4. Zander, M. *Erdöl Kohle Erdgas Petrochem.*, in press (1989).
5. Blümer, G.-P.; Zander, M. *DGMK-Compendium 77/78* (Suppl. to *Erdöl Kohle Erdgas Petrochem.*) pp.235-251.
6. Zander, M. *Fuel* **1987**, 66, 1459
7. Zander, M. Abstract of Papers, International Conference on Carbon (Carbon '88), Newcastle upon Tyne, UK, 1988, pp. 55-57.
8. Zander, M.; Palm, J. *Erdöl Kohle Erdgas Petrochem.* **1985**, 38, 162.
9. Zander, M.; Haase, J.; Dreeskamp, H. *Erdöl Kohle Erdgas Petrochem.* **1982**, 35, 65.
10. Zander, M. *Fuel* **1986**, 65, 1019.
11. Zander, M. *Erdöl Kohle Erdgas Petrochem.* **1985**, 38, 496.
12. Sato, M.; Matsui, Y.; Fujimoto, K. Abstract of Papers. 17th Biennial Conference on Carbon, Lexington, Kentucky, 1985, pp.326-327.
13. Cerny, J. *Fuel* **1989**, 68, 402.
14. Zander, M.; Palm, J. *Erdöl Kohle Erdgas Petrochem.* **1987**, 40, 408.
15. Stein, S.E. *Carbon* **1981**, 19, 421.
16. Stein, S.E.; Griffith, L.L.; Billmers, R.; Chen, R.H. *J.Org.Chem.* **1987**, 52, 1582.
17. Lewis, I.C.; Singer, L.S. in *Polynuclear Aromatic Compounds, Advances in Chemistry Series 217*, p.269, American Chemical Society, Washington, DC 1988.

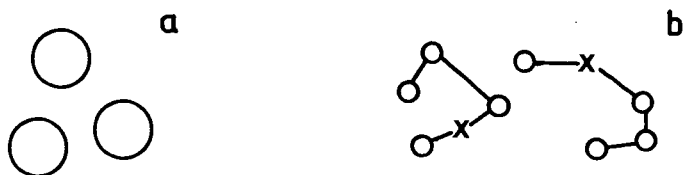


Fig.1. Structure models of higher-molecular TS-fraction constituents: a) "monomeric", b) "oligomeric" model.

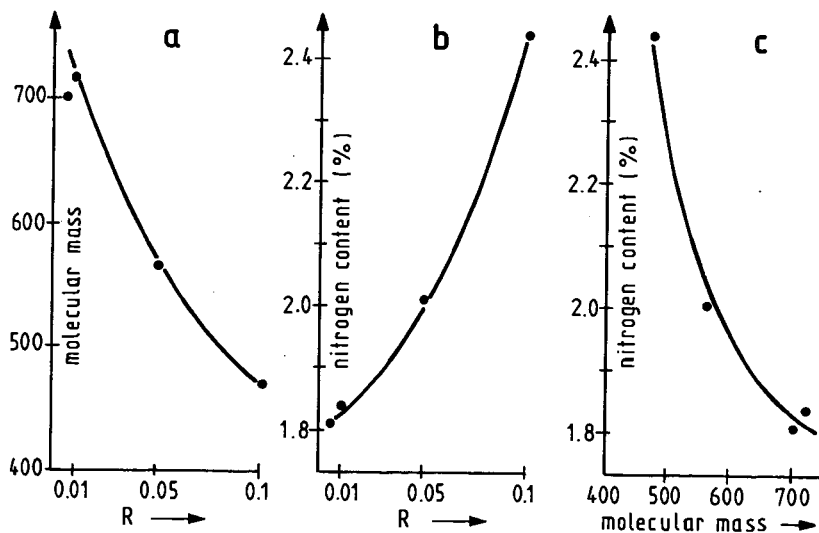


Fig.2. Charge-Transfer-Fractionation. - Relation between ratio R (per weight) of picric acid: pitch dissolved and molecular mass (a) or nitrogen content (b) of CT fractions obtained; (c) relation between molecular mass and nitrogen content of CT fractions.

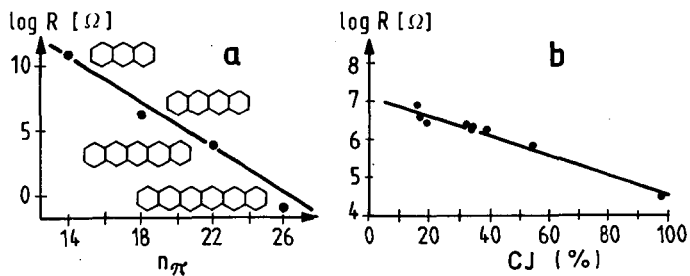


Fig. 3. (a) Relation between electrical resistance R (after addition of 1 % iodine) and number of π -electrons of the polyacenes; (b) relation between R and yield of the chloroform-insoluble fraction of 9 coal-tar pitches.

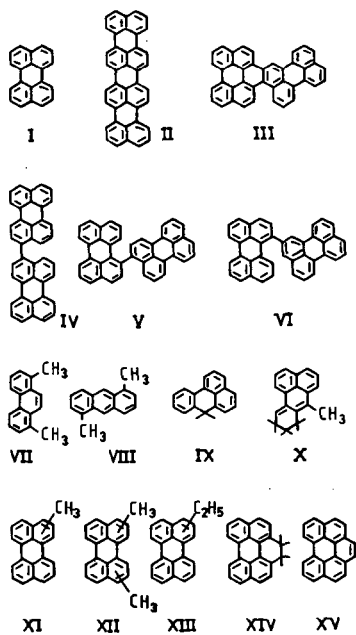


Fig. 4. Identified compounds from the thermolysis ($450^{\circ}C$) of perylene.

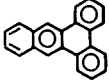
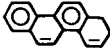
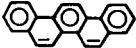
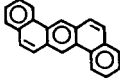
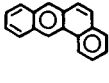
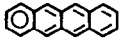
Hydrocarbon	Conversion rate (%)	Hydrocarbon	Conversion rate (%)
	9		36
	20		40
	24		50
	27		53
	30		99

Fig. 5. Carbonization rates (430°C, 4 h) of polycyclic aromatic hydrocarbons

CHARACTERIZATION AND UPGRADING OF COAL LIQUIDS
DERIVED FROM MILD GASIFICATION PROCESSES

John E. Mroczek, Radha P. Krishnan, and Ronald L. Graves

Oak Ridge National Laboratory*
Oak Ridge, Tennessee 37831

ABSTRACT

Mild gasification processes produce coal liquids that have the potential to be upgraded for use as transportation fuels. The quality and yield of these liquids vary widely depending upon the severity of the gasification process. Chemical upgrading of coal liquids may offer a viable and potentially economical alternative to conventional hydrotreating processes. Coal liquids from the United Coal Company Research Corporation, the KILnGAS, the SGI International, and Coalite (United Kingdom) processes have been characterized. These liquids and some of their distillates were subjected to solvent extraction upgrading with formic, acetic, and phosphoric acids to remove the basic nitrogenous fraction. Nitrogen removal ranged from about 50 to as high as 98%, with a recovery factor of about 75%. The most cost-effective reagent appears to be 25 vol % phosphoric acid.

INTRODUCTION

Mild gasification of coal has been shown to be capable of producing relatively light liquids, possibly suitable as an engine fuel, and char that may be suitable for boiler fuel or other purposes. Process conditions greatly influence the product quality; in particular, liquid product quality suffers with increasing yield (Graves et al., 1984). Some liquid upgrading (or blending) will be required even under mild gasification conditions before these liquids can be successfully utilized as transportation fuels. However, the severity and cost of upgrading are predicted to be less compared with conventional hydrotreating. The economics of upgrading mild gasification liquids varies with the raw liquid quality (Graves and Fox, 1984).

Complete and consistent data for mild gasification liquids are sparse in the literature. Often times, the data are of limited use since they have not been obtained by standard methods. Complete chemical and physical analyses of the liquids are essential to (1) determine the feasibility and degree of upgrading needed to produce marketable products from these liquids, (2) evaluate

*Operated by Martin Marietta Energy Systems, Inc., for the U.S. Department of Energy under contract DE-AC05-84OR21400.

the performance of these liquids as transportation fuels, and (3) optimize the mild gasification processes with respect to product yield and product quality.

In this paper, recent results pertaining to the characterization and chemical upgrading of coal liquids from typical mild gasification processes are presented. The studies were conducted at the Oak Ridge National Laboratory (ORNL) for the Morgantown Energy Technology Center (METC), Department of Energy (DOE). The liquid characterization and upgrading are being conducted in conjunction with the char characterization.

LIQUID CHARACTERIZATION

Coal liquid samples from four mild gasification processes were examined in this study. The liquids examined came from the United Coal Company Research Corporation's mild gasification process development unit (UCCRC MGU) in Bristol, Virginia; from the KILnGAS commercial module being operated by the Allis-Chalmers Coal Gas Corporation in East Alton, Illinois; from the low-temperature pyrolysis process being tested by SGI International at the Salem Furnace Company in Pittsburgh, Pennsylvania; and from the Coalite low-temperature carbonization commercial plant in the United Kingdom. The latter product was supplied by UCCRC. Information on the processes is limited since it is deemed proprietary by the process developers.

PROCESS DESCRIPTION

UCC MGU. The UCC system is a batch process capable of processing up to 68 kg (150 lb) of coal per batch, over a 5-h duration, at temperatures of up to 816°C (1500°F) under atmospheric pressure to mild vacuum. Two 0.2-m- (8-in.-) diam. stainless steel tubes, each connected to 0.2 x 2.4 m (0.7 x 8 ft) tall sweep gas heaters located adjacent to the individual reactor tubes comprise the reactor system. Coal is fed to the reactor at the top, and the resulting char is withdrawn at the bottom. The liquids are condensed from the reactor effluent gas. Noncondensable gas is either recycled as sweep gas or flared (Chu, 1988).

Tests have been conducted on 38 mm x 0 (1.5 in. x 0) and 3 mm x 0 (1/8 in. x 0) Kentucky HK bituminous coal containing 33.8 wt % volatile matter, 59.4% fixed carbon, 5.0% ash, and 1.8% moisture. Ultimate analysis of the coal is C - 78.18%, H - 5.24%, N - 1.46%, S - 0.98%, Cl - 0.13%, and O - 9.01%. The optimum reactor temperature is considered to be 538°C (1000°F) for the best liquid quality. A small amount of sweep gas is maintained through the reactors to enhance the heatup rate (1.4 -18°C/min) and to reduce the residence time of the product gas in the reactor. Liquid yield on "as-received" coal is 12 to 15%, of which 4% is water.

KILnGAS Commercial Module (KCM). This is a 600-ton/d coal gasification demonstration plant which uses a ported, pressurized, rotary kiln gasifier. Coal entering the feed end of the gasifier is progressively dried and heated by hot producer gas as it moves toward the discharge end. The hot coal is devolatilized and then reacted with air and steam. Gasification occurs about midway through the gasifier and continues to the discharge end. Agglomerated ash is removed at the discharge end. Gasification occurs at 1037°C (1900°F) at 3.1 bar (45 psi) pressure. Devolatilization occurs around 537°C (1000°F).

The gasifier, which measures 3.2 x 41 m (10 x 136 ft), is divided into five zones with multiple air/steam ports in each zone.

The KILnGAS process can gasify a wide variety of coals without requiring pretreatment. Most of the tests, however, have been done on high-sulfur Illinois No. 6 coal. Condensable hydrocarbons and tars are separated from the reactor effluent gas. The tar is recycled to the gasifier, and the condensates are processed in the wastewater pretreatment plant where the oils are recovered (Parekh, 1982).

SGI Pilot Plant. The SGI system is a small, batch-fed atmospheric pyrolyzer with a nominal operating temperature of 537°C (1000°F) and a residence time of 20 min, and is capable of feeding 22.7 kg (50 lb) of coal per batch. The coal tested is a Montana Rosebud subbituminous coal containing 39.0 weight % volatile matter, 51.8% fixed carbon, 19.8% moisture, and 5.0% ash. Ultimate analysis of this coal is C - 54.8%, H - 3.7%, N - 0.8%, S - 0.6%, and Cl - 0.02%. Liquid yield (naphtha and distillates) is 11 to 13% on a moisture-ash-free coal basis (Esztergar, 1987).

Coalite Commercial Plant. This is a commercial, low-temperature carbonization plant operating in the UK. Bituminous coal with a volatile content of 35% is carbonized in metal retorts at about 600°C (1112°F). The volatile products are condensed in water-cooled take-off pipes. The remaining noncondensable gases pass through electrostatic precipitators and are further condensed before they are recycled and used for heating the retorts. Liquid yield on an "as-received" coal basis is about 9% (W. A. Bristow, 1947).

CHARACTERIZATION METHODS AND RESULTS

The coal liquids were characterized by standard ASTM procedures in most cases; however, other well-accepted procedures were used for some parameters. The following properties were included in the characterization:

Elemental analysis (Leco analyzer)

Carbon

Hydrogen

Nitrogen \geq 1.0 wt %; (for N <1.0%, use modified Method 351.2, EPA

Methods for Chemical Analysis of Water and Waste)

Sulfur

Oxygen (by neutron activation)

- Water content (ASTM 96-73)
- Specific gravity (ASTM D 287-67)
- Viscosity (ASTM D 88)
- Heating value (ASTM D-2015-85)
- Simulated distillation curve by gas chromatography (ASTM D-2887)
- Aliphatics/Aromatics (Proton NMR)

Two liquid samples were provided by UCCRC and were designated as UCC-1 (parametric run) and UCC-2 (production run).

A summary of the data obtained on the four coal liquids is presented in Table 1. For illustration, the simulated distillation curve for the UCC-1 liquid is shown in Fig. 1.

The following trends can be observed in Table 1:

1. H/C ratios of the coal liquids are less than the corresponding ratio for diesel fuel. Some degree of upgrading and/or blending will be required to enhance the H/C ratio if these liquids are to be substituted for diesel fuel.
2. Except for the SGI liquid, the H/C ratios are slightly lower than those found for liquids produced in a batch reactor in a previous study (Graves and Fox, 1984) where the carbonization temperature was below 500°C.
3. The viscosity of coal liquid is much higher than that of diesel fuel.
4. Aromatic carbon contents for the coalite and UCCRC liquids are similar but much higher than the aromaticity of the diesel fuel. Increase in aromaticity with a concomitant decrease in H/C ratio is indicative of increasing aromatic ring condensation. A priori, increased hydrogen content leads to decreased aromaticity (White et al., 1987).
5. Aromaticity of the KILnGAS liquid is the highest of all the liquids, which is attributable to process conditions. Process conditions in the KILnGAS gasifier are much more severe compared with Coalite, UCCRC, and SGI. The higher pressure, temperature, and longer residence time in the reactor could cause thermal cracking for this product, indicative of greater aromatic ring condensation (product contained elevated amounts of naphthalene).
6. The SGI liquid measured the lowest aromatic carbon, even less than that of diesel fuel. The sample from Test 1003, is a second-stage liquid, which is perhaps a much lighter fraction compared with the raw liquid. The high hydrogen and low oxygen contents of this liquid are puzzling.

UPGRADING STUDIES

Hydrotreating is the conventional technology used in the petroleum industry for heteroatom removal and product upgrading. It has also been used for upgrading liquids derived from several different coal liquefaction and shale oil processes. In a previous DOE-sponsored program designed to study the upgrading of coal- and oil shale-derived liquids, fixed-bed hydrotreating at three different severity levels was used to produce gasoline, jet, and diesel fuels from SRC II, Exxon Donor Solvent, and H-coal liquids. Satisfactory fuels were obtained, although high hydrogen consumption was observed [1000 to 3000 SCF/bbl, depending on the severity level and the coal liquid (Guerin, 1986)]. It was found that the hydrotreating operation was very sensitive to asphaltene-like impurities in the feed liquid. In addition to reducing their detrimental effect on catalyst performance, the removal of these impurities enabled significant reduction (factors of 1.5- to 3-fold) in the size of the hydrotreater reactor for jet fuel production (Sullivan, 1981).

Hydrotreating, requiring high-pressure equipment, catalysts, and hydrogen, is expensive and difficult because of the nature of the coal liquids. Chemical means of upgrading have the potential to be more cost effective. Primary emphasis, in the upgrading studies reported in this work, was on the removal of the basic nitrogen fraction from these coal condensibles by solvent extraction with acidic reagents. Principal reagents tested included formic, acetic, and

phosphoric acids in concentrations ranging from 25 to 90 vol %. The effect of acid strength was briefly examined on an early UCCRC condensible using acetic (pKa = 4.75), monochloroacetic (pKa = 2.85), and trichloroacetic (pKa = 0.70) acids at 50 vol % concentrations.

Extraction Studies on UCCRC Liquids

Illustrated in Table 2 is a comparison of formic and acetic acid extractions at 50, 75, and 90 vol % (formic only) concentrations using one of the early samples of UCCRC coal condensibles. Early samples from the UCCRC MGU were obtained under nonoptimum operating conditions and at a higher operating temperature of about 1300°F (optimum temperature is now considered to be about 1000°F). This, of course, resulted in a somewhat more viscous and more highly aromatic liquid product having an H/C ratio of 0.88. Extraction data in Table 2 indicate better extraction by acetic acid, with 50.9% of the nitrogen removed by 75 vol % acetic acid. Oxygen assays show little tendency for the organic phase to retain water for extraction with either of these two acids. Qualitatively, acetic acid also showed better extraction of the basic nitrogenous fraction than either monochloroacetic or trichloroacetic acids, suggesting that increased acid strength did not improve nitrogen removal.

Phosphoric acid was tested as a nitrogen extractant during the course of this work, based on similar experiments on shale oil (Johnson, 1981). Acid concentrations of 25, 50, and 75 vol % were tested, utilizing the same UCCRC condensible liquid and contacting procedure employed with acetic and formic acids. Unextracted nitrogen assays were 0.46, 0.44, and 0.37 wt %, respectively, with the highest acid concentration providing the greatest removal (66%). A third phase, which made clean separations difficult to achieve, was formed for the higher concentrations (50 and 75 vol %) in these experiments. Note, however, that even at 25 vol % phosphoric acid concentration, the nitrogen removal was 57.4%, which is still better than that obtained with 75 vol % acetic acid extraction (50.9%).

A more representative sample of the UCCRC coal condensible liquid is UCC-1 in Table 1. Extractions of the nitrogen content of this product were attempted with both acetic and phosphoric acids. However, extraction with 75 vol % acetic acid proved impossible because, at this concentration, the two liquids were completely miscible. This suggests that the UCC-1 liquid is different from the previous liquids tested. The acetic acid concentration was reduced to 50 vol %, and nitrogen removal was compared to that obtained with 25 vol % phosphoric acid. Nitrogen content was reduced to 0.36 and 0.34 wt %, respectively, or 36% removal with acetic acid and 39% removal with phosphoric acid. Nitrogen removal was less complete for this liquid compared with the previous UCCRC samples, suggesting that the liquid generated at the lower gasifier temperature had a lower basic nitrogen content.

Extraction Studies on a KILnGAS Condensible

A relatively large sample (about 5 gal) of a KILnGAS condensible, described as a "high-naphthalene-content" product, was received through the courtesy of the Allis-Chalmers Coal Gas Corporation. Its elevated aromatic content was verified by the NMR analysis shown in Table 1. A vacuum distillation of this product was performed, and the fraction boiling under 650°F was collected. The nitrogen content was reduced by about 53% (to 0.31 wt %), and the H/C ratio was increased to 0.83. Little change was noted for the other heteroatoms. Extractions were performed on both the raw liquid and the distillate with varying concentrations of acetic acid. The results, shown in Table 3, indicate 67% reduction in nitrogen content for extraction of the raw product with 75 vol % acetic acid and 58% reduction for the distillate.

Extraction Studies on an SGI Liquid

The condensible product from SGI International was described as a second-stage product using coal from the Rosebud Mine in Montana. Few details are known about this particular sample; however, its appearance and analysis (see Table 1) suggested that, at the very least, it was some sort of distillate. Its analytical properties, with the exception of the nitrogen assay, were better than the typical commercial diesel fuel shown in Table 1. The aromatic content, as measured by NMR, and the oxygen and sulfur assays were unusually low for a coal condensible liquid.

Solvent extraction studies with both acetic and formic acids showed nearly complete removal of nitrogen (98 to 99%) at all concentrations tested (see Table 4). Clean separations were observed with this extremely light organic liquid, as indicated by the oxygen assays of the organic phase. The nitrogen removal demonstrated for this product, coupled with the already low oxygen, sulfur, and aromatic assays, is probably sufficient to enable it to be used directly as a fuel in some diesel engines; however, its actual relationship to a working mild gasification process remains to be verified.

CONCLUSIONS

The characterizations of the condensible products from various coal gasification projects give an indication of the need for upgrading in order to produce a fuel suitable for transportation uses. It is evident that lower temperatures (<1000°F) in the gasifier are desirable in order to reduce aromatic content and subsequently increase the H/C ratios.

Solvent extraction studies on limited amounts of three condensible liquids must be deemed tentative. However, based only on raw material prices (acetic acid -- \$0.27/lb; formic acid -- \$0.365/lb; and phosphoric acid, 85% -- \$0.255/lb), the most economical process would utilize 25 vol % phosphoric acid as an extractant. Extraction experiments performed with several condensible samples showed that 75% recovery of the nitrogen-depleted organic phase was achievable with careful attention to experimental procedure. However, it should be pointed out that the aqueous raffinate from any solvent extraction process of this nature may generate an environmental disposal problem that has not been addressed during the course of this work.

REFERENCES

W. A. Bristow, "The Development of Liquid Products from Low-Temperature Carbonization," *J. Inst. Fuel*, Vol. XX, No. 113 (1947).

C. I. C. Chu, Development of Mild Gasification Process, Project Report UCC R&D C-17-20 to Morgantown Energy Technology Center (Sept. 1988).

E. E. Esztegar, personal communication to R. L. Graves, Oak Ridge National Laboratory (May 1987).

C. A. Johnson, C. Ward, H. F. Moore, and R. Hettinger, "Combination Process for Upgrading Oil Products of Coal, Shale Oil, and Crude Oil to Produce Jet Fuels, Diesel Fuels, and Gasoline," U.S. Patent 4,409,092 (1983).

R. L. Graves, S. S. Lestz, S. S. Trevitz, and M. D. Gurney, "Screening Tests of Coal Pyrolysis Liquids as Diesel Fuel Extenders," SAE Technical Paper Series, Paper No. 841002, San Diego (Aug. 1984).

R. L. Graves and E. C. Fox, "Diesel Fuels from Minimally Processed Coal Pyrolysis Liquids -- Exploratory Investigations," presented at the 19th IECEC Meeting, San Francisco (Aug. 1984).

M. R. Guerin, W. H. Griest, C-H. Ho, L. H. Smith, and H. P. Witschi, *Integrated Report on the Toxicological Mitigation of Coal Liquids by Hydrotreatment and Other Processes*, ORNL/TM-10070 (1986).

R. D. Parekh, "Handbook of Gasifiers and Gas Treatment Systems," DOE/ET/10159-T24 (DE 83004846) (1982).

R. F. Sullivan and D. J. O'Rear, *Refining and Upgrading of Synfuels from Coal and Oil Shales by Advanced Processes*, FE-2315-60 (1981).

C. M. White, M. B. Berry, C. E. Schmidt, and L. J. Douglas, "Relationship Between Refractive Indices and Other Properties of Coal Hydrogenation Distillates," *Energy & Fuels*, Vol. 1, 99 (1987).

Table 1. Summary of coal liquids characterization data

Properties	Coalite	UGC-1 (parametric run)	UGC-2 (production run)	Kiln- GAS	SGI	Typical commercial diesel fuel
Elemental analysis (wt %)						
C	80.83	84.24	83.69	88.45	87.34	86.5
H	8.57	9.42	9.34	5.58	12.96	12.8
S	0.72	0.42	0.39	4.6	0.07	0.3
N	1.02	0.56	0.68	0.66	0.40	0.01
O (by neutron activation)	7.74	4.89	5.11	1.6	0.171	
H/C	1.27	1.34	1.34	0.76	1.77	1.78
Water content, %	1.80	0.790	0.900	0.14	0.004	nil
Specific gravity (at 25°C)	1.03	0.972	0.989	1.133	0.872	0.85
Viscosity (at 25°C), CP	290.0 ^a	12.06 ^b	25.55 ^b	34.0 ^b	18.0 ^b	3.0 ^b
Heating value, Btu/lb	16,300	17,100	17,000	16,500	19,400	18,150
Aromatic hydrogen content, wt %	30.4	30.2	26.9	86.1	8.7	14-16
Aromatic carbon content, wt %	57.7	55.9	52.4	94.8	20.0	34-37
Aliphatic hydrogen content, wt %	61.8	59.2	68.1	13.9	91.3	84.0
Simulated distillation data						
Initial BP, °C	147	48	58	58	142	
Final BP, °C	437	397	425	431	433	
Average BP, °C	234	214	211	218	273	
Percentage of oil distilled at 246°C	56	67	75	66	34	

^aMeasured by a Brookfield viscometer.

^bMeasured by a Canon-Fenske viscometer.

CASIM average temperature corresponding to the 50% boiling point for diesel fuel.

Table 2. Extraction studies on a UCCRC liquid with aqueous formic and acetic acids

Element	Raw liquid	Organic-phase concentration, wt %					
		Formic acid			Acetic acid		
		50 ^a	75 ^a	90 ^a	50 ^a	75 ^a	90 ^a
Nitrogen	1.08	0.85	0.74	0.59	0.56	0.53	b
Oxygen	5.24	4.70	4.64	7.96	4.54	4.79	b

^aVol %.

^bInsufficient sample for analysis.

Table 3. Extraction of nitrogen from raw and distilled KILnGAS products using acetic acid

Acetic acid (vol %)	Remaining nitrogen, wt %	
	Raw KILnGAS ^a	<650°F distillate ^b
25	0.31	0.22
50	0.32	0.17
75	0.22	0.13
90	0.21	NA ^c

^aOriginal N content, 0.66 wt %.

^bOriginal N content, 0.31 wt %.

^cNot analyzed.

Table 4. Extraction studies on an SGI liquid with aqueous formic and acetic acids

Element	Raw SGI	Organic-phase concentration, wt %							
		Formic acid				Acetic acid			
		25 ^a	50 ^a	75 ^a	90 ^a	25 ^a	50 ^a	75 ^a	90 ^a
Nitrogen	0.40	<0.01	<0.01	0.01	<0.01	<0.01	<0.01	0.02	<0.01
Oxygen	0.16	0.12	0.13	0.11	0.10	0.14	0.11	0.10	0.08

^aVol %.

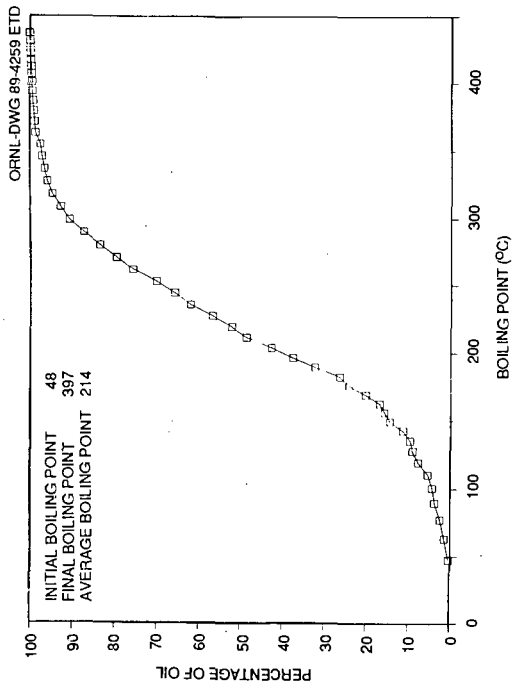


Fig. 1. Simulated distillation curve for UCC-1 coal liquid.

Catalytic Cracking of a Gas Oil
Derived from Eastern Canadian Oil Shale

S. H. Ng

Synthetic Fuels Research Laboratory, CANMET
Energy, Mines and Resources Canada
Ottawa, Ontario, Canada K1A 0G1

Introduction

Large oil shale deposits have been discovered in Central and Eastern Canada.¹ In the past few years, considerable research was conducted on Eastern oil shales.²⁻⁵ Primary liquid products from retorting of oil shales are superior to Canadian heavy oil and tar sand bitumen.⁵ In a continuing effort to evaluate the processability of the shale oil produced, a catalytic cracking study on its gas oil fraction was recently undertaken at CANMET. This paper reports the primary results.

Experimental Section

The raw shale oil was produced by retorting a New Brunswick oil shale from Albert Mines near Moncton, New Brunswick. The retort system in the pilot plant has been reported previously.⁵ The shale oil was distilled under vacuum to give the gas oil fraction which constituted 80 wt % of the feed. For comparison, a conventional gas oil was obtained from a refinery which processes the Alberta crudes transported to Eastern Canada through the Interprovincial Pipe Line (IPPL). The two gas oils were analyzed using ASTM or other accepted methods. The results are shown in Tables I and II.

Three equilibrium catalysts DA-440, Nova D and GX-30 obtained from Davison of W. R. Grace were used in this study. Prior to their characterization and testing, the catalysts were decoked at 590 °C for 3 h. Surface characteristics were determined by both N₂ adsorption-desorption technique and by mercury porosimetry. Zeolite surface areas and zeolite contents were estimated based on a method reported in the literature.⁶ Their physical and chemical properties are given in Table III.

Catalytic cracking of the gas oils was performed in a microactivity test (MAT) unit which was modified from the ASTM D3907 version. It consists of a fixed bed quartz reactor packed with 4.2 g of catalyst heated at 470-530 °C in a three-zone furnace. Feeds were delivered using a syringe pump with catalyst/oil ratio varying from 2-6 while keeping the hourly weight space velocity (WHSV) constant at 20 h⁻¹. A flow of nitrogen purge gas at 20 mL/min was maintained throughout the 20-min test period. Liquid products were collected in a glass receiver cooled in an ice-water bath whereas the gaseous products were trapped using water displacement. After the test, both products were quantitatively measured before analysis. The amount of coke formed on the spent catalyst was also determined. Conversion was calculated based on the fraction of liquid product having a boiling point above 216 °C.

Denitrogenation of the shale vacuum gas oil (VGO) was done by both extraction in which dimethylsulfoxide (DMSO) containing 6 wt % 2N sulphuric acid was used as solvent, and adsorption in which an Attapulugus clay was used as adsorbent.

Results and Discussion

Table I shows that the quality of the shale VGO is better than or equivalent to that of the IPPL gas oil except its nitrogen contents are much higher. The basic nitrogen is undesirable in FCC feedstocks as it can neutralize the acid sites of the cracking catalysts resulting in a rapid loss of activity.⁷⁻⁹ The high nitrogen level is also reflected by the polars in the hydrocarbon type analysis (Table II). Polars in the shale oil may also include oxygen compounds. If these polars are considered crackable, the conversion constraints based on the compositional analysis can be estimated at 80.6 and 81.1 wt % for IPPL and shale VGO respectively, assuming that the diaromatics and the more highly condensed structures including aromatic sulphurs cannot be converted to light products with boiling points less than 216 °C due to the stability of the benzene rings.

Figure 1 shows the effects of temperature and catalyst/oil ratio (C/O) on conversion. Significant differences can be seen between the two feedstocks. For IPPL gas oil, the conversion tends to level off and approaches its limit at high severity. Furthermore, it is less sensitive to the temperature change. On the other hand, for shale VGO, the conversion increases sharply and linearly with C/O ratio and is far below its expected limit even at much higher severity. The conversion is obviously very temperature-dependent. This suggests that the catalysts were seriously poisoned during cracking by the basic nitrogen of shale VGO as this type of poisoning is mainly a surface adsorption phenomenon and high temperature tends to promote desorption. Between the two catalysts, Nova D is apparently more active in cracking IPPL conventional gas oil due to its higher zeolite content. This agrees with Davison's microactivity results (Table III). However, this trend is reversed for shale VGO, with DA-440 being more active. This suggests that the shale oil contains larger molecules which do not have access to the small pores of the zeolite but can be cracked by the matrix of DA-440 which has a larger pore diameter (Table III). A similar phenomenon was also observed in a separate cracking study which deals with other nonconventional gas oils including those derived from resids, tar sand bitumens and heavy oils.¹⁰

For IPPL gas oil, favourable and optimum gasoline yield (54 wt %) is obtained at about 73% conversion beyond which overcracking seems to take place. The gasoline yield decreases slightly with increased temperature at constant conversion. Between the two catalysts, DA-440 is slightly more selective for gasoline production. This does not necessarily mean that it produces a better gasoline, in terms of higher octane number, as DA-440 is not an octane-enhancing catalyst but Nova D is. It is known that the dealuminated ultra-stable Y-zeolite catalysts (USY) yield higher octane gasoline by producing more olefinic compounds,¹¹ compared with the rare earth exchanged Y zeolite catalysts (REY). For shale VGO, the gasoline yield increases linearly and monotonously with conversion without obvious effects of temperature and catalyst. The experimental maximum gasoline yield is less than 30 wt % which is unacceptably low.

The coke yields of the two gas oils increase exponentially (IPPL) or linearly (shale oil) with conversion. At constant conversion, higher temperature

for the same catalyst tends to lower the coke yield because C/O ratio can be reduced to achieve the same conversion. Contrary to the literature,¹¹ Nova D (USY) yields more coke than its counterpart DA-440 (REY) in cracking shale VGO whereas for IPPL gas oil, Nova D shows slightly better or equivalent coke selectivity than DA-440. A similar phenomenon was also observed in a separate cracking study involving other nonconventional feedstocks.¹⁰ It is thus believed that the superiority of USY catalysts over REY catalysts with respect to coke selectivity depends also on the nature of the feedstock.

It has been observed that a linear correlation exists between the second-order conversion (conversion/[100 - conversion]) and the coke yield. The linear relationship is expected based on the equations proposed by Wollaston et al.¹² For IPPL gas oil, the straight lines at different temperatures pass through the origin indicating that all the coke formed results from catalytic cracking and is therefore "catalytic" coke.¹³ However, for shale VGO, the straight lines intersect the x-axis at different coke values. These values obtained at 0% conversion represent neither "catalytic" coke nor "contaminant" coke since the nickel and vanadium contents of the catalysts are rather low (Table III). This suggests that they belong to the "additive" coke resulting from the basic nitrogen of the shale gas oil which contains little Conradson carbon - another possible precursor for the "additive" coke.¹³ The "additive" coke found is independent of the catalyst type and is estimated at 1.47, 1.25, 1.09 and 0.97 wt % at 470 °C, 490 °C, 510 °C and 530 °C, respectively.

Product distribution for the two feedstocks at 50% conversion is shown in Table IV. It can be seen that the shale VGO produces more gases, less gasoline and much more coke compared with IPPL gas oil. The high decant oil yield (39 wt %) for IPPL VGO may be misleading as the majority of its precursor is crackable at higher severity. At 73% conversion, this value drops to 8 wt % raising the gasoline yield from 35 to 54 wt %.

Three methods have been used to achieve higher conversion of the shale oil. The first is to crack with GX-30, a very active catalyst because of its higher zeolite content. The other methods involve upgrading of gas oils by removing some of the nitrogen compounds using either DMSO/acid extraction or Attapulugus clay adsorption. One disadvantage of the rejection methods is the accompanying loss of the hydrocarbon value. Table V shows the weight recovery and the nitrogen contents of the upgraded feedstocks. It is evident that the clay method is superior to the extraction technique since it removes almost 50% more basic nitrogen for the same recovery. Table VI shows a comparison of cracking yields of raw and treated feedstocks cracked at various conditions while keeping catalyst/oil ratio constant at 6. For the untreated shale oil, although the use of GX-30 results in some improvement over DA-440 in conversion and gasoline yield, the coke yield is unacceptably high. Evidently, DMSO raffinate shows better performance than the raw shale oil whereas the clay treated shale oil is the best due to its lowest basic nitrogen content.

Let us consider two approaches in further evaluation of the data: one involves cracking of the raw shale oil as a whole whereas the other involves the separation of the shale oil into two fractions prior to individual cracking under the same conditions. In the latter case, the recovered fraction contains less nitrogen and is therefore better in quality whereas the rejected fraction is assumed, for simplicity, to be unconvertible either because of its high nitrogen level or a refractory nature. One can calculate their cracking yields on a

"total oil" basis by multiplying the yields, based on the recovered portion, with the weight fraction of recovery. The results are illustrated in Fig. 2. Here, the increases in conversion and gasoline yields of the treated shale oils over those of the untreated ones reflect the net poisoning effect on the catalyst by the basic nitrogen.

Based on the data obtained from nitrogen rejection methods (extraction or adsorption), linear correlation can be established between the cracking results, in terms of conversion and gasoline yield, and the basic nitrogen content (1750-4600 ppm) of MAT feeds. A cracking study was also made on the blends prepared from IPPL and raw shale oil. The data points obtained from this dilution method appear to coincide with those from rejection methods over the same basic nitrogen range. This suggests that the rejected portion of the raw shale oil would have been cracked if the catalyst had not been poisoned by the basic nitrogen in the first place. Also, the basic nitrogen content of the shale oil, rather than its compositional differences from the IPPL gas oil, is the determining factor for the cracking yields. Following the trends created by the dilution method, the shale oil produces a cracking result similar to that of IPPL at the same basic nitrogen level, i.e., 72 vs 73.5 wt % in conversion and 51 vs 53 wt % in gasoline yield at 510 °C and a catalyst/oil ratio of 4.

Acknowledgement

The authors would like to thank Dr. T. de Bruijn and Dr. J. Kriz of CANMET for many valuable discussions and suggestions.

REFERENCES

- (1) Duncan, D. C. Oil Shale (Eds. Yen, T. F.; Chilingarian, G. V.), 1976, p.19, Elsevier, New York.
- (2) Furimsky, E.; Synnott, J.; Boorman, R. S.; Salter, R. S. Fuel Process. Technology, 1984, 8, 293-306.
- (3) Boorman, R. S.; Salib, P. F.; Gilders, R.; Gemmell, D. E. Can. Inst. Min., Proc. 3rd Meeting, Fredericton, N. B. 1982.
- (4) Karman, D.; Kresta, S. PREPRINTS, Div. of Petrol. Chem., ACS, 1987, 32(1), 94-96.
- (5) Salib, P. F.; Barua, S. K.; Furimsky, E. Can. J. Chem. Eng. 1986, 64(6), 1001-1007.
- (6) Johnson, M. F. J. Catal. 1978, 52, 425-431.
- (7) Fu, C. M.; Schaffer, A. M. Ind. Eng. Chem. Prod. Res. Dev. 1985, 24(1), 68.
- (8) Scherzer, J.; McArthur, D. P. Oil Gas J. Oct. 27, 1986, pp 76.
- (9) Scherzer, J.; McArthur, D. P. Ind. Eng. Chem. Res. 1988, 27(9), 1571-1576.
- (10) Ng, S. H. Unpublished results.
- (11) Ritter, R. E.; Creighton, J. E.; Chin, D. S.; Roberie, T. G; Wear, C. C. Catalogram, Davison, 1986, 74, 5.
- (12) Wollaston, E. G.; Haflin, W. J.; Ford, W. D; D'Souza, G. J. Hydrocarbon Process. 1975, 54(19), 93.
- (13) Cimbalo, R. N.; Foster, R. L.; Wachtel, S. J. Oil Gas J. 1972, 70(20), 112.

Table I. Feedstock Inspection Data

Properties	IPPL	Shale
*API	24.2	25.0
Aniline point, °C	93.7	80.0
Conradson carbon, wt %	0.43	0.18
Total nitrogen, ppm	1150	7150
Basic nitrogen, ppm	310	4570
Total sulphur, wt %	0.66	0.52
Viscosity at 40 °C, cSt	65.0	17.3
Simulated distillation, °C		
IBP	305	209
10%	369	290
50%	444	394
90%	538	489
FBP	594	536

Table II. Feedstock Compositional Analysis (wt %)

Hydrocarbon type	IPPL	Shale
Paraffins	23.8	21.8
Monocycloparaffins	14.3	13.5
Condensed cycloparaffins	24.2	13.1
Monoaromatics	13.2	16.9
Diaromatics	9.3	11.4
Polynuclear aromatics	7.9	6.1
Polars	4.3	15.4
Aromatic sulphur	2.2	1.4

Table III. Properties of Cracking Catalysts

Properties	DA-440	Nova D	GX-30
Type	REY	USY	REY
BET surface area, m ² /g	75.0	95.5	107.5
Zeolite surface area, m ² /g	43.7	48.4	66.8
Relative zeolite content, wt %	7.3	8.1	10.8
Pore volume, mL/g	0.245	0.266	0.257
Avg. pore diameter, Å	280	208	355
V, ppm	141	351	538
Ni, ppm	374	114	400
Al ₂ O ₃ , wt %	42.1	45.3	33.1
Unit cell dimension, Å	24.42	24.28	24.39
Microactivity (Davison), wt %	70	72	78

Table IV. Comparison of Product Yields at 50% Conversion*

Gas oil Catalyst Reactor temperature, °C	IPPL DA-440 470	Shale DA-440 530
Total dry gas, wt %	1.0	3.5
C ₃ + C ₄ , wt %	8.5	13.0
C ₅ + gasoline, wt %	35.0	30.0
Light cycle oil, wt %	14.0	27.0
Decant oil, wt %	39.0	20.5
Coke, wt %	2.6	6.6

* Extrapolated data

Table V. Weight Recovery and Nitrogen Contents of Upgraded Shale Oils

Shale oil	Untreated	DMSO	Clay
Recovery, wt %	100	85.3	86.1
Total nitrogen, ppm	7150	5618	3496
Basic nitrogen, ppm	4570	3007	1745

Table VI. Cracking Yields (wt %) at C/O = 6

Shale oil	Temp. °C	Catalyst	Conver- sion	C ₅ + Gasoline	Coke
Raw	510	DA-440	45.0	25.2	6.5
DMSO treated	510	DA-440	53.2	31.7	6.4
Clay treated	510	DA-440	65.3	40.0	6.4
Raw	530	DA-440	47.9	26.5	6.6
Raw	530	GX-30	59.8	31.7	9.1
Clay treated	530	DA-440	70.0	42.5	6.4

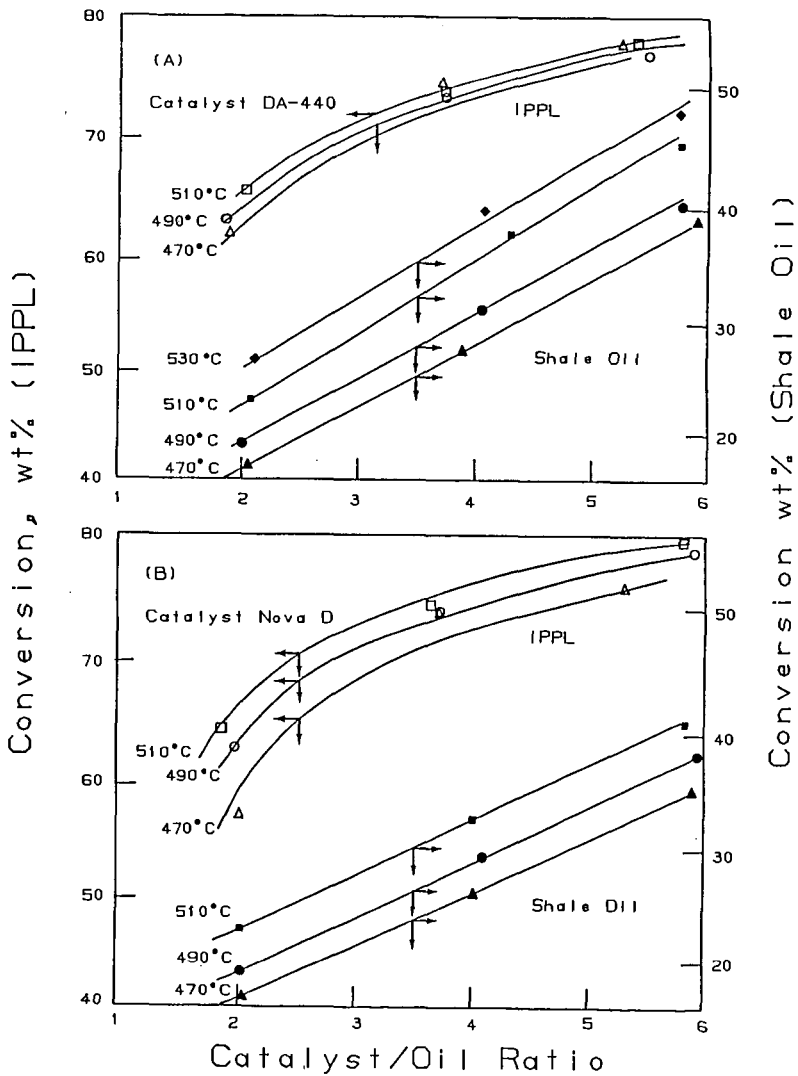


Figure 1. Effects of temperature and catalyst/oil ratio on conversion.

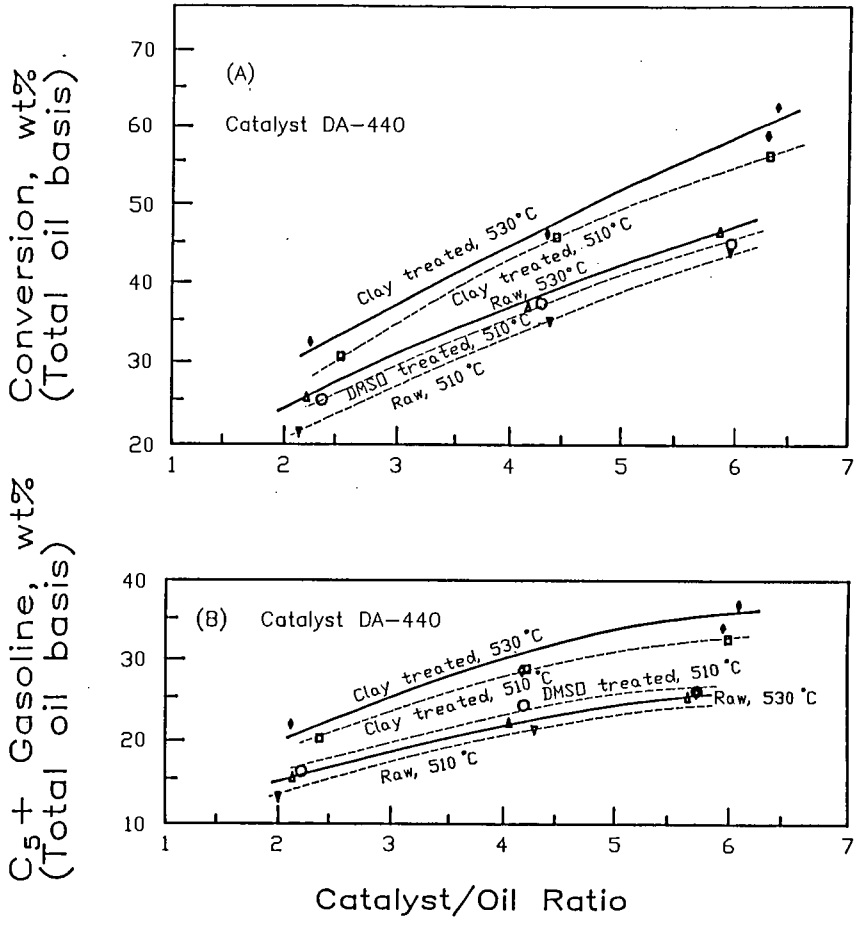


Figure 2. Conversions and gasoline yields of raw and treated shale gas oils calculated on total oil basis.

INFLUENCE OF STEAM ON COAL DEVOLATILIZATION AND ON
THE REACTIVITY OF THE RESULTING CHAR¹

M. Rashid Khan
Texaco Research Center, Texaco Inc
P.O. Box 509, Beacon NY 12508

F. Y. Hsieh²
Morgantown Energy Technology Center
Morgantown, West Virginia

ABSTRACT

Improved reactivity of the mild gasification char is highly desirable for the economic viability of a mild gasification process aimed at producing liquid fuel from coal by pyrolysis. In this study, it is demonstrated that devolatilization of coal in the presence of steam atmosphere increases pyrolysis volatile (and liquid) yield and produces a more reactive char. Devolatilization of coal was effected either in a thermogravimetric analyzer or in a slow heating rate organic devolatilization reactor (SHRODR). The chars prepared in steam have a lower oxygen chemisorption capacity than the chars prepared in helium. Fourier transform infra-red (FTIR) spectroscopic studies indicate that the steam char has a higher concentration of hydroxyl groups than the char prepared in He. This implies that pyrolysis of coal in steam may introduce some hydroxyl functional groups which may have a favorable influence during subsequent char gasification/combustion.

INTRODUCTION AND BACKGROUND

It is well known that gasification reactivity of coal char is a strong function of rank of parent coal and pyrolysis conditions used to generate the char (e.g., maximum heat-treatment-temperature, heating rate, and soak time at peak temperature). Numerous studies have been addressed on the influence of thermal history of pyrolysis and the role of the minerals and cations on the reactivity of the resulting char (1-12). However, relatively little attention has been received on the influence of gas atmosphere used during pyrolysis on the reactivity of the resulting char.

Sharma and coworkers (13) studied the low temperature (up to 650°C) pyrolysis of coal in argon, steam, and hydrogen under 1 to 66 atmosphere. Based on very limited studies, it was concluded that pyrolysis gas atmosphere or pressure had no influence on the reactivities of the resulting chars. Christosora and coworkers (14) studied the effect of pyrolysis atmosphere (argon, steam, and hydrogen) on the reactivity (in steam) of produced chars (900°C char) and observed that the

¹ Work performed at Morgantown Energy Technology Center.

² Post-doctoral trainee through the Oak Ridge Associated Universities

presence of reactive gases (steam and hydrogen) did not affect the rates of reaction of product chars. It was suggested that the pressure of reactive gases (1 bar) during pyrolysis was too low to effect deeper penetration of the reactive gases into the char structure thus causing changes in the chemical and physical properties of chars that would otherwise affect the reactivity of char.

The purpose of this study is to investigate by means of systematic experiments the effect of steam on the pyrolysis weight loss of coals and on the reactivities of resulting chars. The hypothesis of this study is that pyrolysis of coal under steam atmosphere may introduce oxygen containing functional groups to the coal/char structures which may have positive contribution to the reactivity of char.

EXPERIMENTAL

The coals were devolatilized in a thermogravimetric analysis system (Dupont 1090 thermal analyzer) and in a slow heating rate organic devolatilization reactor (SHRODR) either in He or in steam/He mixture. For the devolatilization in the TGA system, steam was introduced to the TGA system by bubbling He through a filtered dish of a sealed saturator. The temperature of saturator was maintained at a constant temperature of 25°C. The saturation pressure of steam at room temperature is 3 kPa. For the devolatilization in the SHRODR, steam was introduced to the reactor by pumping water to the reactor at the rate of 0.2 cc/min. The analyses of coals used in this study are presented in Table 1. Wyodak coal was acid-washed with 0.1 N HCl solution according to the procedures described by Morgan, et al. (15) to remove exchangeable cations in the coal. The extract solution was analyzed by atomic absorption spectrometry. The exchangeable cation content of Wyodak coal were determined and given in Table 2.

Chemisorption was carried out at 155°C and 0.1 MPa O₂ for 15 h using the TGA. The oxygen chemisorption capacity (OCC) or the active surface area of chars (ASA) were calculated from the amount of oxygen chemisorbed on the chars. Isothermal char reactivities were determined using TGA at 400°C in 0.1 MPa O₂.

The reproducibilities of coal pyrolysis (devolatilization) and char reactivities determination in the TGA system can be seen in Figures 1a and 1b, respectively. It is obvious that the reproducibility of our experiments was very good.

RESULTS AND DISCUSSION

Effect of Steam on Pyrolysis Weight Loss of Coals

Tables 3 and 4 summarized the pyrolysis weight loss of Wyodak coal and Pittsburgh No. 8 coal during pyrolysis in He and steam (3 kPa) up to 650° and 950°C. Weight loss (both for temperature up to 650° to 950°C) is a function of coal rank. The weight loss of Wyodak coal (subbituminous coal) is higher than that for the Pittsburgh No. 8 coal (high volatile bituminous coal). The steam gasification process is thermodynamically favorable when the temperature is higher than 500°C. Table 3 shows that pyrolysis of coals in steam up to 650°C increases weight loss by 3.5 percent for Wyodak coal and 7.0 percent for Pittsburgh No. 8 coal. Wyodak coal contains relatively high concentration of exchangeable cations (Table 2) which are excellent catalysts for steam gasification. As shown in Table 4, pyrolysis of Wyodak coal up to 950°C in steam increases weight loss by 28.8 per-

cent. However, weight loss for Pittsburgh No. 8 coal is increased by only 6.0 percent. These results suggest that steam has small but significant effect on the weight loss of coals at lower pyrolysis temperature (Ca 650°C). However, steam appears to have a significant influence on the weight loss of Wyodak (sub-bituminous) coal at higher pyrolysis temperature (950°C). Tables 3 and 4 also indicate that steam has very little effect on the pyrolysis weight loss of acid-washed Wyodak coal both in the high (950°C) and low (650°C) temperature pyrolysis. This demonstrates that the effect of steam on the pyrolysis weight loss of Wyodak coal is mostly due to the catalytic effect of the exchangeable cations present in this low-rank coal.

Table 5 shows the effect of steam and heating rate on the pyrolysis weight loss of Pittsburgh No. 8 coal up to 900°C. The results suggest that heating rate has relatively small influence on devolatilization of coal in He. In contrast, the overall weight loss during pyrolysis of coal in steam is a strong function of heating rate. The weight loss during devolatilization in steam is 37 percent at 50°C/min which increases to 50 percent when a heating rate of 5°C/min was utilized. This increase in weight loss is attributable to gasification of coal/char by steam which is facilitated by longer residence time at slow heating rates.

Influence of Steam Atmosphere on the Reactivities of the Resulting Chars

Table 6 shows the effect of steam on the reactivities of chars prepared at low (650°C) and high (950°C) temperatures. There are several ways to express the reactivity of chars. As continuations of a previous study (5), we are reporting the reactivity data using maximum gasification rate (R_m) and the time for 10 percent char conversion ($T_{0.1}$). It can be seen that the 650° steam-prepared chars have higher R_m and shorter $T_{0.1}$ than those for the 650° helium-prepared chars. The 950° steam-prepared chars also have higher R_m (except for acid-washed Wyodak coal char) than those for the 950° helium-prepared chars. However, the $T_{0.1}$ of 950° steam-prepared chars are longer than $T_{0.1}$ of 950° helium-prepared chars. By viewing the total gasification profiles of 950° chars, it is evident that the 950° steam-prepared chars are less reactive than 950° helium-prepared chars. It appears that R_m does not serve as a good parameter for describing char reactivity in some cases. This is not surprising keeping in mind that char reactivity is a function of char conversion. In order to express the char reactivity properly, we suggest that it is appropriate to report both the maximum gasification rate and the time needed for certain levels of char conversion (e.g., $T_{0.1}$).

Table 7 compares the reactivities and oxygen chemisorption capacity (OCC) for various chars prepared at 650°C. It can be seen that steam-prepared chars have lower OCC and higher reactivity than helium-prepared chars. Long and Sykes (18,19) studied the mechanism of steam-carbon reaction and suggested that steam can dissociate to form an absorbed hydrogen atom and a hydroxyl group which is absorbed on a neighboring carbon atom of the char. They also suggested that the absorbed hydroxyl groups can undergo further reaction to form carbonyl groups and finally desorb as carbon monoxide. Hence, a probable explanation for the lower OCC of steam-prepared chars is that the "newly formed hydroxyl groups" could occupy some of the active sites for oxygen chemisorption and, therefore, lower the OCC of chars. These hydroxyl groups of chars could undergo gasification reaction to form monoxide and, thereby, enhance the reactivity of chars. The FTIR spectra demonstrate that steam-prepared char has slightly higher concentration of hydroxyl groups than those for the helium-prepared char. This implies that the "absorbed

hydroxyl groups" (or part of them) serve as surface complexes on the char surface which could have positive contribution to char reactivity. The data shown in Table 7 indicate that the enhanced effect of steam on the char reactivity (R_m) is dominant for the bituminous coal (Pittsburgh No. 8 coal) than for the subbituminous coal (Wyodak coal). This is perhaps due to the higher concentration of cations in Wyodak coal which catalytically promote char gasification. After acid-washing, the catalytic effect became less significant and the effect of steam on char reactivity became more dominant.

Because steam gasification reaction is highly favorable at 950°C, the lower reactivity of 950° steam-prepared chars as compared with 950° helium-prepared chars can be attributed to the relatively severe conditions which was utilized for coal pyrolysis.

Table 8 presents the effect of steam on the pyrolysis tar yields of Pittsburgh No. 8 coal in a fixed-bed reactor (SHRODR) and isothermal reactivity of produced char at 400°C. It can be seen that pyrolysis of coal in the presence of steam enhances the tar yield and reactivity of produced chars. Sharma and his coworkers (13) observed that pyrolysis of coal in steam increases the weight loss. However, there was no report regarding the effect of steam on the pyrolysis tar yield. We propose that steam can dissociately sorb on the char surface. This could reduce the recombination reactions and thereby suppress the char formation and increase the tar yield. In order to further confirm the enhanced effect of steam on char reactivity, a non-isothermal reactivity test has also been performed.

Steam-prepared and helium-prepared chars were heated in a TGA unit under 0.1 MPa oxygen at 10°C/min from 400°C to 900°C. Figure 2 shows the non-isothermal gasification profiles of these two chars. It is clear that the steam-prepared char is more reactive than helium-prepared char. Figure 3 shows the non-isothermal gasification rates DTG curves for the two chars. The maximum gasification rate of steam-prepared char is 25 percent higher than that for the helium-prepared char. The temperature for the maximum gasification rate of steam-prepared char is 8°C lower than that for the helium-prepared char. These results again confirm that pyrolysis of coal in the presence of steam at relatively lower temperature (650°C) enhances both the tar yield and reactivity of the resulting chars.

SUMMARY AND CONCLUSIONS

The above results demonstrate that pyrolysis of coal in the presence of steam at relatively lower temperature ($\leq 650^\circ\text{C}$) not only increases the weight loss and tar yield but also enhances the reactivity of the resulting char. Steam can dissociatively absorb on the char surface and thereby inhibit the recombination reactions between tar-free radicals and char-free radicals and, thereby, suppress the retrogressive reactions and increasing tar yield. The newly formed "hydroxyl surface complexes" can undergo further reaction to form carbon monoxide during gasification. Devolatilization of coal in the presence of steam at relatively higher

temperature (950°C) enhances the pyrolysis weight loss, primarily due to the steam gasification of coal char. However, the char prepared at elevated temperatures in steam is less reactive perhaps due to loss of volatiles in the presence of steam during the pyrolysis step.

ACKNOWLEDGEMENT: Funding for this work was provided by the US Dept of Energy, Morgantown Energy Technology Center.

REFERENCES

1. Bradbury, A. G. W., and F. Shafizadel, "Chemisorption of Oxygen on Cellulose Char," Carbon, 1980, 18, 109.
2. Furimsky, E., "Effect of H/C Ratio on Coal Ignition," Fuel Processing Technology, 1988, 19, 203.
3. Van Heek, K. H., and H.-J. Mühlen, "Effect of Coal and Char Properties on Gasification," Fuel Processing Technology, 1987, 15, 113.
4. Rybak, W., "Reactivity of Heat-Treated Coals," Fuel Processing Technology, 1988, 19, 107.
5. Khan, M. R., "Significance of Char Active Surface Area for Appraising the Reactivity of Low- and High-Temperature Chars," Fuel, 1987, 66, 1626.
6. Radovic, L. R., K. Steczko, P. L. Walker, Jr., and R. G. Jenkins, "Combined Effects of Inorganic Constituents and Pyrolysis Conditions on the Gasification Reactivity of Coal Chars," Fuel Processing Technology, 1988, 10, 311.
7. Patel, M. M., D. T. Grow, and B. C. Young, "Combustion Rates of Lignite Char by TGA," Fuel, 1988, 67, 165.
8. Solomon, P. R., M. A. Serio, and S. G. Herringer, "Variations in Char Reactivity with Coal Type and Pyrolysis Conditions," ACS Division of Fuel Chemistry Preprints, Vol. 31, No. 3, pp. 186.
9. Floess, J. K., J. P. Longwell, and A. F. Sarofim, "Intrinsic Reaction Kinetics of Microporous Carbons," Energy and Fuel, 1988, 2(6), 756.
10. Smith, L. W., "The Intrinsic Reactivity of Carbons to Oxygen," Fuel, 1978, 57, 409.
11. Hshieh, F. Y., and G. N. Richards, "Factors Influencing Chemisorption and Ignition of Wood Chars," Combustion and Flame, in Press.
12. Tsai, C. Y., and A. W. Scaroni, "Reactivity of Bituminous Coal Chars During the Initial Stage of Pulverized-Coal Combustion," Fuel, 1987, 66, 1400.
13. Sharma, D. K., A. Sulimma, and K. H. Van Heek, "Comparative Studies of Pyrolysis of Coal in Inert Gas, Steam, and Hydrogen Under Pressure," Erdoel Kohle, Erdgas, Petrochem, 1986, 39(4), 173.
14. Christosora, C. T., H.-J. Mühlen, K. H. Van Heek, and H. Jüntgen, "The Influence of Pyrolysis Conditions on the Reactivity of Char in H₂O," Fuel Processing Technology, 1987, 15, 17.
15. Ternan, M., and M. V. C. Sekhar, "The Catalytic Steam Gasification of Chars from Various Sources by K₂CO₃," Fuel Processing Technology, 1985, 10, 77.
16. Morgan, M. E., and R. G. Jenkins, "Pyrolysis of a Lignite in an Entrained-Flow Reactor. Effect of Cations on Total Weight Loss," Fuel, 1986, 65, 757.
17. Garcia, X., and L. R. Radovic, "Gasification Reactivity of Chilean Coals," Fuel, 1986, 65, 292.
18. Long, F. J., and K. W. Sykes, "The Mechanism of the Steam-Carbon Reaction," Proc. Roy. Soc. A., 1948, 183, 377.
19. Long, F. J., and K. W. Sykes, "The Effect of Specific Catalysts on the Reaction of the Steam Carbon System," Proc. Roy. Soc. A., 1952, 215, 100.

TABLE 1

Proximate and Ultimate Analysis of
Pittsburgh No. 8 Coal, Wyodak Coal
(PSOC 1520)

	Pittsburgh No. 8 Coal	Wyodak Coal
% C, daf	83.74	73.78
% H, daf	5.46	4.62
% N, daf	1.56	1.11
% S, daf	2.15	1.38
% O, daf (by difference)	7.09	19.11
<hr/>		
% Ash (as-received basis)	7.27	9.08
% Moisture	0.57	26.69
H/C Atomic (daf)	0.78	0.75
O/C Atomic (daf)	0.064	0.19

TABLE 2

Exchangeable Cation Content
of Wyodak Coal

Cation	% of Dry Coal
Ca	1.30
Mg	0.275
K	0.005
Na	0.020
Fe	0.275

TABLE 3

Effect of Steam^a on the Pyrolysis Weight Loss of
Coals Up To 650°C (Heating Rate = 20°C/min)

Sample/Pyrolysis Atmosphere	Weight Loss During Pyrolysis Up To 650°C, % of Coal (Dry Base)
Wyodak Coal/He	39.7
Wyodak Coal/Steam	43.2
Acid-Washed Wyodak Coal/He	38.2
Acid-Washed Wyodak Coal/Steam	38.2
Pittsburgh No. 8 Coal/He	30.2
Pittsburgh No. 8 Coal/Steam	37.2

^a Pressure of Steam: 3 kPa

TABLE 4

Effect of Steam^a on the Pyrolysis Weight Loss of
Coals Up To 950°C (Heating Rate = 20°C/min)

Sample/Pyrolysis Atmosphere	Weight Loss During Pyrolysis Up To 950°C, % of Coal (Dry Base)
Wyodak/He	57.6
Wyodak/Steam	86.4
Acid-Washed Wyodak Coal/He	49.5
Acid-Washed Wyodak Coal/Steam	50.8
Pittsburgh No. 8 Coal/He	41.5
Pittsburgh No. 8 Coal/Steam	47.5

^a Pressure of Steam: 3 kPa

TABLE 5
Effect of Steam and Heating Rate on the
Pyrolysis Weight Loss of Pittsburgh
No. 8 Coal Up To 900°C

Heating Rate (°C/min)	Weight Loss During Pyrolysis Up To 900°C	
	He	Steam
5	38.0	50.0
10	37.0	44.5
20	37.0	40.5
50	37.0	37.0

TABLE 6
Effect of Steam on the Reactivities of Chars Prepared
at Low (650°C) and High (950°C) Temperature

Sample/Pyrolysis Temperature and Atmosphere	Maximum Gasification Rate at 400°C, %/min (daf)	Time for 10% Conversion (To.1), min
Wyodak/TGA 650/He	10.14	10.0
Wyodak/TGA 650/Steam	10.84	9.0
Wyodak/TGA 950/He	1.58	40.0
Wyodak/TGA 950/Steam	2.81	42.5
Acid-Washed Wyodak/TGA 650/He	3.56	13.0
Acid-Washed Wyodak/TGA 650/Steam	4.06	13.0
Acid-Washed Wyodak/TGA 950/He	1.16	36.7
Acid-Washed Wyodak/TGA 950/Steam	1.05	42.5
Pittsburgh No. 8/TGA 650/He	1.06	30.5
Pittsburgh No. 8/TGA 650/Steam	1.31	28.0
Pittsburgh No. 8/TGA 950/He	0.45	64.5
Pittsburgh No. 8/TGA 950/Steam	0.58	81.0

TABLE 7

Comparison of Reactivities and Active Surface Areas for Various Chars^a

Sample/Pyrolysis Temperature and Atmosphere	g^b , (% of Char, daf)	Rm^c (400°C) ($g\ g^{-1}\ h^{-1}$, daf)	ASA^d , (g/m^2)	$k^e \times 10^3$ ($g\ m^{-2}\ h^{-1}$)
Pittsburgh No. 8/TGA 650/He	5.73	0.64	172	3.72
Pittsburgh No. 8/TGA 650/Steam	4.93	0.79	148	5.34
Wyodak/TGA 650/He	8.51	6.08	255	23.84
Wyodak/TGA 650/Steam	6.91	6.50	207	31.40
Acid-Washed Wyodak/TGA 650/He	5.62	2.14	169	12.66
Acid-Washed Wyodak/TGA 650/Steam	5.35	2.44	161	15.16

^a Pyrolysis was performed at 20°C/min.^b Chemisorption capacity. Chemisorption was performed at 155°C in oxygen for 15 h.^c Maximum gasification rate at 400°C in oxygen.^d Active surface area or oxygen chemisorption capacity (OCC).^e Reactivity per unit active surface area.

TABLE 8

Influence of Steam on the Pyrolysis Tar Yield for Pittsburgh No. 8 Coal and the Reactivity of the Resulting Chars^a

Pyrolysis Atmosphere	Tar Yield, % of Coal (daf)	Maximum Gasification Rate at 400°C, %/min (daf)	Time for 10% Conversion, min
He	14.5	1.11	31.6
Steam	16.3	1.36	23.1

^a Pyrolysis was performed in SHRODR at 500°C, 20 min.

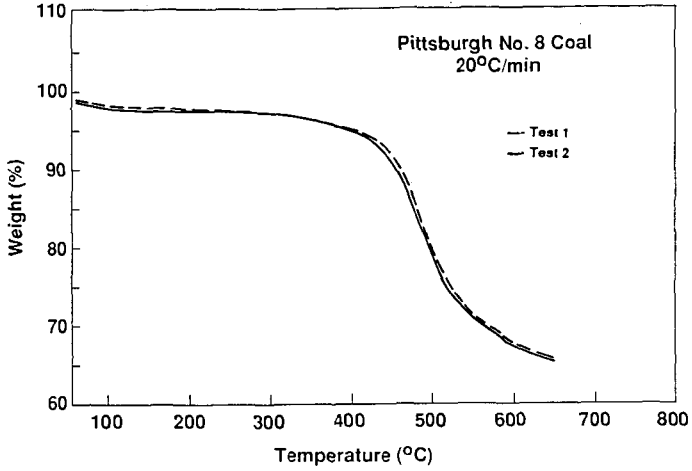


FIGURE 1a. Reproducibility of TGA Devolatilization Runs

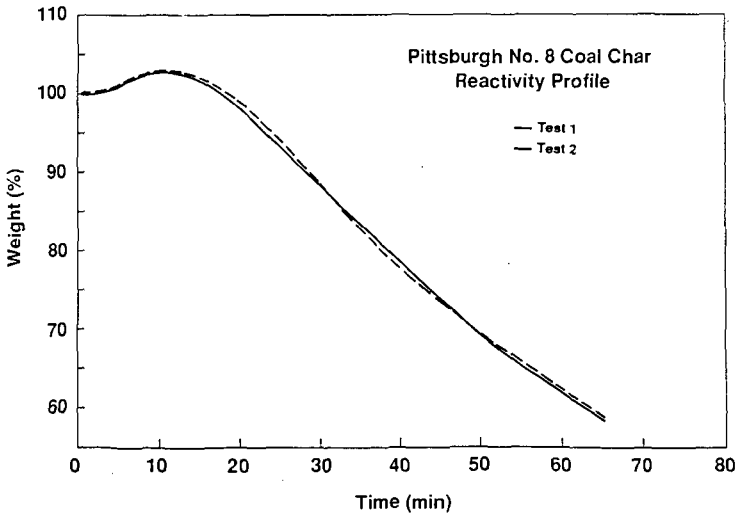


FIGURE 1b. Reproducibility of TGA Reactivity Profiles

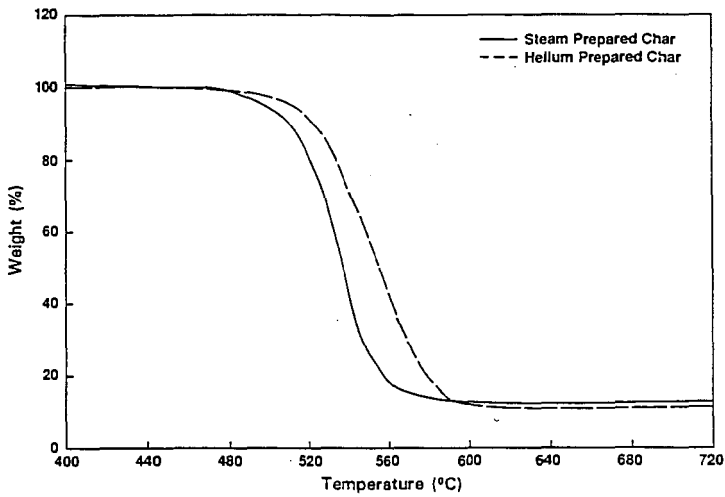


FIGURE 2. Comparison of Non-isothermal Gasification Profiles of Chars Prepared Under Helium and Steam

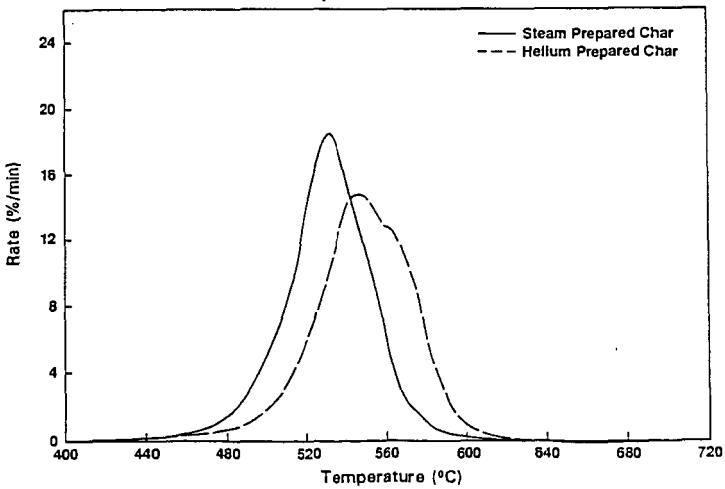


FIGURE 3. Comparison of Non-isothermal Gasification Rates of Chars Prepared Under Helium and Steam

COMBUSTION CHARACTERISTICS OF MILD-GASIFICATION CHARS

C. Stuart Daw
Oak Ridge National Laboratory*
Bldg. 9108, P. O. Box 2009, Oak Ridge, TN 37831

INTRODUCTION

The commercial success of mild coal gasification (MG) depends on economical utilization of the byproduct char. While various utilization options are being considered (e.g., coke manufacture, activated carbon production, and further gasification), the boiler fuel market is likely to be the largest potential consumer. A key concern is the combustion performance of MG chars relative to more conventional boiler fuels. This paper summarizes recent results of MG char characterizations conducted by Oak Ridge National Laboratory (ORNL) for Morgantown Energy Technology Center (METC) of the Department of Energy (DOE). The char characterizations are being conducted in conjunction with MG liquid characterizations.

EXPERIMENTAL METHODS AND MATERIALS

Char and Reference Fuel Samples

Char samples were obtained from two MG processes, one developed by the United Coal Company (UCC) and the other by SGI International (SGI). A single UCC char sample was obtained from a typical test on the UCC MG test unit [test run P1/12; United Coal Company (1988)]. In this case, the parent coal was Kentucky Williamson No. 2 seam, a high-volatile, bituminous coal. Three SGI char samples were obtained, each representing successively higher devolatilizations of Montana Rosebud subbituminous coal. These samples were produced in cooperative tests between SGI and Peabody Coal Company [Estergar(October 1988)]. Four widely-used reference fuels were also included to extend the applicability of the results: Texas lignite; Kentucky No. 9 high-volatile, bituminous; delayed petroleum coke, and anthracite.

Table 1 summarizes proximate, ultimate, and BET analyses of the char samples, typical analyses of the parent coals, and reference fuel analyses. It is clear that all the SGI chars have more volatiles and much greater surface area than the UCC char. Such differences are believed to be due both to the parent coals and to higher temperature and residence time in the UCC process.

Thermogravimetric Tests

Low-temperature combustion tests were conducted for each char and reference fuel using a Netsch model STA 429 thermogravimetric (TG) analyzer. Previous studies [e.g., Jenkins et al (1973),

* This work was conducted at Oak Ridge National Laboratory operated by Martin Marietta Energy Systems, Inc. for the U.S. Department of Energy under contract DE-AC05-84OR21400. By acceptance of this article, the publisher acknowledges the U. S. Government's right to retain a nonexclusive, royalty-free license in and to any copyright.

Ceely and Daman (1981), Khan (1987)] have demonstrated the usefulness of TG comparisons of coals and chars. Standard operating procedure involved heating approximately 20 mg of 105-125 μm particles from ambient up to 1273 K. Heating rate was 10 K/min, and gas flow was 190 cc/min. Dry air (21% oxygen) was injected directly into the sample crucible. Sample weight, rate of weight change, and temperature were continuously monitored.

The limiting external oxygen mass-transfer rates for similar conditions have been determined previously [Daw and Mitchell (1986)]. These limits were reevaluated during the current tests based on the observed burning rates for previously tested reference fuels and on the asymptotic high-temperature burning rates of the chars [see Mulcahy and Smith (1969)]. Measured burning rates were corrected to true intraparticle rates by the relationship of Young and Smith (1981):

$$RI = R/[1 - (R/RMT)]^n \quad (1)$$

where RI is the internally-limited burning rate (i.e., the rate limited solely by intraparticle processes), RMT is the maximum rate possible due to external mass transfer of oxygen, R is the observed burning rate, and n is the effective reaction order in oxygen. In most cases such corrections were small.

Fixed-Bed Reactor Tests

Higher-temperature combustion tests were conducted using the fixed-bed reactor at Babcock and Wilcox's (B&W) Alliance Research Center. This reactor was constructed for the Atmospheric Fluidized Bed Combustion Fuels Characterization Program sponsored by the Electric Power Research Institute (EPRI). B&W has used this reactor to characterize a range of coals, refuse derived fuels, and coal-cleaning refuse for EPRI and Consolidated Edison Company of New York [Chandran et al (1988, 1989)]. Described in detail elsewhere [Chandran et al (1987)], the reactor is a 5.1-cm diameter quartz vessel containing a bed of spent fluidized bed combustor sorbent. The bed is heated electrically, and preheated nitrogen/oxygen mixtures enter the top, flowing down through the bed. Fuel particles are injected batchwise via a solenoid valve, and they land on top of the bed where they devolatilize and burn. The reactor is designed for gas velocities, temperatures, gas compositions, and particle sizes similar to those expected for AFBC. The operating ranges for each of the fuels in this study were: 1045-1215 K gas temperature, 3-10 volume % oxygen, 1.5-1.6 atm total pressure, and 1.3-1.5 m/s superficial gas velocity.

Fuel particles were prescreened into two narrow fractions: 1) 105-125 μm (115 μm mean) and 2) 500-595 μm (547 μm mean). The fuel batch weight was chosen such that the reactor oxygen concentration decreased by less than 10% at the maximum combustion rate. Devolatilization and combustion were monitored by continuous analysis of the reactor exit gas for carbon dioxide, carbon monoxide, and hydro-carbons. Net carbon loss-vs.-time was determined by integrating total gas carbon concentration. Particle temperatures were estimated by heat balances accounting for conduction, convection, radiation, and heat of combustion.

EXPERIMENTAL RESULTS AND DISCUSSION

Thermogravimetric Results

Figures 1 and 2 illustrate the observed variation in the rate-vs-temperature profiles for the reference fuels. From these plots it is clear that the UCC char ignites and burns more slowly than all three SGI chars at the conditions tested. Many different ignitability/reactivity measures can be derived from TG profiles. Table 2 lists some example measures to illustrate comparisons of the fuels tested here. While minor variations occur depending on the measure used, the general trends are readily apparent: 1) Texas lignite⁰ is by far the most ignitable and reactive; 2) the SGI chars and Kentucky 9 bituminous are similar and slightly less ignitable and reactive than lignite; 3) the UCC char and petroleum coke are similar and significantly less ignitable and reactive than the SGI chars and Kentucky 9; and 4) anthracite is by far the most difficult to burn.

Fixed-Bed Reactor Results

Figure 3 compares the fixed-bed profiles for 115 μm particles of each fuel exposed to 3% oxygen at 1100-1120 K. As with the TG results, the fixed-bed profiles clearly distinguish among the fuels. Texas lignite burns by far the most rapidly, followed closely by Kentucky No. 9 bituminous and the SGI chars. Petroleum coke, UCC char, and anthracite are again much slower. Quantitative comparisons can be made using various profile measurements such as: 1) burning rate at char ignition, 2) degree of fixed carbon conversion after a fixed elapsed time, and 3) time to achieve a given fixed-carbon conversion. For the fuels tested the basic profile shapes following char ignition are similar, and thus all three of the above measures give identical rankings. Measurement 1 above, the burning rate at char ignition, is selected as the key index for further discussion.

Table 3 compares the estimated initial char burning rates for the profiles in Figure 3. The fuel ranking resulting from these burning rates is virtually identical with the rankings developed from burning rates evaluated at other fixed-bed conditions. An important point emerging from these comparisons is that the relative fuel reactivities are consistent over the range of fixed-bed and TG conditions tested.

Combined Burning-Rate Expressions

Estimates of the true intra-particle combustion rate at char ignition, RI, were made for each fuel and test condition (both TG and fixed-bed) using Eqn. 1. As expected, the corrected rates were found to follow the standard Arrhenius rate expression:

$$RI = A \exp(-E/Rg T_p) PO_2^n = kw PO_2^n \quad (2)$$

where A is the pre-exponential rate coefficient, E is the effective activation energy, Rg is the ideal gas constant, T_p is particle temperature, PO₂ is bulk-gas-oxygen partial pressure, and

kw, was determined assuming n to be 0.5. Within the scope of this study it is not possible to select with certainty any value of n between 0.5 and 1. Essenhigh(1981) has shown that Zone 2 combustion (combustion in which pore diffusion is a significant controlling factor) should exhibit an effective reaction order of 0.5. As discussed below, the Arrhenius fits of the present data suggest Zone 2 burning. Selection of n=0.5 is also consistent with earlier fixed-bed data [Daw (1988)] and conforms more closely to the comprehensive study by Suuberg et al (1988).

Figure 4 depicts the combined Arrhenius fits for the chars and reference fuels (note: the horizontal axis is the reciprocal of estimated particle temperature not gas temperature). Comparing slopes, the activation energies for all four chars do not seem to differ greatly. Table 4 summarizes the Arrhenius parameters quantitatively. Within experimental uncertainty, all the activation energies fall within the 4.8 to 9.6 kJ/mole (20 to 40 kcal/mole) expected for Zone 2 burning [Essenhigh (1981)]. Thus the assumption of 0.5 oxygen reaction order is reasonable.

CONCLUSION

The above results suggest that the bituminous char tested is more suitable for firing in non-sensitive applications, such as fluidized beds, stokers, or U-flame boilers. The subbituminous chars evaluated may be sufficiently reactive for pulverized firing in bituminous boilers with little or no supplemental fuel.

REFERENCES

- Coely, F. J. and Daman, E. L., "Combustion Process Technology," in Chemistry of Coal Utilization, M. A. Elliot, editor, John Wiley and Sons, pp 1313-1387, 1981.
- Chandran, R. R., Duqum, J. N., Jafari, M. C., Rowley, D. R., and Perna, M. A., "Fuels Characterization Project- Interim Report," Report by Babcock and Wilcox to EPRI, RDO:88:4753-06-55:D1, 1987.
- Chandran, R. R., Duqum, J. N., Perna, M. A., Rowley, D. R., Daw, C. S., Petrill, E. M., and McGowin, C. R., "AFBC Fuels Characterization Program Results For Different Coals, Refuse-Derived Fuel (RDF), and Coal-Cleaning Refuse," EPRI Seminar on Fluidized-Bed Combustion Technology for Utility Applications, vol 1, Palo Alto, California, May 1988.
- Chandran, R. R., Duqum, J. N., Perna, M. A., Sutherland, D. D., Rowley, D. R., Pirkey, J., and Petrill, E. M., "Ranking Fuels and Sorbents for Utility Scale AFBC Application," Tenth International Conference of Fluidized Bed Combustion, San Francisco, May 1989.
- Daw, C.S., "Second Interim Report to the Tennessee Valley Authority on the Analysis of the Kentucky Fixed-Bed Reactor Data from the Babcock and Wilcox Alliance Research Center," April 1988.
- Daw, C. S. and Mitchell, R. E., "Char Combustion Kinetics for Kentucky No. 9 Coal," Proceedings of the AFB Technology for Utility Applications Seminar sponsored by the Electric Power Research Institute, Palo Alto, California, April 1986.
- Essenhigh, R. H., "Fundamentals of Coal Combustion," in Chemistry of Coal Utilization, M. A. Elliot, editor, John Wiley and Sons, pp 1153-1312, 1981.
- Esterger, E. P., SGI International, La Jolla, California, personal communication, October 1988.

Jenkins, R. G., Satyendra, P. N., and Walker, P. L., Jr., Fuel, vol 52, pp 288-293, October 1973.

Mulcahy, M. F. R. and Smith, I. W., Rev. Pure and Appl. Chem., 19, pp 81-108, 1969.

Sauberg, E. M., Wojtowicz, M., and Calo, J. M., "Reaction Order for Low Temperature Oxidation of Carbons," Proceedings of the Twenty-Second International Symposium on Combustion, The Combustion Institute, Pittsburgh, Pennsylvania, p 1988.

Young, B. C. and Smith, I. W., Proceedings of the Eighteenth International Symposium on Combustion, The Combustion Institute, Pittsburgh, Pennsylvania, p 1245, 1981.

United Coal Company, Project Status Report, UCC R&D C17-20, Contract No. DE-AC21-87MC23289, September 16, 1988.

Table 1. Ultimate and proximate analyses of the test chars, parent coals, and reference fuels.

Chars:	Ultimate*				Tot. S	Pyr. S	Sul. S	Org. S
	C	H	N	Cl				
UCC	83.88	3.18	1.46	0.077	0.70	0.036	0.0061	0.66
SGI 4	63.40	3.07	1.00	0.0037	0.78	0.055	0.053	0.67
SGI 20	68.31	2.34	1.13	0.0009	0.99	0.016	0.0094	0.96
SGI 48	66.50	3.27	1.12	0.0022	0.64	0.16	0.021	0.46
Parent Coals:								
KY WIL. 2 (UCC)	78.18	5.24	1.46	0.13	0.98	-	-	-
MT ROS. (SGI)	54.82	3.72	0.79	0.02	0.63	0.33	0.040	0.42
Ref. Fuels:								
TX LIG.	33.27	3.28	0.77	-	0.75	-	-	-
KY 9	65.82	4.72	1.40	-	3.48	-	-	-
PET. CK.	85.75	3.87	1.46	-	5.18	-	-	-
ANTH.	79.80	1.79	0.78	-	0.53	-	-	-

Chars:	Proximate*				FC	BET ⁺
	WATER	ASH	VM			
UCC	2.32	5.86	11.49	80.33	0.197	
SGI 4	10.82	15.27	18.34	55.57	22.6	
SGI 20	6.84	15.63	13.99	63.54	30.5	
SGI 48	8.61	11.52	23.72	56.15	11.2	
Parent Coals:						
KY WIL. 2	1.80	5.00	33.80	59.40	-	
MT ROS.	19.84	9.16	39.02	51.82	-	
Ref. Fuels:						
TX LIG.	33.27	7.25	30.58	28.90	-	
KY 9	6.78	10.81	37.75	44.66	-	
PET. CK.	1.10	2.14	13.86	82.90	0.230	
ANTH.	4.23	10.85	5.74	79.18	-	

* All analyses as weight percent on an as-received basis (i.e., moisture and ash included).

+ BET surface area by N₂ adsorption (m²/g).

Table 2. Example measures of TG reactivity for the fuels tested.

Fuel	Tign	Rign	Tmax	FCCL	FCCh	T50
UCC	753	7.2×10^{-4}	847	0.10	0.50	823
SGI 4	723	9.6×10^{-4}	753	0.39	0.71	785
SGI 20	703	5.9×10^{-4}	801	0.33	0.71	793
SGI 48	713	1.3×10^{-3}	778	0.45	0.84	781
TX LIG.	668	2.6×10^{-3}	681	0.84	0.91	703
KY 9	748	1.9×10^{-3}	798	0.28	0.59	798
PET. COKE	761	7.8×10^{-4}	823	0.0	0.36	838
ANTHRACITE	793	2.7×10^{-4}	918	0.0	0.05	883

Tign = char ignition temperature (K) ; Rign = rate at char ignition (g/g s) or (l/s); Tmax = maximum burning rate temperature (K); FCCL = fractional fixed carbon conversion at 773 K; FCCh = fractional fixed carbon conversion at 823 K; T50 = temperature at which fixed carbon conversion reaches 0.5 (K)

Table 3. Typical fixed-bed combustion results for 115 micron particles in 3% oxygen at 1100-1120 K.

Fuel	Tg	Vo	Tp	Rign
UCC	1120	1.51	1127	0.059
SGI 4	1120	1.48	1174	0.30
SGI 20	1114	1.69	1164	0.36
SGI 48	1120	1.45	1183	0.47
TX LIGNITE	1101	1.60	1189	1.5
KY 9	1103	1.59	1141	0.59
PET. COKE	1116	1.67	1132	0.090
ANTHRACITE	1114	1.46	1117	0.024

Tg = gas temperature (K) ; Vo = superficial gas velocity (m/s) ; Tp = estimated particle temperature (K); Rign = burning rate (l/s)

Table 4. Arrhenius char combustion parameters derived from the combined combustion data.

Fuel	A*	E ⁺	r ²
UCC	1.7×10^4	5.71 ± 0.57	0.990
SGI 4	7.2×10^4	6.70 ± 0.57	0.997
SGI 20	3.0×10^4	7.00 ± 0.88	0.994
SGI 48	4.9×10^4	5.61 ± 0.53	0.997
TX LIGNITE	1.8×10^5	5.38 ± 0.31	0.999
KENTUCKY 9	1.6×10^4	7.05 ± 0.91	0.996
PET. COKE	2.0×10^4	5.73 ± 0.55	0.990
ANTHRACITE	2.8×10^4	6.47 ± 1.15	0.974

A = Arrhenius pre-exponential factor ($s^{-1} atm^{-0.5}$);
 E_a = activation energy (kJ/mole) and 95% confidence interval;
 r² = coefficient of determination for regression

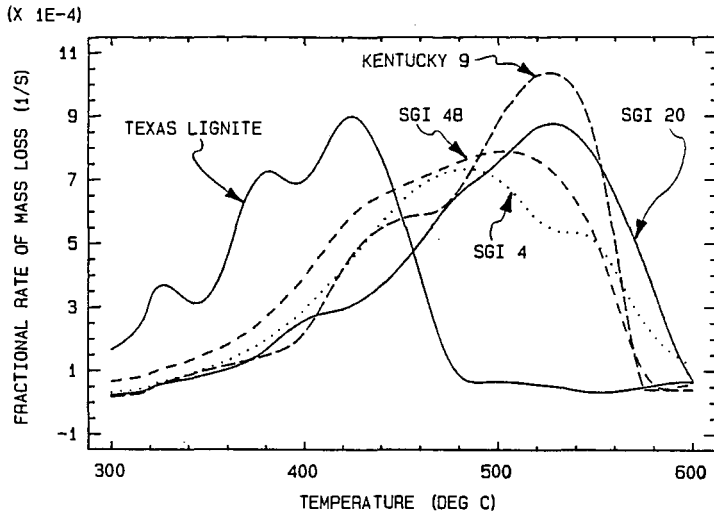


Figure 1. TG rate profiles for the more reactive fuels.

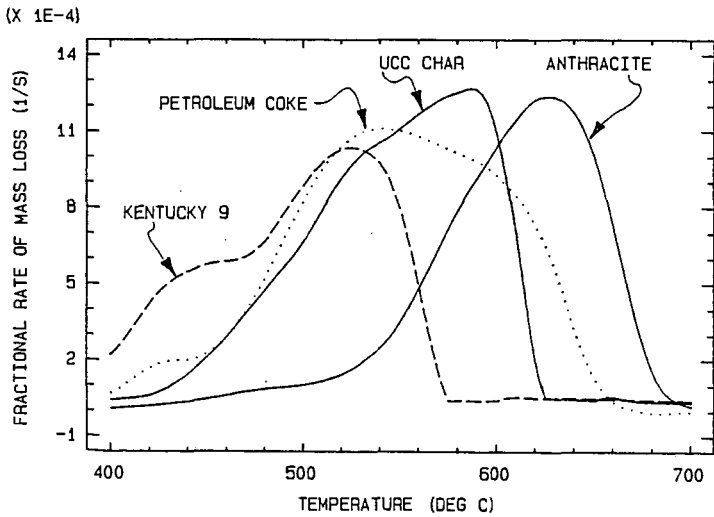


Figure 2. TG rate profiles for the less reactive fuels.

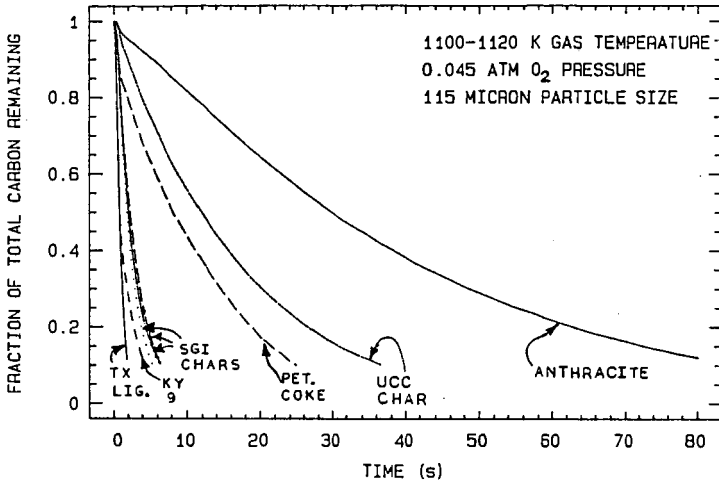


Figure 3. Comparison of the fixed-bed profiles for all the fuels at one test condition.

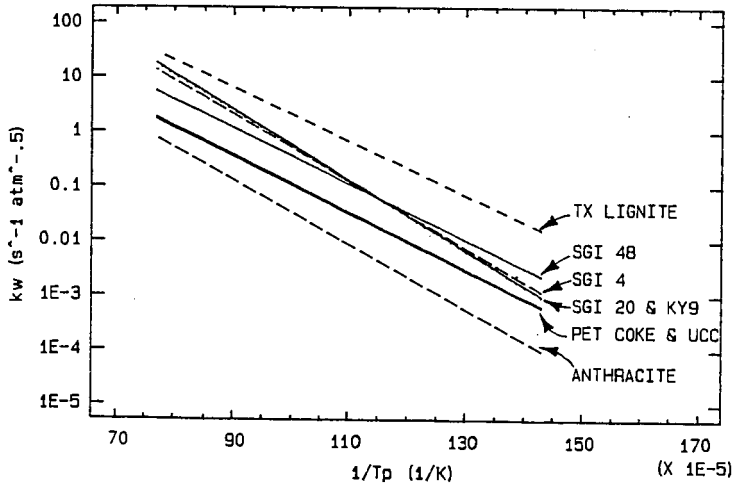


Figure 4. Comparison of Arrhenius plots for all the fuels tested.

REACTIVITY OF MILD GASIFICATION CHARs DERIVED FROM AN ILLINOIS COAL

M. Rostam-Abadi¹, J. A. DeBarr¹, W.T. Chen¹, D. P. McCollor², and S. A. Benson²

¹ Illinois State Geological Survey, 615 E. Peabody Drive, Champaign, IL 61820

² University of North Dakota, Energy and Minerals Research Center, Grandfork, North Dakota 58202

INTRODUCTION

In recent years, some emphasis has been given to producing premium liquids by mild gasification of coal¹⁻³. The principle product from the mild gasification process is a partially devolatilized coal that must be effectively utilized (burned or gasified) to help the overall economics of the process. The loss of volatile matter indicates loss of hydrocarbon materials from the coal that can influence reactivity and combustion characteristics such as ignition, flame stability and carbon burn-out.

A large number of studies have been conducted on the oxidation reactivity and combustion properties of coal chars⁴⁻⁶. However, the majority of these studies have focused on chars prepared in laboratory reactors under rapid heating rates (10⁴°C/sec). A few studies have dealt with the ignition⁷ and reactivity of industrial process chars⁸. Reactivities of chars prepared under mild pyrolysis conditions have been recently reported⁹. Fuels prepared in laboratory reactors by heating coals at 12.5 to 20°C/min to 500°C were more reactive than either the parent coals or chars produced at higher pyrolysis temperatures. The present authors reported the reactivities of chars prepared from an Illinois coal under various pyrolysis conditions¹⁰. The results suggested that lower pyrolysis temperatures, higher heating rates, and shorter soak times increased reactivity.

In this paper, the reactivities and ignition temperatures of chars derived from an Illinois coal in a pilot scale reactor under mild gasification conditions are reported. The paper focuses on the influence of volatile matter and particle size on char reactivity.

EXPERIMENTAL

Char Preparation

Chars, also referred to as partially devolatilized (PD) coals, were produced in the Mild Gasification Unit at United Coal Company Research Corporation in Bristol, Virginia in October 1986. The coal was from the Illinois Basin Coal Sample Program, Sample IBC-103. The details of PD coal production have been reported elsewhere¹¹. In brief, the PD coals were prepared by heating the coal under a slight vacuum in a fixed bed reactor (8-inch diameter, and 8-foot long) which was located inside a natural gas fired furnace. The furnace temperature was kept at 760°C during the production runs. Three PD coals designated as PD-1, PD-2, and PD-3 were prepared at residence times of 1.70, 2.90 and 3.17 hours.

Five size fractions of coals and PD coals were prepared by grinding the -8 mesh fuels in a rod mill. The crushed samples were dry sieved to obtain 65x100, 100x150, 150x200, 200x270, and 270x400 mesh fractions. The samples were stored under nitrogen to prevent oxidation.

Ignitability Tests

An ignitability test apparatus, shown in figure 1, was used to determine ignition temperatures of fuels. It consisted of an oxygen reservoir, a sample holder tube, a quartz reactor tube and an electric furnace. Fuel particles were injected into the reactor by oxygen gas through a built-in orifice. Six thin wire (0.0076 cm) type K thermocouples spaced at 2 cm apart measured axial temperature variations inside the reactor. The thermocouples were interfaced with a computer for automatic data collection. Typical data acquisition rates were six simultaneous measurements at 50 millisecond intervals.

In a typical ignition test, 20 mg of sample was injected into the preheated (between 390 and 500°C) reactor. The volume of oxygen carrier gas used to inject the sample was 10 cc at 5 to 7 psig. The relatively low pressure and volume of the carrier gas ensured that the fuel particles traveled with velocities approaching their free fall velocities inside the reactor.

Criteria for positive ignition were a brilliant flash and an abrupt increase in temperature inside the reactor during the test. If a negative test was noted, the reactor temperature was increased in 5°C increments and the test procedure was repeated.

Thermogravimetric Tests

An Omniherm thermogravimetric analyzer (TGA) which was interfaced with a computer was used to obtain burning profiles (non-isothermal TGA) and isothermal reactivity data. Burning profiles were obtained by heating a sample mass of < 5 mg at a constant rate of 20°C/min in air to 850°C. A gas flow rate of 200 cc/min (STP) was used.

In isothermal reactivity tests, a sample mass of 2 to 4 mg was heated at 50°C/min under nitrogen flow to 550°C. The sample was then cooled to between 400 and 525°C and the nitrogen flow was replaced with dry air flowing at 200 cc/min. The weight of the char remaining, the rate of weight loss, and temperature were monitored by the computer at 5 to 40 second intervals depending on the reaction temperature. A modified TGA quartz furnace tube was used to obtain reliable rate data in the initial stage of oxidation¹². The objective was to achieve the desired oxygen concentration in the furnace tube as quickly as possible.

Drop Tube Furnace Tests

These tests were conducted using the University of North Dakota Energy and Minerals Research Center drop tube furnace (DTF). The details of the furnace assembly, are given elsewhere¹².

Combustion tests were performed on the 65x100 and 270x400 mesh size fractions of the coal and three PD coals. The furnace temperatures selected were 900°C and 1300°C. The gas in the tube furnace (6.5 cm i.d.) contained 3% oxygen - 97% nitrogen and flowed at a nominal rate of 5 l/min. The flow rate was chosen to keep the residence times within a single furnace segment for nearly all the tests. The flow rate was adjusted to give residence times of 0.1 and 0.8 seconds. Carbon conversion efficiencies were calculated using the ash tracer method.

RESULTS AND DISCUSSION

Characterization of Fuels

The analyses of the coal and PD coals are summarized in tables 1 and 2. The volatile matter content, hydrogen and fixed carbon were nearly identical for the five size fractions of coal. However, for PD coals, volatile matter and hydrogen contents increased while carbon contents decreased with decreasing particle size range. The amount of volatiles increased from 24.8% to 29.2% for PD-1, from 15.7% to 21.3% for PD-2, and from 11.5% to 15.7% for PD-3 as particle size range decreased from 65x100 mesh to 270x400 mesh. Hydrogen content remained unchanged for PD-1 samples but increased by 21% for PD-2 and by 41% for PD-3 samples.

Comparison of the devolatilization profile (non-isothermal TGA under nitrogen atmosphere) of the fuels indicated that a major decomposition stage for the coal and PD coals occurred between 380 and 530°C¹². The average weight losses were 25.6, 14.0, 7.4, and 4.8% for coal, PD-1, PD-2, and PD-3 respectively. These results confirmed the presence of varying amounts of coal-like materials in the PD-coals. This was attributed to the manner in which PD coals were prepared. Because the reactor was externally heated, the temperature at the wall of the reactor was much higher than at the center. Therefore, the coal particles near the wall were highly devolatilized whereas those at the center were not. The devolatilization profiles suggest that a fraction of coal was never devolatilized during processing.

Burning Profiles

Burning profiles obtained for the 65x100 mesh coal, PD-1, PD-2, and PD-3 coals are shown in figure 2. The profiles are offset to avoid overlap. The onset of burning was about 375°C for all the samples. However, there are clear differences among the burning profiles. Raw coal exhibited a single-burn profile, while double-burn profiles were observed for PD-1, PD-2 and PD-3. The second burn appeared as a shoulder peak for PD-1 and became more pronounced for PD-2 and PD-3. The double-burn behavior observed for the PD coals suggested the presence of at least two types of combustibles in the fuels. The two portions of combustibles burned in two distinct stages with peak burn rates at approximately 500°C and 550°C. The higher reactivity constituents (low temperature burn) had burning properties similar to coal and was present in larger concentrations in PD-1 followed by PD-2 and PD-3¹². Fuels with higher volatile matter content burned more rapidly. For example at 500°C, the amount of combustible materials burned (not shown) was 70% for the raw coal, 55% for PD-1, 40% for PD-2, and 20% for PD-3. Differences in volatile matter had the greatest impact on burn-out temperatures which were 580, 630, 660 and 690°C for the coal, PD-1, PD-2 and PD-3. The results indicate that under the conditions used, raw coal was the most readily combusted fuel, followed by PD-1, PD-2 and finally PD-3.

Ignition Temperatures

The effect of volatile matter on ignition temperatures is presented in figure 3. Ignition temperatures varied between 406 and 494°C and were independent of volatile matter (except for 270x400 mesh fuels) in the range of 28 to 41% (daf). Below 28%, the volatile matter effect on ignition temperature appears to be significant among all the different particle size fractions tested (ignition temperature increased between 40 and 70°C). However, it has been shown in the literature that the role of volatile matter on the ignition temperature is little or none⁷ (heterogeneous ignition

theory). Therefore, the differences in ignition temperatures observed could be attributed to inherent reactivity differences among the fuels tested.

The influence of particle size on ignition temperature is illustrated in figure 4. The particle size dependence of ignition temperature appeared to be rather mild with a spread of 30°C separating the studied size fractions. With the exception of the 65x100 mesh fraction (180µm average particle size), the ignition temperatures for the coal and PD coals increased with decreasing particle size. Ignition curves exhibited a minimum at 100x150 mesh size range (130µm).

The presence of a minimum on the ignition curves and the observed narrow temperature difference among different size fractions could be attributed to contributions of particle and cloud ignition. According to the Semenov thermal explosion theory¹³, which is commonly used to model single coal particle ignition, large particles ignite at lower temperatures. However, it has been shown that under dust cloud conditions, ignition temperatures of fine particles are lower than those of large particles¹⁴. In this work, regardless of particle size range, a constant sample mass of 20 mg was used. Therefore, samples containing finer particles had higher solid mass density (mass/unit reactive volume) than those containing coarser particles, and the ignition approximated cloud ignition rather than particle ignition. As a result, there was a shift from dust cloud ignition to single particle ignition as particle size range increased. Because the opposite nature of these two mechanisms offset the other, a minimum and a narrow temperature difference were observed for ignition curves of the fuels:

Isothermal Reactivity Studies

Initial reactivity tests were conducted at 475°C. The data were used to calculate apparent rate, R,

$$R = \frac{-1}{f} \frac{df}{dt} \quad (1)$$

and

$$f = (M - M_a) / (M_o - M_a) \quad (2)$$

where f = fraction combustible remaining at time t, M = mass of sample at time t, M_o = initial sample mass, M_a = mass of sample at complete conversion, i.e. ash. At 475°C, the rates were the same for all particle sizes, indicating the data were obtained under diffusion-free conditions. The apparent rates at 50% conversion were 0.013, 0.025 and 0.062 g/g/min for PD-1, PD-2 and PD-3, respectively. The rate for a char (18% volatile matter) that was prepared in the TGA at 500°C under nitrogen atmosphere was 0.2 g/g/min.

Additional tests were performed at temperatures between 400 to 525°C to evaluate activation energies for the oxidation of 200x270 mesh fuels. In figure 5, the values of ln(-df/dt/f) evaluated at 50% burn-off are plotted against 1/T. The activation energies obtained from the slopes of the plots were 146, 137, 134, and 125 kJ/mole for the 500°C char, PD-1, PD-2 and PD-3. The observed activation energies are comparable with previously reported values for various types of coal chars^{8,9}. The data shown in figure 5 indicate that the 500°C char is 2.5, 6.2, and 9.5 times more reactive than PD-1, PD-2, and PD-3.

Drop Tube Furnace Tests

Figure 6 shows carbon conversion at 900°C for 0.1 and 0.8 second residence times for 65x100 mesh and 270x400 mesh size fractions of coal and PD coals. Carbon conversions ranged from 10 to 28% at 0.1 second residence time and from 10 to 75% at 0.8 seconds residence time as volatile matter content increased from 12 to 40% (daf basis). These data indicate that 1) the fraction of carbon burned increased with increasing volatile matter, with a larger increase noted at 0.8 seconds, and 2) the effect of residence time on carbon loss was more pronounced for fuels with higher volatile matter content. The particle size effect on carbon conversion was small, although it was more pronounced at longer residence times.

Carbon conversion data at 1300°C are shown in figure 7. Carbon conversion increased with increasing volatile matter and increasing residence time. The data indicate that the effects of volatile matter and residence time on carbon conversion were more pronounced at the higher furnace temperatures. The percent of carbon combusted at 1300°C and 0.8 second residence time varied between 62 and 90 for the 65x100 mesh size fractions and between 72 and 99 for the 270x400 size fractions as volatile content of fuels increased from 10.5 to 40% (daf basis). Data also revealed that carbon conversion curves at 1300°C and 0.1-second were almost identical to those at 900°C and 0.8 second. This observation indicates that temperature and residence time are interrelated.

The DTF data suggest that variables which had significant influence on the combustion efficiency were temperature and residence time, followed by fuel type (volatile matter) and particle size. Statistical analyses of the test data indicated that: 1) there was no interaction between volatile matter and any other variable, and 2) external particle surface area was a contributing factor. This indicates that at high combustion temperatures, burning rates were partially controlled by the external mass transfer rate. Finally, DTF data revealed similar trends in reactivity as that obtained with the TGA method.

CONCLUSIONS

Fuels used in this study consisted of a mixture of highly devolatilized coal and relatively unheated coal with the proportion of each depending on the overall volatile matter content. Burn-out temperature and ignition temperatures increased significantly with decreasing volatile matter below 28%. High-temperature drop tube furnace tests revealed that temperature and residence time affected combustion efficiencies most, followed by fuel volatile matter content and particle size.

ACKNOWLEDGEMENTS

This work was funded in part by grants from the Illinois Coal Development Board through the Center for Research on Sulfur in Coal.

REFERENCES

1. Khan, M. R., 1987, Fuel Science and Technology International, 5(2), p. 185-291.
2. Chu, C. I. C., C. J., Im, B. L. Gillespie, 1989, DOE Report, DE-AC-2187MC23289.
3. Williams, A. D., M. D. Stephenson, C. W. Kruse, and M. Rostam-Abadi, 1988, Final Technical Report, Center for Research on Sulfur in Coal, Champaign, IL, August.
4. Nsakala, N. Y., R. L. Patel, and T. C. Lao, 1982, Final Report, EPRI AP-2601.

5. Solomon, P. E., M. A. Serio and S. G. Heninger, 1986, ACS preprints, 31(3) p. 200-205.
6. Tsai, C.-Y. and A. W. Scaroni. 1987, Fuel, 66(10) p. 1400-1406.
7. Chen, M. R., L. S. Fan and F. H. Essenhigh. 1984. Twentieth Symposium (Int.) on Combustion, p. 1513-1521.
8. Wells, W. F., S. K. Kramer, L. D. Smoot, A. U. Blackham, 1984, Twentieth Symposium (International) on Combustion, p. 1539-1546.
9. Khan, M. R. 1987. ACS preprint, 32(1), p. 298-309.
10. Rostam-Abadi, M., J. A. DeBarr, 1988, ACS preprint, 33(4), p. 864-874.
11. Rostam-Abadi, M., J. A. DeBarr, R. D. Harvey, R. R. Frost and C. W. Kruse, 1987. Final Report, Center for Research on Sulfur in Coal, Champaign, Illinois, August.
12. Rostam-Abadi, M., J. A. DeBarr, W.-T. Chen, S. A. Benson and D. P. McCollor, 1988. Final Report, Center for Research on Sulfur in Coal, Champaign, IL, August.
13. Semenov, N. N., 1935, Oxford, Clarendon Press.
14. Cassel, H. M., and I. Liebman, 1969, Combustion and Flame, 37, p. 207-10.

Table 1. Analyses of coal*, wt% (dry basis)

Volatiles Matter	39.2	Hydrogen	4.9
Fixed Carbon	52.4	Carbon	73.8
H-T Ash	8.4	Nitrogen	1.7
BTU/lb	13437	Oxygen	8.7
Moisture	5.4	Sulfur	2.3
		Chlorine	.2

*Illinois hvBb coal. Predominantly Springfield (No. 5), 20% Herrin (No. 6) blended at washing plant.

Table 2. Characterization data for chars

Particle size, mesh	65x100	100x150	150x200	200x270	270x400
<u>PD-1</u>					
volatile matter	24.8	24.6	25.7	27.8	29.2
fixed carbon	75.2	75.3	74.3	72.2	70.8
hydrogen	3.9	3.9	3.9	4.0	4.0
<u>PD-2</u>					
volatile matter					
carbon	15.7	15.9	17.3	19.5	21.3
hydrogen	84.2	83.8	82.7	79.9	78.7
	2.5	2.7	2.8	2.9	3.1
<u>PD-3</u>					
volatile matter	11.5	11.7	12.4	13.7	15.7
carbon	88.5	88.3	87.5	85.5	84.2
hydrogen	1.8	1.9	2.0	2.2	2.5

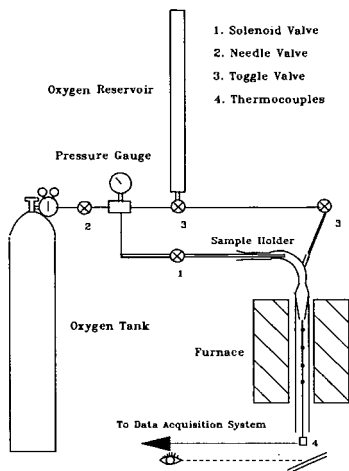


Figure 1. Ignitability test apparatus

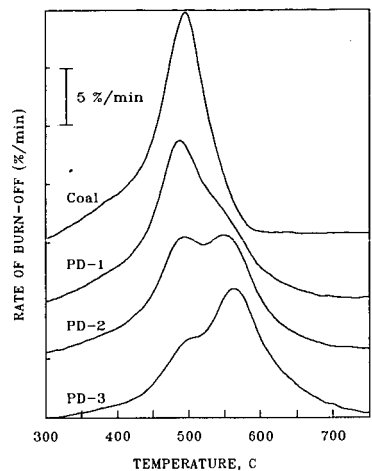


Figure 2. Burning profiles for coal and PD coals

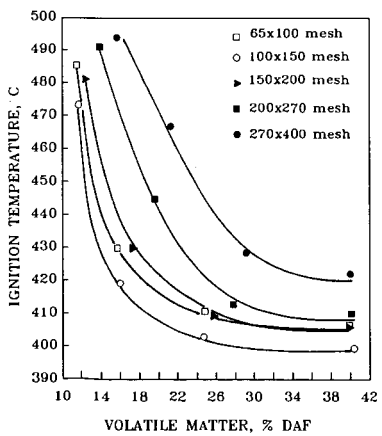


Figure 3. Effect of volatile matter on ignition temperature.

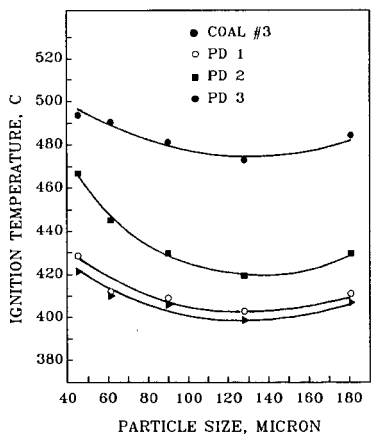


Figure 4. Effect of particle size on ignition temperature.

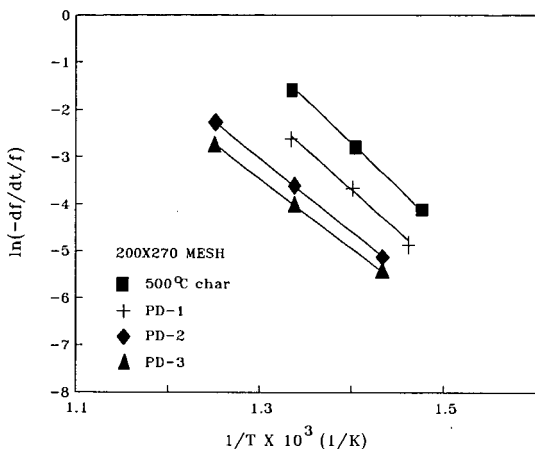


Figure 5. Arrhenius plot from isothermal TG data for 200x270 mesh fuels.

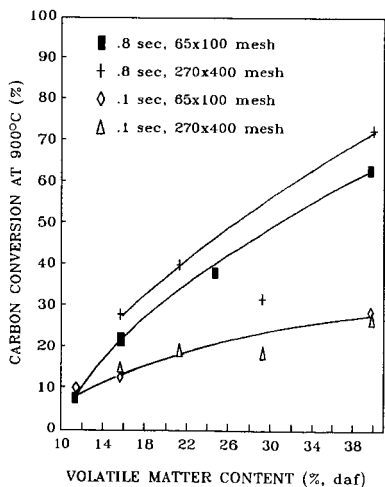


Figure 6. Effect of volatile matter content on carbon conversion in the drop tube furnace at 900°C.

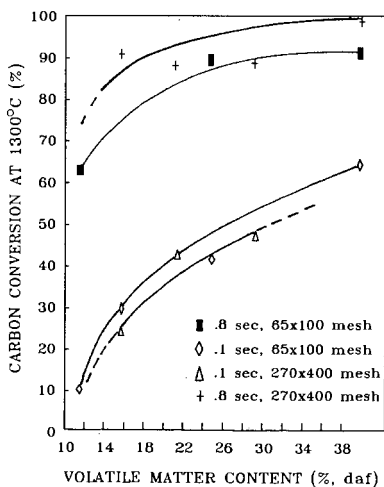


Figure 7. Effect of volatile matter content on carbon conversion in the drop tube furnace at 1300°C.